Near-Capacity Sphere Decoder Based Detection Schemes for MIMO Wireless Communication Systems

By

Goodwell Kapfunde

A thesis submitted in partial fulfilment of the requirements of the University of Hertfordshire for the degree of Doctor of Philosophy

The programme of research was carried out in the Science and

Technology Research Institute (STRI),

University of Hertfordshire,

Hatfield, Hertfordshire, United Kingdom, 2013

January 2013

ACKNOWLEDGMENTS

First and foremost, I have been greatly privileged to have this great opportunity to work with some of the highly experienced supervisors in the world. This work could not have come into existence if not for the wonderful discussions I have had while at University of Hertfordshire. I am particularly grateful for the supervision, support and mentorship of my supervisor, Professor Yichuang Sun. His expertise, understanding, and encouragement are the driving forces behind the success of this work.

Professor Yichuang Sun was a great inspiration in my technical development and provided me with great insights into relevant engineering problems. It is an honour and great pleasure to be supervised by him. His interest in my professional and personal development has made my experience at University of Hertfordshire valuable in many ways than I anticipated. I have learnt a lot from him through numerous meetings and discussions. He has always reserved time for these meeting even if pressed with other important commitments.

My sincere gratitude also goes to my second advisor Dr. Nandini Alinier for her valuable time and continuous support throughout this work. She has played a key role in my development ever since my arrival at University of Hertfordshire and she was always available for discussion whenever I needed it.

I would also like to thank Dr. Fabien Delestre and Dr. Gbenga Owojaiye for diverting their precious time to assist me in every aspect of this work. I also want to thank my research colleagues and other members of staff for their support and encouragement. I particularly would like to extent my warm appreciation to the School of Engineering and Technology for ensuring availability of all the necessary resources required in executing this work.

Finally, I would like to thank my family and friends whose moral and spiritual support was vitally important during the most stressful and trying times. I would like to dedicate this

thesis to my family. Without their unconditional and unwavering love and support, this work would not have been possible. I cannot conclude without thanking the ALMIGHTY GOD for the grace and guidance HE has granted me throughout my life.

ABSTRACT

The search for the closest lattice point arises in many communication problems, and is known to be NP-hard. The Maximum Likelihood (ML) Detector is the optimal detector which yields an optimal solution to this problem, but at the expense of high computational complexity. Existing near-optimal methods used to solve the problem are based on the Sphere Decoder (SD), which searches for lattice points confined in a hyper-sphere around the received point. The SD has emerged as a powerful means of finding the solution to the ML detection problem for MIMO systems. However the bottleneck lies in the determination of the initial radius.

This thesis is concerned with the detection of transmitted wireless signals in Multiple-Input Multiple-Output (MIMO) digital communication systems as efficiently and effectively as possible. The main objective of this thesis is to design efficient ML detection algorithms for MIMO systems based on the depth-first search (DFS) algorithms whilst taking into account complexity and bit error rate performance requirements for advanced digital communication systems. The increased capacity and improved link reliability of MIMO systems without sacrificing bandwidth efficiency and transmit power will serve as the key motivation behind the study of MIMO detection schemes.

The fundamental principles behind MIMO systems are explored in Chapter 2. A generic framework for linear and non-linear tree search based detection schemes is then presented Chapter 3. This paves way for different methods of improving the achievable performance-complexity trade-off for all SD-based detection algorithms. The suboptimal detection schemes, in particular the Minimum Mean Squared Error-Successive Interference Cancellation (MMSE-SIC), will also serve as pre-processing as well as comparison techniques whilst channel capacity approaching Low Density Parity Check (LDPC) codes will be employed to evaluate the performance of the proposed SD. Numerical and simulation

results show that non-linear detection schemes yield better performance compared to linear detection schemes, however, at the expense of a slight increase in complexity.

The first contribution in this thesis is the design of a near ML-achieving SD algorithm for MIMO digital communication systems that reduces the number of search operations within the sphere-constrained search space at reduced detection complexity in Chapter 4. In this design, the distance between the ML estimate and the received signal is used to control the lower and upper bound radii of the proposed SD to prevent NP-complete problems. The detection method is based on the DFS algorithm and the Successive Interference Cancellation (SIC). The SIC ensures that the effects of dominant signals are effectively removed. Simulation results presented in this thesis show that by employing pre-processing detection schemes, the complexity of the proposed SD can be significantly reduced, though at marginal performance penalty.

The second contribution is the determination of the initial sphere radius in Chapter 5. The new initial radius proposed in this thesis is based on the variable parameter α which is commonly based on experience and is chosen to ensure that at least a lattice point exists inside the sphere with high probability. Using the variable parameter α, a new noise covariance matrix which incorporates the number of transmit antennas, the energy of the transmitted symbols and the channel matrix is defined. The new covariance matrix is then incorporated into the EMMSE model to generate an improved EMMSE estimate. The EMMSE radius is finally found by computing the distance between the sphere centre and the improved EMMSE estimate. This distance can be fine-tuned by varying the variable parameter α.

The beauty of the proposed method is that it reduces the complexity of the preprocessing step of the EMMSE to that of the Zero-Forcing (ZF) detector without significant performance degradation of the SD, particularly at low Signal-to-Noise Ratios (SNR). More specifically, it

will be shown through simulation results that using the EMMSE preprocessing step will substantially improve performance whenever the complexity of the tree search is fixed or upper bounded.

The final contribution is the design of the LRAD-MMSE-SIC based SD detection scheme which introduces a trade-off between performance and increased computational complexity in Chapter 6. The Lenstra-Lenstra-Lovasz (LLL) algorithm will be utilised to orthogonalise the channel matrix H to a new near orthogonal channel matrix $\overline{H}$.The increased computational complexity introduced by the LLL algorithm will be significantly decreased by employing sorted **QR** decomposition of the transformed channel $\overline{H}$ into a unitary matrix and an upper triangular matrix which retains the property of the channel matrix. The SIC algorithm will ensure that the interference due to dominant signals will be minimised while the LDPC will effectively stop the propagation of errors within the entire system. Through simulations, it will be demonstrated that the proposed detector still approaches the ML performance while requiring much lower complexity compared to the conventional SD.

TABLE OF CONTENTS

ACKNOWLEDGMENTS ..... **i**
ABSTRACT ..... **iii**
TABLE OF FIGURES ..... **ix**
LIST OF SYMBOLS USED ..... **xi**
NOTATION ..... **xiv**
ACRONYMS ..... **xvi**
1. Introduction **1**
1.1 A General Overview of Wireless Communication Systems 1
1.2 Multiple-Input Multiple Output Detection Algorithms 2
1.3 Motivation 5
1.4 Thesis Contributions 8
1.5 Thesis Outline 9
1.6 Declaration 11
2. Preliminaries **12**
2.1 Introduction 12
2.2 Multiple-Input Multiple-Output Systems 13
2.2.1 Traditional antenna configurations for wireless systems 13
2.2.2 Multiple-antenna systems 14
2.3 MIMO Channel Configurations 15
2.3.1 Centralized transmitter and receiver 15
2.3.2. Decentralized transmitters and central receiver 15
2.3.3. Central transmitter and decentralized receivers 16
2.4 MIMO Transmission Schemes 17
2.4.1 Spatial diversity schemes 17
2.4.2 Spatial Multiplexing Schemes 20
2.5 Diversity Gain 24
2.6 Spatial Multiplexing Gain 26
2.7 The diversity gain vs. multiplexing gain 27
2.8 MIMO Capacity and Channel Coding Schemes 29
2.8.1 Capacity-approaching codes 30
2.8.2 MIMO channel capacity 33
2.8.3 MIMO System Setup and Assumptions 36
2.8.4 MIMO System description 38

2.8.5 Equivalent Real-Valued MIMO System Model 39
3. MIMO Detection Strategies 41
3.1 Introduction 41
3.2 The ML Detector 42
3.2.1 Maximum Likelihood Sequence Detection 43
3.2.2 The MAP Detector 45
3.2.3 Analytical Results of the ML Detector 46
3.2.4 Summary of ML Detection Schemes 47
3.3 Linear Detectors 48
3.3.1 The Zero-Forcing Detector 48
3.3.2 The Minimum Mean Squared Error Detector 49
3.3.4 Results and Discussion of Linear Detection Schemes 51
3.3.5 Summary of Linear Detection 52
3.4 Non-Linear Detectors 53
3.4.1 Successive Interference Cancellation Detector 54
3.4.2 Vertical Bell Labs Layered Space-Time Detector 56
3.4.3 Results of Non-Linear Detection Schemes 58
3.4.4 Summary of Non-Linear Detection Schemes 59
3.5 Lattice Reduction Techniques 61
3.5.1 Performance Results and Discussion 64
3.5.2 Summary of the LRAD detection Schemes 66
3.6 Introduction to tree search based detection schemes 66
3.6.1 Basic Sphere Detection Terminology 67
3.6.2 Tree Search Based Detection Schemes 70
3.6.3 Classification of Tree Search Algorithms 72
4. Sphere Decoding 74
4.1 Introduction 74
4.2 The Sphere Detection Concepts 75
4.3 Design Description 77
4.3.1 System Model 77
4.3.2 Tree representation of sphere decoding 79
4.3.3 OSIC-based QR Decomposition 80
4.3.4 Upper and Lower Bound Sphere Radius 81
4.3.5 The Depth Tree Search Algorithm 83
4.4 Optimization Techniques 91
4.4.1 Finke-Pohst Enumeration Strategy 91
4.4.2 Schnorr-Euchner Enumeration Strategy 92

4.4.3 Tree Pruning 92
4.5 Simulation Setup of the Proposed Sphere Detector 93
4.6 Performance Results and Discussion 94
4.7 Summary of the Sphere Decoder Results 97
4.8 Conclusion 97
5. Initial Radius Selection 99
5.1 Introduction 99
5.2 Selection of Initial Sphere Radius 101
5.2.1 Fixed Radius Search 103
5.2.2 Adaptive Radius Search 104
5.2.3 System Model 105
5.3 Linear detection schemes 109
5.4 The proposed sphere decoder 111
5.5 Performance Results and Discussion 114
5.6 Conclusions 118
6. The LRAD-SD-based Detection Schemes 119
6.1 Introduction 119
6.2 System Model 120
6.3 MIMO detection schemes 122
6.3.1 Lattice Reduction Aided Detection schemes 123
6.3.2 LRAD-MMSE-SIC-SE-SD System Description 125
6.4 Performance Results and Discussion 127
6.5 Computational Complexity Analysis 130
6.6 Summary 134
6.7 Conclusions 134
7. Conclusion and Future Work 135
7.1 Conclusions 135
7.2 Future Work 137
7.2.1 Tree search based Algorithms and sequential Detection 137
7.2.2 MIMO Detection Problem Size 137
7.2.3 Sphere Detection Computational Complexity Analysis 137
7.2.4 Initial Radius Selection 138
7.3.5 Hardware Implementation of the Proposed Detection schemes 138
References 139

TABLE OF FIGURES

Figure 2-1Traditional SISO Antenna Configuration 13

Figure 2-2 Traditional SIMO and MISO Antenna Configuration 14

Figure 2-3 Example of Multiple-Input-Multiple-Output System 14

Figure 2-4 Central transmitter and central receiver MIMO System 15

Figure 2-5 Decentralized Transmit and Central Receive MIMO system 16

Figure 2-6 Centralized Transmit and Decentralized Receive Cooperative MIMO System 17

Figure 2-7 Generalised STBC Block diagram 19

Figure 2-8 Generalised VBLAST Architecture 22

Figure 2-9 Example of MIMO System Multiplexing Structure 26

Figure 2-10 Spatial Multiplexing Gain Diversity trade-off 29

Figure 2-11 Discrete time transmission model 30

Figure 2-12 Graphical Representation of LDPC Codes 32

Figure 3-1 Simulation Results For ML 47

Figure 3-2 Block diagram of a Zero-Forcing Equalizer 49

Figure 3-3 Block diagram of an MMSE Filter 50

Figure 3-4 Simulation Results for coded and uncoded ZF and MMSE Detection 51

Figure 3-5 Block Diagram of a Successive Interference cancellation Detector 55

Figure 3-6 Block Diagram of the VBLAST Detector 56

Figure 3-7 Performance Results for Linear Versus Non-Linear detectors 58

Figure 3-8 Block diagram of an LRAD 63

Figure 3-9 LRAD performance results for 4-QAM and 64-QAM 4x4 MIMO setup 64

Figure 3-10 LRAD performance results for4-QAM and 64-QAM 4x6 MIMO setup 65

Figure 3-11 Tree search diagram illustrating sphere detection terminologies 68

Figure 4-1 Geometrical representation of sphere detection algorithm 76

Figure 4-2 Block diagram of a complete MIMO System 78

Figure 4-3 BPSK Binary Tree representation of sphere detection algorithm 83

Figure 4-4 Binary Tree diagram illustrating Pruning and Depth-First-Search algorithm 89

Figure 4-5 Illustration of selection of the best candidate in sphere detection 90

Figure 4-6 Illustration of the Finke-Pohst Enumeration Strategy 91

Figure 4-7 Illustration Schnorr-Euchner Enumeration Strategy 92

Figure 4-8 Performance comparison for 4x4 and 4x6 MIMO Setup for the proposed SD 95

Figure 4-9 Performance comparison for coded and uncoded 4x4 MIMO setup for the proposed SD 96

Figure 5-1 ML block diagram 106

Figure 5-2 Geometric Representation of the Sphere Decoding Algorithm 107

Figure 5-3 Complexity results for SE-SD 16-QAM-4x4 MIMO system 114

Figure 5-4 Complexity results for SE-SD 16-QAM-4x6 MIMO system 115

Figure 5-5 Performance of the proposed SE-SD for uncoded 64-QAM-4x4 MIMO setup .. 116

Figure 5-6 Performance results for the proposed SE-SD for uncoded 4x6 MIMO setup 117

Figure 6-1 MIMO system transmission model 121

Figure 6-2 Proposed LRAD-MMSE-SIC-SE-SD block diagram 126

Figure 6-3 Performance results for (a) coded and (b) uncoded 4x4 MIMO System Setup ... 128

Figure 6-4 Performance results for proposed LRAD-MMSE-SIC-SD 129

Figure 6-5 Average arithmetic operations without statistical pruning 131

Figure 6-6 Average arithmetic operations with statistical pruning 133

LIST OF SYMBOLS USED

The most frequently used symbols throughout the thesis are presented in this section. These symbols are applicable all the sections in this thesis. Symbols which are applicable to specific sections are defined within those sections.

A	Size of real-valued modulation alphabet
$\boldsymbol{\mathcal{A}}$	Real signal set of cardinality A
B_l	Length bias term at layer l
B_c	Coherence bandwidth
B_s	System bandwidth
C	Channel capacity
c	Vector of bits transmitted per vector symbol
$c_{l,i}$	Bit transmitted at bit index i on layer l
$d\big(x(c)\big)$	Euclidean distance between $\boldsymbol{y}$ and $\mathbf{Hx}$(c)
$d_l(\cdot)$	Euclidean distance increment at layer l
E_b	Signal energy per bit
E_s	Signal energy per (vector) symbol
$\mathbf{G}$	Linear filter matrix
$\mathbf{H}$	Channel transfer or lattice generating matrix (real valued model)
$h_{i,j}$	Channel gain between transmit antennaj and receive antenna i
I	Average mutual information

$\mathbf{I}$	Identity matrix (TT^{-1})
K	Number of information bits per transmitted block
l	Layer index, with $1 \leq l \leq N_L$
L	Number of bits per modulated symbol (complex valued model)
$L_a(c_{l,i})$	A priori log-likelihood ratio of bit $c_{l,i}$
$L_e(c_{l,i})$	Extrinsic log-likelihood ratio of bit $c_{l,i}$
$L_p(c_{l,i})$	A posteriori log-likelihood ratio of bit $c_{l,i}$
$\mathcal{L}$	Subset search list with hypotheses on the transmit signal, $\lvert\mathcal{L}\rvert = M$
$\mu(\mathbf{x}(c))$	Metric corresponding to the hypotheses that $\mathbf{x}(c)$ was transmitted
$\mu_l(\cdot)$	Branch metric at layer l
M	Number of leaf nodes a tree search algorithm has to find
n	Receiver noise (real-valued model)
N	Number of coded bits per transmitted block
N_L	Number of layers
N_M	Number of branch metric computations during a tree search
N_{r}	Number of receive antennas (complex-valued model)
N_{2t}	Number of receive antennas (real-valued model, $N_{2t} = N_{\mathrm{t}}$
N_{s}	Number of vector symbols transmitted per block
N_t	Number of transmit antennas

N_0	Noise power spectral density (double-sided, complex baseband)
P_e	Probability of a transmission (block) error
$\boldsymbol{\Psi}$	Interference matrix after linear equalisation ($\boldsymbol{\Psi} = \mathbf{GH}$)
$\boldsymbol{\varphi}_{nn}$	Noise covariance matrix (real-valued model)
$\boldsymbol{\varphi}_{xx}$	Transmit covariance matrix (real-valued model)
R_0^2	Initial hyper-sphere radius
$R_l^2\{[\mathbf{x}]_{N_L}^{l+1}\}$	Remaining radius of the hyper-sphere in sphere detection at layer l, depending on the incomplete transmit signal estimate $[\mathbf{x}]_{N_L}^{l+1}$
R_d	Data rate
R_c	Code rate
R	Spectral efficiency
S	Stack size of a sequential detector (LISS)
ξ	Scaling factor for mean squared error of channel estimate, relative to the operating SNR
$\mathbf{x}$	Transmitted vector signal (real-valued model)
$\boldsymbol{y}$	Received vector signal (real-valued model)

NOTATION

- Bold lowercase letters **x** denote vectors
- $\|\mathbf{x}\|$ denotes the Euclidean distance or the l_2-norm of the vector **x**.
- The notation $[\mathbf{x}]_j^i$ is used to refer to the vector of elements i through j from **x**.
- Bold uppercase letters A denote matrices
- $\left(\mathbf{x}_{l,i}^{-1}\right)$ means that the i^{th} element in layer l is equal to -1
- $\left(\mathbf{x}_{l,i}^{+1}\right)$ means that the i^{th} element in layer l is equal to +1
- $\boldsymbol{x}_{i,j}$ or $[\mathbf{A}]_{i,j}$ denote the i^{th} row and j^{th} column of the matrix A.
- $\mathbf{x}^{(i)}$ denotes the i^{th} row vector and $\mathbf{x}_j$ denotes the j^{th} column vector.
- $\boldsymbol{A} \in \boldsymbol{\mathcal{A}}^{[N_L \times N_r]}$ denotes a matrix with N_L rows and N_r columns whose components are taken from the set $\boldsymbol{\mathcal{A}}$.
- $\boldsymbol{A} \subset \boldsymbol{\mathcal{A}}^{[N_L \times N_r]}$ indicates that $\boldsymbol{A}$ is a subset of the set $\boldsymbol{\mathcal{A}}$.
- $\mathbf{0}_{N_L}$ denotes the $N_L \times N_L$ matrix of zeros while $\mathbf{0}_{N_L,1}$is the $N_L \times 1$ row vector of zeros.
- $\mathbf{1}_{N_L}$ denotes the $N_L \times N_L$ matrix of ones while $1_{N_L,1}$is the $N_L \times 1$ row vector of ones.
- $\mathbf{x}_l^k$ denotes the vector **x** at node k in layer l
- $[\cdot]^{-1}$ denotes the inverse of a matrix
- $[\cdot]^T$ denotes the transpose of a matrix
- $[\cdot]^H$ denotes the Hermitian transpose of a matrix.
- $[\cdot]^*$ denotes the complex conjugate transpose of a matrix
- $[\cdot]^\dagger$ denotes the Moor-Penrose pseudo-inverse or simply the pseudo-inverse.
- The set of real, complex and integer numbers are donated by $\mathbb{R}$, $\mathbb{C}$ and $\mathbb{Z}$, respectively.
- Real valued numbers and imaginary numbers will be denoted by $\mathfrak{R}$ and $\mathfrak{I}$ respectively.
- The binary field is denoted by with elements $\{+1, -1\}$
- Binary mapping will be carried out as follows: $0 \leftrightarrow +1$and $1 \leftrightarrow -1$).

- Rounding-off to the nearest integer larger than x is denoted by $\lfloor x \rceil$
- rounding-off the nearest integer smaller than x is denoted by $\lceil x \rceil$
- $E_s/(N_t N_0)$ denotes the signal-to-noise ratio where N_t is the number of transmit antennas and N_0 is the noise spectral density
- The Probability Density Function (p.d.f) of the continuous random variable x is denoted by p (x). The expected value of a random variable X is denoted by {X}. Probabilities are denoted by P[·].

ACRONYMS

AAS	Advanced Antenna Systems
ADSL	Asynchronous Digital Subscriber Line
APP	A Posteriori Probability
AWGN	Additive White Gaussian Noise
BER	Bit Error Rate
BFS	Breadth First Search
BICM	Bit interleaved Coded Modulation
BLAST	Bell Laboratory Layered Space-Time
BS	Base Station
CDMA	Code Division Multiple Access
CLP	Closest Lattice Point
CLPP	Closest Lattice Point Problem
CPDF	Conditional Probability Density Function
CSD	Conventional Sphere Decoder
CSI	Channel State Information
D-BLAST	Diagonal Bell Labs Layered Space-Time
DFE	Decision Feedback Equalization
DFS	Depth First Search
EMC	Ergodic MIMO Capacity
EMMSE	Extended Minimum Mean Squared Error
DSP	Digital Signal Processing
FDA	Fano Detection Algorithm
FEC	Forward Error Correction
ILSS	Integer Least Square Solution

ISI	Inter-Symbol Interference
LD	Linear Detection
LDC	Linear Dispersion Codes
LDPC	Low Density Parity Check
LLL	Lenstra-Lenstra-Lovasz (lattice reduction) algorithm
LLR	Log-Likelihood Ratio
MAI	Multiple Access Interference
MAP	Maximum A Posteriori Probability
MFS	Metric First Search
MIMO	Multiple Input Multiple Output
MISO	Multiple Input Single Output
ML	Maximum Likelihood
MLD	Maximum Likelihood Detector
MLSE	Maximum Likelihood Sequence Estimator
MMSE	Minimum Mean Squared Error
MMSE-SIC	MMSE-Successive Interference Cancellation
MPIC	Multistage Parallel Interference Cancellation
MUD	Multi-User Detection
MRC	Maximum Ratio Combining
NLD	Non-Linear Detectors
NP-hard	Non-deterministic Polynomial-time hard
OFDM	Orthogonal Frequency Division Multiplexing
MOC	MIMO Outage Capacity
OSIC	Ordered Successive Interference Cancellation
PARC	Per-Antenna Rate Control
PCCC	Parallel Concatenated Convolutional Codes

PED	Partial Euclidean Distance
PIC	Parallel Interference Cancellation
PSA	Post-Sorting-Algorithm
PSK	Phase Shift Keying
QAM	Quadrature Amplitude Modulation
QoS	Quality of service
QRD	QR Decomposition
SD	Sphere Detector
SDMA	Space Division Multiple Access
SE	Schnorr-Euchner
SE-SD	Schnorr-Euchner Sphere Detector
SIC	Successive Interference Cancellation
SIMO	Single Input Multiple Output
SNR	Signal-to-Noise Ratio
SQRD	Sorted QR decomposition
STBC	Space Time Block Coding
STC	Space-Time Coding
STTC	Space Time Trellis Coding
SVD	Singular Value Decomposition
SVP	Shortest Vector Problem
V-BLAST	Vertical Bell Labs Layered Space-Time
ZF	Zero Forcing
ZF-SIC	ZF- Successive Interference Cancellation

1. Introduction

1.1 A General Overview of Wireless Communication Systems

The idea of transmitting radio signals over wireless communication channels date back in the 1890s. The first wireless communications radio link was discovered by Gugliemo Marconi, popularly known as the "father of wireless communications", in 1895. In this year, he succeeded in establishing the first recognised wireless communication link by transmitting a series of dots and dashes, also known as the Morse code, from the Isle of Wight over a wireless communication channel to a receiver in a tugboat located at approximately 30km away from the transmitter.

Although the transmitted radio signals were accurately interpreted by the receiver, there was little or no knowledge about the fundamental limits of the rates at which radio signals can be transmitted over such a radio link reliably. In these infantry stages of wireless communication systems, the communications community remained in the wilderness of darkness until Shannon's pioneering work in 1948 on the capacity limits of an Additive White Gaussian Noise (AWGN) channel [1]. It was until then that communication engineers understood the fundamental limits on the communication rate of reliable transmission [1]. Since then wireless communication systems have seen a tremendous growth with an incredible rate of expansion in the past few decades. Today, advanced digital communications systems transmit digital signals over billions of kilometres via satellite communication links.

Today, the goal of a communication system designer is to design high speed communication links with high spectral efficency and at the same time provide good Quality of Service (QoS), i.e., improved link reliability leading to minimisation of the probability of error. The system designer goals also include the reduction of transmission power and bandwidth and

minimization of complexity and cost of implementation of the proposed wireless communication systems. The ultimate result is increased capacity at significantly low interference. Currently, communication technologies based on Long Term Evolution (LTE) are being designed to provide high data rate in both the uplink and the downlink. More ambitiously, system designers are developing wireless systems to supplant the standard wired last mile (access network) of service providing a wireless alternative to cable modems and digital subscriber lines, a wireless backbone for Wi-Fi (IEEE802.11) hotspots as well as providing general telecommunications and data services [2]. However, little is known about the performance characteristics of such wireless systems, neither how to optimize the design of such wireless systems, particularly when the complexity of the system design is taken into account as a practical constraint.

1.2 Multiple-Input Multiple Output Detection Algorithms

Several techniques have been proposed to achieve these design goals. Examples of such techniques include the design of more spectral efficient higher order modulation schemes such as Quadrature Amplitude Modulation (QAM), Phase Shift Keying (PSK) and Low Density Parity Check (LDPC) codes channel coding schemes. However, the use of higher order modulation and coding schemes pose more challenges: limited range [3]-[4], thus demanding more transmit power and transmission of redundant bits instead of information carrying bits. Furthermore, the channel becomes more subject to Inter Symbol Interference (ISI) as the modulation order increases, thus, reducing the reliability and consequently the performance and capacity of wireless communication systems.

As communication engineers strive to address existing issues, they are often confronted with more serious and more pressing new challenges. The radio communication channel is a dynamic process which is never constant, but which is instead continuously varying with

time, space and frequency. Communication channels are generally non-orthogonal, i.e., the electromagnetic signals radiated from different transmit antennas superimpose at each receive antennas [5]. If perfect Channel State Information (CSI) is available at the transmitter, the channel can be orthogonalised by using appropriate signalling techniques. However, such information is often unavailable or cannot be exploited due to limited computational resources at the receiver side. In such scenarios, the detection of received signals becomes a daunting task for the receiver as the complexity of optimal detector rises exponentially with the number of received bits per transmitted vector symbol.

One of the candidates for Digital Signal Processing (DSP) technologies which has provided solutions to the constraints and technical burden placed on spectrum by exploiting the spatial domain of the transmission medium is Multiple-Input Multiple Output (MIMO) systems [6]. Equipping both the transmitter and the receiver with multiple antennas can result in significant increase in diversity gain, spectral efficiency [7]-[10], link range and reliability without additional bandwidth and transmit power. However, due to the non-orthogonality of the transmission channel, these benefits come at the cost of potentially high detection complexity, particularly in cases where a large number of transmit antennas and large constellation sizes are used [11].

The brute-force Maximum Likelihood (ML) detector yields an optimal solution in detection of both coded and uncoded MIMO signals transmitted over non-orthogonal channels, but however, at the expense of huge and practically unbearable computational complexity due to the excessively high number of lattice points visited during the detection process. The need to reduce the number of visited lattice points, and consequently computational complexity, has motivated intense research in the design of more powerful sub-optimal detectors which are capable of fine-tuning the visited lattice points. These include the Sphere Decoder (SD) [12],

the Fano Detection Algorithm (FDA) [13] and the Lattice Reduction-Aided Detection (LRAD) schemes [14]-[15].

The SD or the Finke-Pohst (FP) detection algorithm [12], [16] was proposed as an efficient algorithm for finding the solution to the ML detection problem in MIMO digital communication systems. It is an effective method for ML detection for MIMO systems [17]. The SD criterion is based on finding the Integer Least-Squares Solution (ILSS) of a system of linear equations where the unknown vector is comprised of integers but the coefficient matrix and the given vector is comprised of real numbers [18]. This problem is equivalent to finding the closest lattice point to a given point and is known to be NP-hard [18]. The SD detection problem has been reformulated into a tree search problem, which can be regarded as a search for leaf nodes in a tree which maximizes certain metric [19].

However, the complexity of the SD is very sensitive to the initial radius R_0, of the hyper-sphere [19]-[21], which in turn determines the number of lattice points inside the hyper-sphere. As a result, researchers have shifted their attention towards finding an optimal initial sphere radius which minimizes the number of lattice points visited during the detection process, and consequently, the computational complexity of the SD.

The desire to achieve a near-optimal SD detection at low computational complexity has resulted in bridging the gap between the study of Multi-User Detection (MUD) and MIMO detection. Several sub-optimal detection strategies have been used as pre-processing techniques in MIMO detection. The main aim being to improve the reliability of SD input signals and consequently reducing the computational cost of the sphere decoder and at the same time increasing the performance of the SD [22]-[24]. Among them are the Linear Detectors (LD) and Non-Linear Detectors (NLD). Examples of NL detectors include the Decorrelating detector, also known as the Zero-Forcing (ZF) equalizer [22]-[23] and the

Minimum Mean Squared Error Detector (MMSE) [24]. NLD include the Vertical Bell Layered Space-Time (V-BLAST), also known as the Ordered Successive Interference Cancelation (OSIC) [27], and its variations, i.e., the Parallel Interference Cancellation (PIC) and the Decision Feedback Detector (DFD) [25]-[26], [28].

This thesis focuses on the performance and complexity analysis of MIMO detection algorithms. More powerful codes such as LDPC codes and suboptimal detection schemes will be combined with the SD to achieve quasi-optimal solution to the MIMO detection problem with minimum complexity.

1.3 Motivation

The increasingly high demand for wireless communications services and the increasing users' expectations for multi-media services have led to the explosive increase in different applications of wireless technology in the last decade. With this current trend, present wireless communication systems will not be able to handle the expected high data rates traffic. The demand for high data rates for future wireless communications systems has resulted in the congestion of radio frequency spectrum. Frequency spectrum, which is subject to physical constraints and regulation, is a scarce and limited resource, and thus a precious resource. This fact has consequently led to the need for the design of wireless technologies which utilise the radio frequency spectrum as efficiently as possible. The solution lies in the design of MIMO systems with high spectral efficiency. It has been demonstrated that MIMO technology is the most promising technology as it can improve link reliability without sacrificing bandwidth efficiency and transmit power.

However, the increase in spectral efficiency comes at the expense of a potentially high computational cost of the receiver design. The non-orthogonality of the transmission channels has motivated intense research into the design of MIMO detectors. Chapter 2 of this thesis

sheds some light on the fundamental principles and benefits of MIMO systems including increased capacity, improved diversity gain and spatial multiplexing gain.

Whilst MIMO systems are capable of achieving near-channel capacity, the major challenge lies in the design of the MIMO detectors due to non-orthogonality of MIMO channels. The ML detector yields an optimal solution to the detection of MIMO signals transmitted over non-orthogonal channels, however, at the expense of its computational complexity which arises due to the excessively high number of lattice points visited during the detection process. Several suboptimal MIMO detection strategies have been introduced in the literature to slice the complexity of the ML detector. Chapter 3 discusses linear and non-linear detection schemes including MMSE and the Successive Interference Cancellation (SIC). Most researchers to date have not investigated techniques which eliminate error propagation effectively. An MMSE-SIC detection scheme, which effectively reduces error propagation and yield performance gain over linear detection schemes, is investigated in Chapter 4.

Linear detectors are popularly known for their significantly reduced complexity, but the reduced complexity is achieved at strong performance penalty. Tree search detection schemes, which form the core of this thesis, have recently emerged as the most promising approaches towards solving the MIMO detection problem. They model the detection task into a search for leaf nodes in a tree which maximise a certain metric. By tuning the number of lattice points, tree search algorithms are allowed to visit a predetermined number of nodes. Thus, performance and complexity can be flexibly traded off against each other. Research in this area so far concentrated on iterative detection-decoding and sequential detection. In Chapter 4, an SD characterised by the depth-first-search algorithm which is capable of achieving near-ML performance is ivestigated. Both coded and uncoded transmissions will be

investigated in Chapter 4. The state of the art LDPC will be employed to evaluate and improve performance.

The selection of the initial sphere radius is one of the most difficult challenges faced in the design of the sphere detector. A novel Extended Minimum Mean Squared Error (EMMSE) initial radius based on the received signal; noise statistics; the number of transmit antennas; the energy of the transmitted symbols and on the channel matrix is designed in Chapter 5. This proposed initial radius is particularly suitable for reducing the complexity of the SD at low signal-to-noise ratios (SNR).

Finally, it has been shown that non-linear detectors, including sequential detectors, yield better performance compared to linear detection schemes at the expense of one or more or a combination of the following problems: error propagation and increased computational complexity. To overcome these problems, a trade-off between performance and one or more of these issues has to be made. Most work to date has concentrated on searching in original signal space. The state-of-the-art Lattice Reduction Aided SE-SD (LRAD-SE-SD) which searches for the Closest lattice Point (CLP) in the transformed reduced signal space is proposed in Chapter 6. Chapter 6 provides a detailed assessment of preprocessing schemes which aim to reduce the complexity of the SD and improve performance. The investigations cover the case of uncoded transmission, as well as coded transmission. Both average and worst case complexity will be investigated in Chapter 6.

1.4 Thesis Contributions

The novel contributions of this thesis are highlighted below.

- The SIC-based SD characterised by the Depth First Search (DFS) algorithm is proposed in Chapter 4. A tree search representation will be used to illustrate how the proposed algorithm walks over the tree throughout the design. The sphere detection problem will be reformulated into a tree search problem by performing **QR** decomposition on the channel matrix. This allows for the construction of an ordered SIC based subset search list which minimizes the number of visited lattice points, thus reducing the complexity of the SD significantly.
- To avoid the effects of error propagation introduced by the SIC algorithm which could have an adverse effect on the Bit Error Rate (BER) performance of the proposed SD, LDPC codes will be employed to stop error propagation from one stage of the detector to the next. Optimal ordering is also used in this design to eliminate error propagation by allowing the row within the received signal vector with the highest post detection SNR to be detected earlier than others in Chapter 4.
- The selection of the initial sphere radius is one of the most difficult challenges faced in the design of the sphere detector. A novel EMMSE SD initial radius based on the received signal; noise statistics; the number of transmit antennas; the energy of the transmitted symbols and on the channel matrix is proposed in Chapter 5. The proposed initial radius is particularly suitable for reducing the complexity of the sphere decoder at low SNRs. In order to further reduce the complexity of the SD, the **QR** decomposition which is inherent in the Schnorr-Euchner SD (SE-SD) will be utilised. Simulation results show that the proposed initial sphere radius does not only reduce the complexity of the SD, but also significantly improves the BER performance of the SD, particularly at low SNR.

- An efficient SD detection strategy that yields an ML solution at significantly reduced complexity is proposed in Chapter 6. Complexity reduction is achieved by intruding the Lattice Reduction Aided detection (LRAD) scheme and performing **QR** decomposition. The resulting reduced SD structure will be referred to as the LRAD-MMSE-SIC-SE-SD and its computational complexity is independent of the constellation size while it is polynomial with respect to the number of antennas. Performance results of the proposed complete LRAD-MMSE-SIC-SD detection scheme show that the SD complexity is significantly reduced at only marginal performance penalty.

1.5 Thesis Outline

Chapter 2 provides an overview of MIMO systems. The advantages of MIMO which include increased spectral efficiency and/or capacity and diversity gain of wireless communication systems are presented in this Chapter. A brief description of the simulation setup and MIMO transmit strategies used throughout this thesis is provided in this chapter. The concept of channel capacity and channel approaching codes exemplified by LDPC codes is introduced in Chapter 2.

Chapter 3 introduces MIMO detection schemes. Optimal detection schemes are considered in the first part of this chapter. Two classes of optimal detection schemes namely the Maximum Likelihood Sequence Detector (MLSD) and the Maximum A Posteriori Probability (MAP) detection schemes are then discussed. The MLSD will serve as the basis for the SD which forms the core of this work. It will also be used as a yardstick against which the performance of the other MIMO detection strategies is measured.

The fundamental principles underlying both linear and non-linear sub-optimal detection algorithms are discussed to depth in Chapter 3. The de-correlating and the MMSE detectors,

the SIC and the Vertical Bell Laboratory Layered Space-Time (V-BLAST) detection schemes are used as representative examples of both linear and non-linear detection schemes respectively. These sub-optimal detection schemes will be later used as pre-processing schemes as well as comparison techniques for the SD, which is the main focus of this work. It will be shown that non-linear detection schemes yield better performance compared to linear detection schemes, though at slightly increased complexity. A brief survey of the LRAD scheme is also presented in Chapter 3.

A generic framework for tree search based detection schemes is introduced. An overview of the three main classes of tree search detection algorithms, namely the Depth-First-Search (DFS), Breath-First-Search (BFS) and the Metric-First-Search (MFS) is provided in this chapter, leading to the main subject of this work, i.e., the SD in Chapter 4.

The SD characterized by the DFS algorithm will be investigated in Chapter 4. This will be followed by an in-depth description of the proposed SD design. The orthogonalisation of the channel matrix, also referred to as the lattice generating matrix, will be explored in Chapter 4. A survey of the EMMSE initial radius is provided in this chapter. The chapter will be closed with a thorough analysis of the tree search representation of the DFS SD detection algorithm. Note that the terms detector and decoder are interchangeable in the context of sphere detection and will be used with the same meaning throughout this thesis.

In Chapter 5, a simple SE-SD with a novel EMMSE radius based on the received signal; noise statistics; the number of transmit antennas; the energy of the transmitted symbols and on the channel matrix is proposed. The main goal of this chapter is to address the issue of decoding failure and reduction of the computational complexity which is inherent in the SD.

The LRAD-MMSE-SIC-SE-SD detection scheme that introduces a trade-off between performance and the complexity is designed in Chapter 6. The Lenstra-Lenstra-Lovász (LLL)

algorithm will be employed to orthognalise the channel matrix by transforming the signal space of the received signal into an equivalent reduced signal space. It will be shown through simulation results that the computational complexity of this detector is independent of the constellation size while it is polynomial with respect to the number of antennas and signal-to-noise ratio. Finally, an outlook on the future work and the main findings are presented in Chapter 7.

1.6 Declaration

The following papers have been published and parts of their material are included in this thesis:

Published Manuscripts

- G. Kapfunde, Y. Sun, "Performance Evaluation of Linear Detectors for LDPC-Coded MIMO Systems," *University College of London Conference*, London, UK, 2010.
- G. Kapfunde, Y. Sun, N. Alinier, "An Improved Sphere Decoder for MIMO Systems," *3rd International Workshop on the Performance Enhancements in MIMO OFDM Systems (PEMOS)*, Barcelona, Spain, October, 2012.
- G. Kapfunde, F. Tade, Y. Sun, "A Sphere Decoder for MIMO Detection using Improved Initial Sphere Radius", *Applied Radio Systems Research and Smart Wireless Communications (ARSR/SWICOM),* Luton, UK, 2013.

2. Preliminaries

2.1 Introduction

The increasing demand for wireless communication services has led to the congestion of the electromagnetic spectrum. This has consequently accelerated the desire to design wireless communication systems which frees up this scarce and precious resource. Multiple-Input Multiple-Output (MIMO) is a technology which employs multiple antennas at both the transmitter and receiver to improve the performance of wireless communication systems [7]. Performance improvement is achieved by exploiting the spatial domain of the transmission medium. Without the discovery of MIMO systems, there would have been no hope of achieving Shannon Capacity Limit with Single Input Single Output (SISO) systems. It has been demonstrated in [8] that further increases in channel capacity can be gained by the use of MIMO systems.

The idea of using antenna arrays to enhance the performance of wireless communication systems was conceived in the late 1920s [29]. Antenna arrays were then mainly used to enhance the link budget by beam-steering in these early years [29]. The ultimate goal of using antenna arrays was to exploit the receive diversity of a wireless communication system to combat the effects of fading [30] and estimating the angle of arrival of radio signals. Research into antenna arrays accelerated subsequently with the advent of personal mobile communication systems and digital signal processing in the 1970s. As research in antenna arrays gathered momentum, it became clear that antenna diversity may also be extended to cancellation of co-channel interference, thus increasing the capacity of a wireless link [31]. These developments subsequently led to the realization of the true potential of using MIMO systems: to increase the capacity and receive diversity gain of wireless communication systems.

The increasing demand for high data rates for wireless communication systems, coupled with the limited availability of radio frequency spectrum has increased the desire to design wireless communications systems with higher spectral efficiency [32]. The first practical Vertical Bell Laboratory Layered Space Time (V-BLAST) for realizing the performance gains for a MIMO system was developed by Gerard J. Foschini [7] in the mid-1990s at Bell Laboratories, with the theoretical foundation laid by Telatar [3]. It is now widely accepted that by exploiting the available spatial diversity appropriately, the capacity of wireless networks and link reliability can be substantially improved [34]. Due to these desirable features, MIMO systems have found application in modern wireless communication standards including IEEE 802.11n (Wi-Fi), 4G, 3GPP Long Term Evolution (LTE), Worldwide Interoperability for Microwave Access (Wi-MAX), also known as IEEE 802.16 and High Speed Packet Access (HSPA+) [35]-[36].

2.2 Multiple-Input Multiple-Output Systems

2.2.1 Traditional antenna configurations for wireless systems

Traditional wireless communication systems employ a single antenna at the transmitter and receiver and/or smart antenna technology [37].

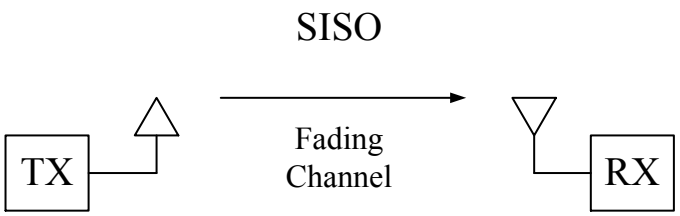

Figure 2-1Traditional SISO Antenna Configuration

The former is known as Single Input Single Output (SISO), while the later (smart antenna) exist in two configurations: Multiple-Input Single Output (MISO) and Single Input Multiple Output (SIMO) [37]. Figure 2-1 and Figure 2-2 show the conceptual diagrams for the respective SISO and smart antenna configurations.

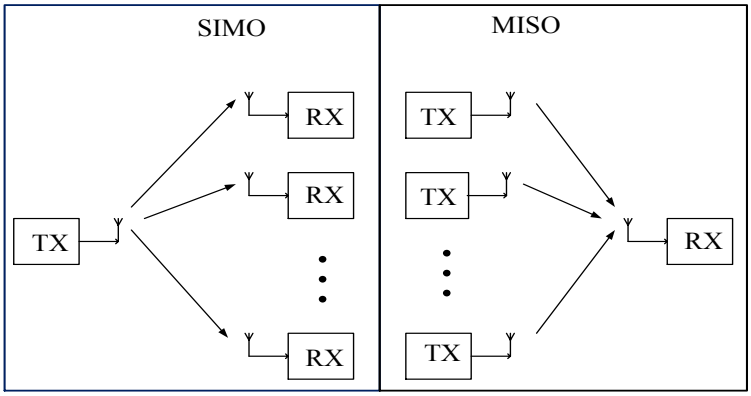

Figure 2-2 Traditional SIMO and MISO Antenna Configuration

2.2.2 Multiple-antenna systems

MIMO systems are considred as an extension of smart antennas technology. Traditional smart antenna technology employ *multiple antennas* at *either* the transmitter *or* receiver *only*, while MIMO systems generally employ multiple antennas at *both* the transmitter *and* the receiver.

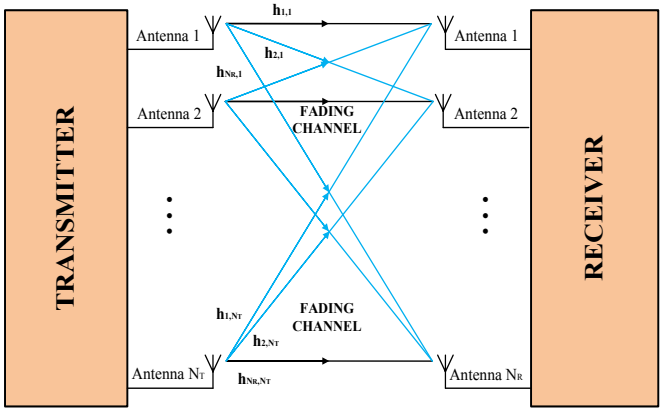

Figure 2-3 Example of Multiple-Input-Multiple-Output System

The demployment of multiple antennas at both the transmitter and receiver combined with advanced signal processing algorithms yields significant advantages both in terms of capacity and diversity gain over both traditional SISO wireless systems and smart antenna systems. Figure 2-3 shows an example of a MIMO system employing multiple antennas at both the transmitter and the receiver.

It is important noting that such a MIMO system cannot only be realized by using physically co-located antennas, but it can also be realized in decentralized or distributed antenna systems [38]-[39].

2.3 MIMO Channel Configurations

2.3.1 Centralized transmitter and receiver

In a typical MIMO system, both the transmitter and the receiver use several antennas with separate modulation and demodulation for each antenna. The interfering channels are the radio links between all pairs of transmit and receive antennas. Figure 2-4 shows an example of this *point-to-point MIMO channel* setting. This type of setup can be practically employed in a high-rate semi-mobile local-area wireless data communications system, where, for example, a laptop computer equipped with a set of antennas mounted on the back side of the display and communicates with an access point that also has several antennas.

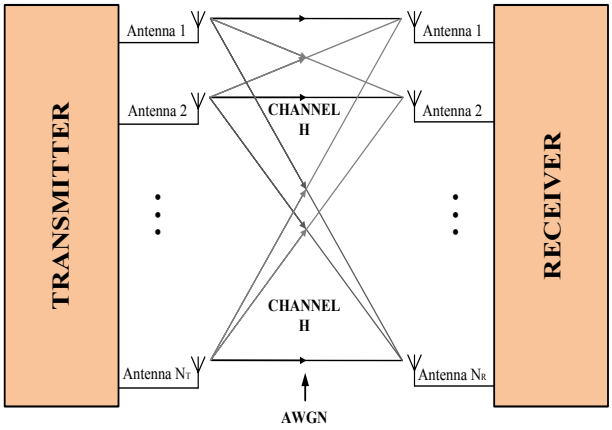

Figure 2-4 Central transmitter and central receiver MIMO System

2.3.2. Decentralized transmitters and central receiver

In the decentralized transmitters and central receiver MIMO configuration, several transmit antennas transmit signals which are received by a central receiver. This type of MIMO system has found application in Multi-User MIMO (MU-MIMO) systems. Here, several transmitters, e.g., mobile phones, transmit radio signals in the uplink direction towards the base station of the multiuser mobile communication system. The joint receiver at the base

station recovers the individual users' signals from the received aggregate signal. Since a number of users transmit at the same time in the same frequency band, the received signal is the superposition of all the active users' signals. This is referred to as multiuser detection problem, and is also known as the MIMO multiple access channels [40]. Figure 2-5 shows the block diagram for MIMO multiple access channels.

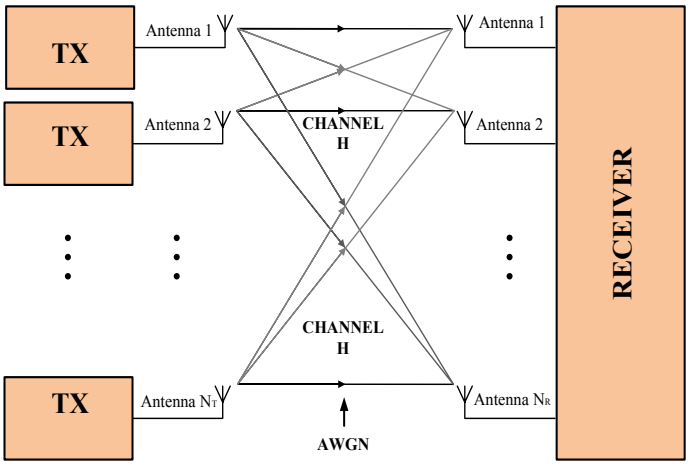

Figure 2-5 Decentralized Transmit and Central Receive MIMO system

This type of MIMO multiple access setup is analogous to digital subscriber line (ADSL) in fixed communication systems where ADSL signals propagate in the upstream direction via twisted pairs from the customers to the central office. This type of channel model will not be discussed further in this thesis.

2.3.3. Central transmitter and decentralized receivers

In the downlink direction of mobile multiuser communication system, the central transmitter transmits mobile signals towards decentralised receivers. An example of this setup is the base station (central transmitter) simultaneously transmitting mobile signals towards mobile phone handsets (decentralized receivers). Figure 2-6 shows this type of MIMO architecture which is referred to as *MIMO broadcast system* [41]-[45].

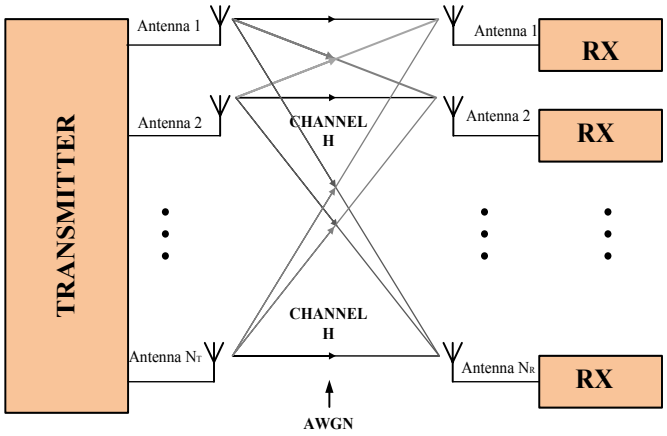

Figure 2-6 Centralized Transmit and Decentralized Receive Cooperative MIMO System

The main features of this MIMO setup is that the endpoints of the channels over which communication takes place are not concentrated at one point. The freedom of mutual interference of the channels from the base station to each of the users is usually assured by using time- or frequency-division-duplex transmission techniques. Separation of the user signals can also be achieved by the use of Code Division Multiple Access (CDMA) by assigning separate spreading codes or signature waveforms to individual users.

The technique that is mostly used to separate user signals in multiple access MIMO systems is *Space Division Multiple Access* (SDMA). This technique employs several transmit antennas at the base station in parallel to "form beams" [46] towards the users. Similarly, this setting is called the downstream direction in ADSL, where high data rate streams of data propagate from the central office towards decentralized customers.

2.4 MIMO Transmission Schemes

2.4.1 Spatial diversity schemes

Diversity can be achieved in different ways: time, frequency and space. Time diversity can be achieved by coding and interleaving data symbols [37]. Here, the coded symbols are dispersed over time in different coherence periods in such a manner that different parts of the code-words experience independent fades. Diversity can alternatively be exploited over frequency in frequency-selective channels. In MIMO channels diversity can be obtained over

space if the transmit or receive antennas are spaced sufficiently far enough. In a cellular network, macro-diversity can be exploited by the fact that the signal from a mobile can be received at two base-stations [37].

Spatial diversity schemes are employed to exploit the full diversity offered by the MIMO channel where high link reliability is of prime interest. Link reliability is achieved by transmitting the *same* bit stream over *all* transmit antennas, i.e., the several copies of the same message is mapped to all transmit antennas. However, link reliability is achieved at the expense of the potential increase in spectral efficiency.

Space-Time-Block-Codes

Space-Time Block Codes (STBC) employs some form of repetition data coding through both space and time to decouple the non-orthogonal MIMO channels into a set of orthogonal SIMO channels to improve the reliability of the transmission. This does not only enable exploitation of the transmit diversity of the system, but it also enables the implementation of low complexity receiver architectures based on Maximum Ratio combining (MRC). In each STBC block, *s* independent modulated data symbols are transmitted over a time interval of *T* samples, resulting in a code rate of the STBC of $R_{STBC} = s/T$. It is important pointing out that the channel has to remain constant over the duration of *T* samples in order to guarantee orthogonality of the code, and thus the reliability of the transmission.

The first STBC transmit strategy was proposed and developed by Alamouti [49] for two transmit antennas and one receive antenna. This scheme was later extended to general orthogonal designs for an arbitrary number of transmit and receive antennas by Tarokh et al. [50]. Both the Alamouti scheme and the generalised coding schemes have a very simple maximum likelihood decoding algorithm based only on linear processing at the receiver.

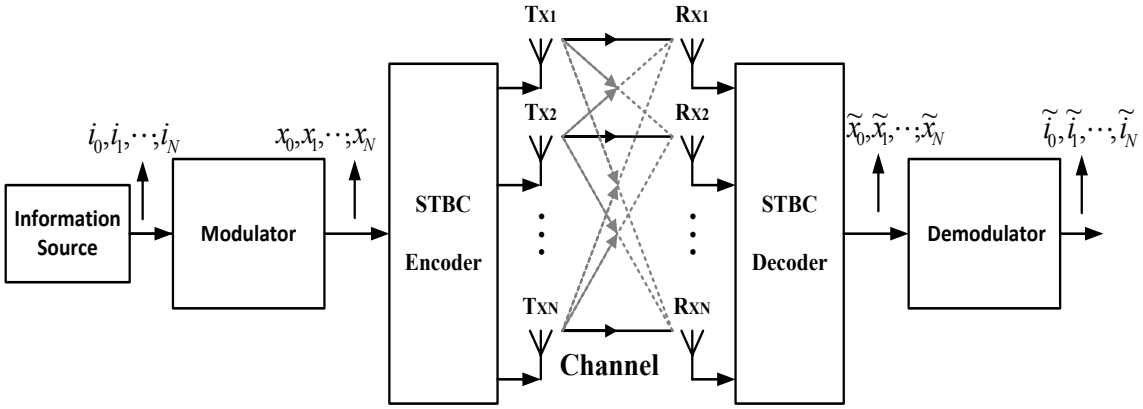

Figure 2-7 Generalised STBC Block diagram

However, the major limitation of the STBC scheme is that full rate codes (i.e., $R_{STBC} = 1$) exist only for up four antennas, if real signalling is employed and for up to two antennas, and if complex signal constellations are used [50]. This limitation can be overcome by sacrificing the orthogonality of the code in order to increase its rate: quasi-orthogonal space-time block codes [51]. The resulting loss in diversity may be avoided by constellation rotation, which however requires more complex receiver architectures [52]. Space-time block coding schemes may equivalently be used along the frequency domain, for example in Orthogonal Frequency Division Multiplexing (OFDM) based systems [53]. Due to their implementation simplicity, STBC are very attractive for improving link reliability in situations where the transmitter is equipped with multiple antennas.

Space-Time Trellis Codes

Space-Time Trellis Codes (STTC) [54] does not only provide diversity gain like STBC, but provides additional coding gain by using Trellis encoding instead of a repetition coding at the transmitter. The major limitation of STTC transmit strategy is that it requires complex receiver architectures based on Maximum Likelihood Sequence Estimation (MLSE). This fact renders STTC some-what less attractive for practical implementation than STBC.

Beamforming

Beamforming [55] can be used to directly address the most dominant eigenmode of the channel provided that the instantaneous Channel State Information (CSI) is available at the transmitter. The array gain of the transmitter can be exploited in addition to the diversity gain of the beamforming MIMO transmit strategy. Again, MRC based receiver structures are sufficient to achieve good performance. This strategy is particularly attractive in very low mobility scenarios, where CSI of sufficient quality can be made available to the transmitter at relatively low overhead, and the beam steering vectors have to be updated only infrequently.

2.4.2 Spatial Multiplexing Schemes

Spatial Multiplexing is more attractive in scenarios where the main goal of a wireless communication system design is to achieve a high spectral efficiency and consequently high data rates. This can be achieved by simultaneously transmitting multiple data streams in parallel over the multiple antennas [56]. This strategy is particularly appealing whenever sufficient time and frequency diversity is available, in order to make up for the loss in spatial diversity (when compared to the diversity schemes discussed above).

Bell Labs Layered Space-Time transmission

The Bell Labs Layered Space-Time (BLAST) transmission architecture was first proposed by J. Foschini for a spatial multiplexing scheme for multiple antennas systems to take advantage of the promising capacity of MIMO channels [7]. It achieves high spectral efficiencies by simultaneously spatially multiplexing coded or uncoded data symbols over fading MIMO channels. The main idea behind the BLAST scheme is the use of an appropriate encoding scheme at the transmitter side in order to achieve good performance when using only suboptimal detection schemes at the receive end i.e., the interference cancellation based detection schemes.

There are two different versions of the BLAST scheme. These are the Vertical BLAST (V-BLAST) [27] and the Diagonal BLAST (D-BLAST) [7]. Both schemes de-multiplex the bit streams into N_t substreams and separately encode, interleave and modulate these streams. In the case of V-BLAST, the bit streams are mapped one-by-one onto each of the transmit antennas. This transmit strategy is sometimes also referred to as Per-Antenna Rate Control (PARC) [57]. Multi-level coding approaches [58] can be thought of as an extension of this scheme, where multiple data streams are transmitted per antenna. It is important to point out that none of the bit streams transmitted using the scheme benefit from the available transmit diversity.

In contrast to the V-BLAST scheme, the D-BLAST exploits the available transmit diversity by transmitting each bit stream in a time-delayed "diagonal" fashion over *all* transmit antennas. Another important difference between the V-BLAST and the D-BLAST is that the layers of the V-BLAST can be coded or uncoded, while the D-BLAST can be used only with coded layers. However, the disadvantage of the D-BLAST is the requirement for an initializing phase at the beginning of each transmission burst. This results in reduced achievable spectral efficiency.

While not requiring instantaneous knowledge of the channel transfer function at the transmitter, both schemes rely on the appropriate assignment of the data rates to the different streams, in order to enable a correct functioning of the interference cancellation based receiver. In order to do this allocation correctly, it is preferable to have at least some statistical knowledge of the channel available at the transmitter. Figure 2-8 shows a block diagram of the V-BLAST architecture. The received signals at each receive antenna is a superposition of M faded symbols plus Additive White Gaussian Noise (AWGN).

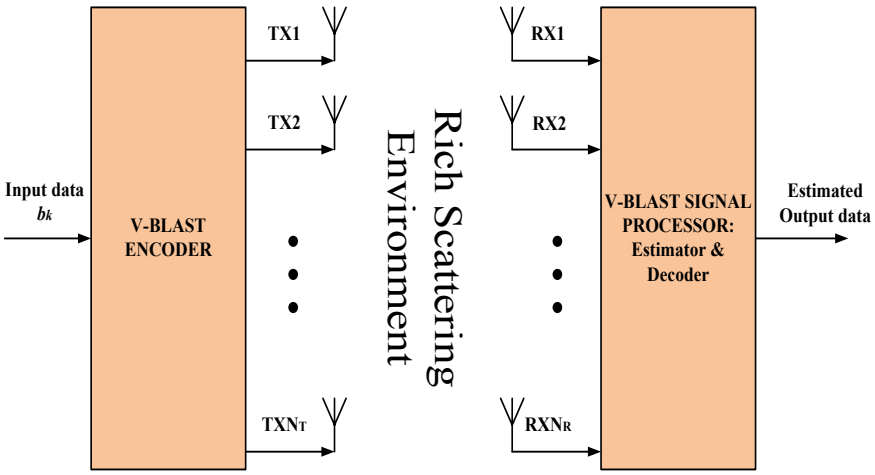

Figure 2-8 Generalised VBLAST Architecture

The transmission of signals is described as follows. A data stream is de-multiplexed into N_t sub-streams, also referred to as layers. For D-BLAST, at each transmission time, the layers circularly shift across the N_t transmit antennas resulting in a diagonal structure across space and time. Unlike the D-BLAST, the layers of the V-BLAST are arranged horizontally across space and time and the cycling operation is removed before transmission. At the receiver, as mentioned previously, the received signals at each receive antenna is a superposition of N_t faded symbols plus AWGN. Although the layers are arranged differently for the two BLAST systems across space and time, the detection process for both systems is performed vertically for each received vector.

Bit Interleaved Coded Modulation

Bit Interleaved Coded Modulation (BICM) [59] consist of a sequence of encoded, interleaved, modulated information and the resulting single symbol stream is then directly mapped onto the transmit antennas. It is a transmit strategy with very low complexity and no channel knowledge is required at the transmitter side. However, due to the non-orthogonality of the MIMO channel, a significant amount of processing is required at the receiver side in order to achieve performance close to channel capacity.

SVD MIMO

Singular Value Decomposition (SVD) MIMO [57]-[60], also known as eigenmode signalling, can be used if instantaneous channel knowledge of sufficient quality is available at the transmitter. The SVD of the channel transfer matrix is used to couple the transmit data directly into and out of the eigenmodes of the channel. The signal processing load is balanced between transmitter and receiver, as the different data streams can be demodulated individually at the receiver side. This requires substantially less processing effort at the receiver than for BICM or BLAST-like schemes. The data rates on the individual eigenmodes can be chosen such that the channel is not overloaded, in order to avoid outage events. Additionally, water filling can be used at the transmitter side, in order to maximize the achievable data rate subject to the given transmit power constraint. However, the additional gains are often not substantial at high Signal-to-Noise Ratio (SNR) in high diversity environments [57].

Diversity-Multiplexing Schemes

There are several situations where it is attractive to combine the benefits of diversity gain and multiplexing gain. This can for example be the case when the number of significant eigenmodes of the channel is lower than the number of transmit antennas, e.g. in the presence of high correlation or in a downlink scenario where the number of antennas at the base station exceeds the number of antennas at the user terminal. In 4G wireless communications, the main emphasis is on obtaining significant gains in overall system capacity and improved spectral efficiency which can be achieved by deploying the optional advanced antenna systems (AAS) [49]. Since diversity is such an important resource, a wireless system typically uses different diversity schemes.

Linear Dispersion Codes

Linear Dispersion Codes (LDC), belong to a class of space-time or space-frequency codes which are defined by linear generator matrices [61]. Examples of special members of this family include STBC, BICM and BLAST. The concept of LDC is to linearly superimpose multiple space-time encoded data streams (strata). The main advantage is that the number of strata may be chosen arbitrarily. However, there is no extra benefit of increasing the number of strata beyond the number of eigenmodes of the channel. The space-time coding can be designed such that all data streams can exploit the full spatial diversity offered by the channel. Examples of LDC include Multi-Stratum Space-Time Codes (MSSTC) [62] and Multi-Stratum Permutation Codes (MSPC) [63]. Like the BLAST schemes, data rates on individual strata should be chosen to ensure achievement of good performance when using suboptimal detection schemes such as the interference cancellation based receiver architectures. Otherwise, close-to-optimum tree search based schemes have to be used to achieve good performance instead [64].

2.5 Diversity Gain

Multiple-antenna channels provide spatial diversity, which can be used to improve the reliability of the link [65]. Diversity schemes play a crucial role in MIMO wireless systems in combatting fading and co-channel interference as well as avoiding error bursts. The premises behind diversity gain is that individual channels experience different levels of fading and interference. By sending signals that carry the *same* information through different paths with different characteristics, multiple independently faded replicas of the same signal are received at the receiver. These versions of the same signal are then combined in the receiver. The ultimate result is that the probability that all the signal components fade simultaneously is reduced. Hence, the reliability of the link is increased, thus leading to improved quality of

service (QoS). It has been shown in [66] that the probability of error at high SNR, averaged over the fading gain as well as the additive noise is:

$$P_e(\text{SNR}) \approx \frac{1}{4} SNR^{-1} \tag{2-1}$$

for uncoded binary phase-shift keying (PSK) signals over a single-antenna fading channel. By equipping the receiver with two antennas and transmitting the same signal, the error probability decreases to [66]:

$$P_e(\text{SNR}) \approx \frac{3}{16} \text{SNR}^{-2} \tag{2-2}$$

The error probability decreases with the exponent of the SNR as can be seen in (2-2). Here, the error probability decreases at a faster rate of $\frac{3}{16}\text{SNR}^{-2}$. The exponent (2) is called the diversity gain D_g of the MIMO system. Thus the performance gain at high SNR is dictated by the exponent of the SNR, which in turn dictates the error probability [67]. The exponent depends on the *number* of independently faded channels over which the transmit signal propagates through. The generalised maximum (full) achievable diversity gain D_{max} of an $N_r \times N_t$ MIMO system is given by the number of independent eigenmodes of a MIMO channel, that is, the total number of independent signal paths that exist between the transmitter and receiver. This corresponds to the product of the number of receive antennas and transmit antennas. In general P_e decays at a rate of SNR^{-D_g} for a multiple antenna system as opposed to SNR^{-1} for a SISO system where $1 \leq D_g \leq D_{max}=N_R.N_t$. The *diversity gain* D_g of a MIMO system depends on the error probability P_e and is given by [67]:

$$\lim_{SNR \to \infty} \frac{\log P_e(\text{SNR})}{\log \text{SNR}} = -D_g \tag{2-3}$$

It is important noting that it is only the Bit Error Rate (BER) which improves due to diversity gain, and not the data rates as can be clearly seen in (2-3). In addition to improved BER, reduced fading can also offer an extra benefit, that is, increased link range. Diversity gain of a MIMO system can also be maximized by using appropriate Space Time Coding (STC) at the transmitter, thus providing the transmit MIMO signals with immunity to severe impairments caused by fading channels. Sensitivity to fading is reduced by the spatial diversity provided by multiple spatial paths which experience different levels of fade at a particular instant.

2.6 Spatial Multiplexing Gain

Whilst diversity gain is achieved by transmitting information through different paths with different characteristics, the spectral efficiency of a MIMO system can be increased by Spatially Multiplexing (SM) *several* data streams in the same frequency band. That is, SM provides high data rates by simultaneously transmitting independent data streams over different spatial channels. Increased capacity is achieved by introducing additional spatial channels that are exploited by using STC at the transmitter. Here, a high rate stream is split or de-multiplexed into a number of sub-streams with lower rates. Each of the sub-streams is mapped to each transmit antenna and then transmitted simultaneously in the same frequency channel.

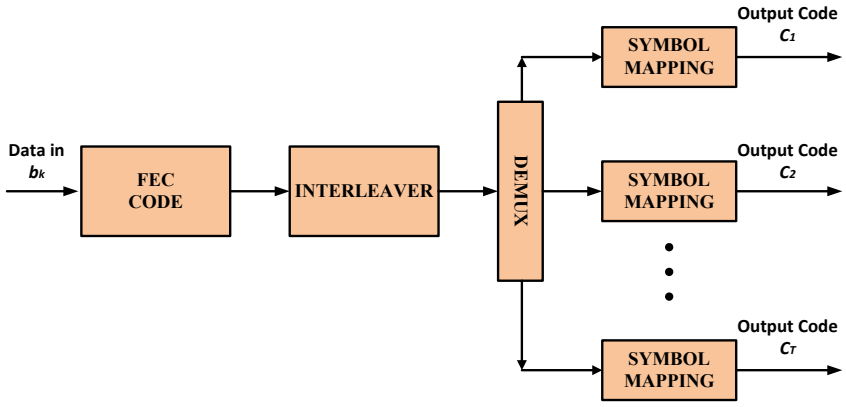

Figure 2-9 Example of MIMO System Multiplexing Structure

The ergodic capacity of a block-fading MIMO channel is [67]:

$$C(\text{SNR}) = \varepsilon\left[\log\det\left(\text{I} + \frac{\text{SNR}}{m}\mathbf{H}\mathbf{H}^{\dagger}\right)\right] \quad \text{(b/s/Hz)} \tag{2-4}$$

$$C(\text{SNR}) = \min\{m,n\}\log\frac{\text{SNR}}{m} + \sum_{\text{i}=|m-n|+1}^{\max\{m,n\}} \varepsilon[\log\chi_{2\text{i}}^2] + 0(1) \quad (\text{b/s/Hz}) \tag{2-5}$$

where χ_{2i}^2 is chi-square distributed with n degrees of freedom, $m = N_t$ and $n = N_r$. In contrast to single-antenna system, the channel capacity increases with SNR as $\min\{m,n\}$ log SNR (b/s/Hz) at high SNR. The implication of equations (2-5) is that MIMO channels can be viewed as $\min\{m,n\}$ independent parallel SISO channels or *spatial channels* between the transmitter and the receiver, where $\min\{m,n\}$ is the total *number of degrees of freedom* for communication. The *spatial multiplexing gain of a MIMO system depends on the data rate* $R_d(\text{SNR})$ and is given by [67]:

$$\lim_{\text{SNR}\to\infty}\frac{R_d\,(\text{SNR})}{\log\,(\text{SNR})} = S_g \tag{2-6}$$

The main feature of SM is that it exploits rich scattering channels to increase multiplexing gain of the system by transmitting independent information symbols in parallel through the spatial channels. This phenomenon is referred to as *spatial multiplexing*.

However, the bottleneck of SM system lies at receivers: the decoding complexity becomes a challenging problem when the number of transmit and receive antennas and the size of modulation constellations increases [68]. The solution to this problem lies in the design of optimal or near-optimal detectors at the receiver.

2.7 The diversity gain vs. multiplexing gain

Traditionally, multiple antennas have been used to increase diversity to combat channel fading as discussed in Section 2.1. Each pair of transmit and receive antennas provides independent channels for signals from the transmitter to the receiver [69]. As discussed in Sections 2.5 and 2.6, the spatial diversity offered by the wireless channel may be exploited in two different ways: to improve link reliability and increase the spectral efficiency. However,

Zheng and Tse showed in [67] that there exists a fundamental trade-off between the two, rendering it impossible to maximize both at the same time.

First, let the spatial multiplexing gain S_g of a system be defined as [67]:

$$S_g = \lim_{\mathrm{SNR} \to \infty} \frac{R_d\,(\mathrm{SNR})}{\log\,(\mathrm{SNR})} \tag{2-7}$$

where R_d is the transmission rate of the system, i.e., the system data rate. The multiplexing gain is upper bounded by the maximum number of parallel sub-channels opened up by the MIMO system, i.e., the number of eigenmodes with non-zero gain. It thus cannot exceed the minimum of the number of transmit and receive antennas: hence, $S_g = \min\{N_t, N_r\}$.

Link reliability is inherently coupled to the fading statistics of the channel, more precisely the number of independent channel realizations over which the signal propagates through. The spatial diversity gain D_g of a system can be defined as [67]:

$$D_g := -\lim_{\mathrm{SNR} \to \infty} \frac{\log\{P_e\,(\mathrm{SNR})\}}{\log(\mathrm{SNR})} \tag{2-8}$$

where the probability of error P_e depends on the transmission rate R_d. It is important to note here that R_d increases with SNR, as implied by the achieved multiplexing gain S_g. The maximum achievable diversity gain of a MIMO system is then given by the number of independent links present in a MIMO channel, i.e., the product of the number of transmit and receive antennas: $D_{max} = N_t . N_r$. The results presented in [67] show that it is not possible to maximise the diversity gain and the spatial multiplexing gain at the same time, i.e., an increased diversity gain will inevitably result in a smaller multiplexing gain.

Figure 2-10 shows a plot of the trade-off between the spatial multiplexing gain and diversity gain of a MIMO system. It can be clearly seen that for a system aiming to maximize the diversity gain, the spatial multiplexing gain S_g will approach zero. Conversely, for a scheme

operating within a constant offset of the full MIMO capacity at any given SNR, the diversity gain will approach zero.

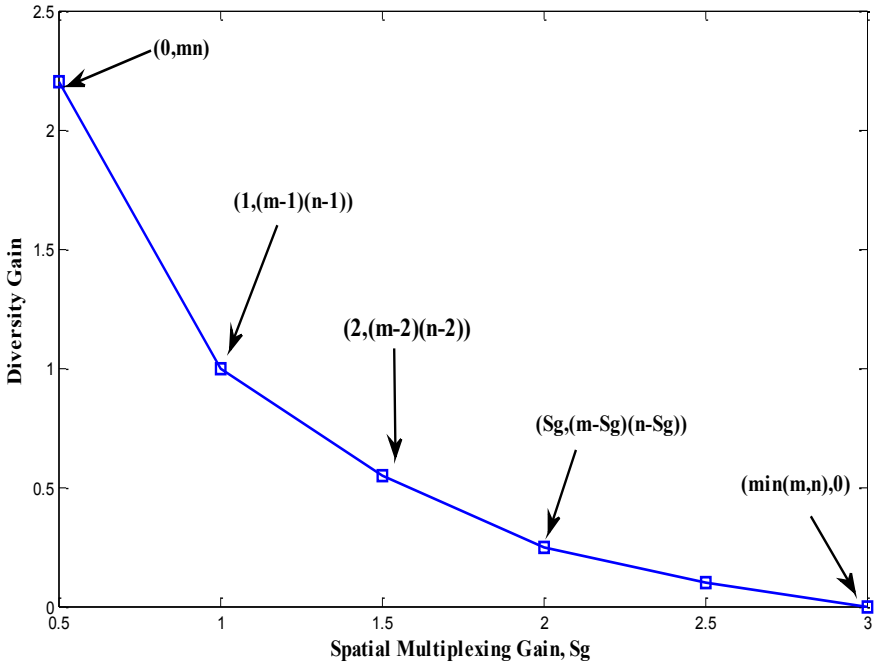

Figure 2-10 Spatial Multiplexing Gain Diversity trade-off

The error probability will no longer decrease with increasing SNR. Therefore a trade-off between the two has to be made to achieve optimal performance of a MIMO system.

2.8 MIMO Capacity and Channel Coding Schemes

In his seminal paper of 1948, Shannon introduced the concept of channel capacity as the maximum rate at which information can be reliably transmitted over a channel [1]. This concept stemmed from the fact that the probability of error asymptotically approaches zero as the duration of transmission tends to infinity. Given the discrete time transmission model:

$$\mathbf{y} = \mathbf{x} + \mathbf{n} \tag{2-9}$$

where $\mathbf{x}$ is the transmitted signal corrupted by some additive noise $\mathbf{n}$, resulting in the signal received as $\mathbf{y}$.

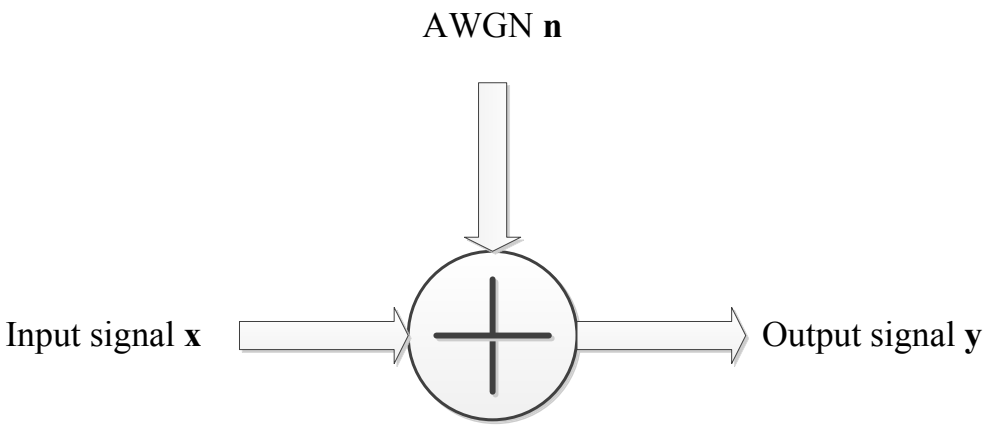

Figure 2-11 Discrete time transmission model

Figure 2-11 shows the given discrete time transmission model. The average mutual information $\boldsymbol{I}(\mathbf{x};\mathbf{y})$ (measure of mutual dependence of $\mathbf{x}$ and $\mathbf{y}$) between the channel input $\mathbf{x}$ and its output $\mathbf{y}$ which determines the rate for which error free transmission is possible is given by [70]:

$$\boldsymbol{I}(\mathbf{x};\mathbf{y}) = \mathbf{H}(\mathbf{x}) - \mathbf{H}(\boldsymbol{y}|\mathbf{x}) = \mathbf{H}(\boldsymbol{y}) - \mathbf{H}(\mathbf{x}|\boldsymbol{y}) \tag{2-10}$$

where $\mathbf{H}(\cdot)$ is the Shannon or marginal entropy and $\mathbf{H}(\cdot\,|\,\cdot)$ is the conditional entropy. The channel capacity is obtained by maximizing $\boldsymbol{I}(\mathbf{x};\mathbf{y})$ over the choice of the input alphabet distribution $p(\mathbf{x})$. For the AWGN channel with complex noise, it is achieved by choosing $\mathbf{x}$ to be zero mean independent identically complex Gaussian distribution, and is given by:

$$C_{AWGN} = \max_{p(x)} \boldsymbol{I}(\mathbf{x};\mathbf{y}) = \log_2 \det(1 + E_s/N_0\,) \text{ Bits/channel use} \tag{2-11}$$

where the result has been normalized to the channel bandwidth used for communication and E_s/N_0 is a measure of the SNR at the receiver.

2.8.1 Capacity-approaching codes

The transmission of a codeword $\mathbf{x} \in \mathbf{C}$ over an AWGN impaired channel can be modelled by equation (2-9). The task of the decoder is to recover the codeword which was transmitted with highest probability, given the received sequence $\mathbf{y}$ and the knowledge of the set of valid

codewords $\mathbf{C}$. This problem is known as Maximum A Posteriori Probability (MAP) decoding and can be stated as:

$$\mathbf{x} := \underset{\mathbf{x}\in\mathbf{C}}{arg\,max}\ P(\mathbf{x}|\mathbf{y}) = \underset{\mathbf{x}\in\mathbf{C}}{arg\,max}\frac{p(\mathbf{y}|\mathbf{x}).P(\mathbf{x})}{p(\mathbf{y})} = \underset{\mathbf{x}\in\mathbf{C}}{arg\,max}\, p\big((\mathbf{y}|\mathbf{x}).P(\mathbf{x})\big) \tag{2-12}$$

where the first equality follows from the application of Bayes' theorem and the second from the fact that the normalization factor $p(\mathbf{y})$ has no impact on the optimization problem. Assume that the codewords $\mathbf{x}$ are chosen from $\mathbf{C}$ with equal probability, $P(\mathbf{x}) = \frac{1}{|\mathbf{C}|}$, the MAP decoding reduces to the Maximum Likelihood (ML) decoding problem:

$$\hat{\mathbf{x}} = \underset{\mathbf{x}\in\mathbf{C}}{arg\,max}\, p(\mathbf{y}|\mathbf{x})\frac{1}{|\mathbf{C}|} = \underset{\mathbf{x}\in\mathbf{C}}{arg\,max}\, p(\mathbf{y}|\mathbf{x}) = \cdots = \underset{\mathbf{x}\in\mathbf{C}}{arg\,min}\, d(\mathbf{y},\mathbf{x}) \tag{2-13}$$

where $d(\mathbf{y},\mathbf{x})$ is an appropriate distance metric (e.g., the Hamming distance in the case of a Binary Symmetric Channel (BSC)) and the Euclidean distance in the case of an AWGN channel [71]. The goal of the detection problem is to find codes and an associated decoding algorithm which allow to solve (2-13) at manageable complexity, preferably at fixed or reduced cost per transmitted bit. However, the ML decoding problem has been shown to be NP-complete for the case of binary linear block codes transmitted over the BSC, which at least strongly suggests that (2-13) cannot be solved in polynomial time by any "straightforward" decoding algorithm for a linear block code of arbitrary structure.

The first major step in approaching the Shannon bound with practical coding schemes was the invention of Low Density Parity Check (LDPC) codes by Robert Gallagher in 1961 [72]. Although his idea was very progressive and forward-looking, it was either ignored or was given little attention, apart from the work of R. Michael Tanner [73] who published a paper describing a graphical method for representing LDPC codes in 1981, see Figure 2-12.

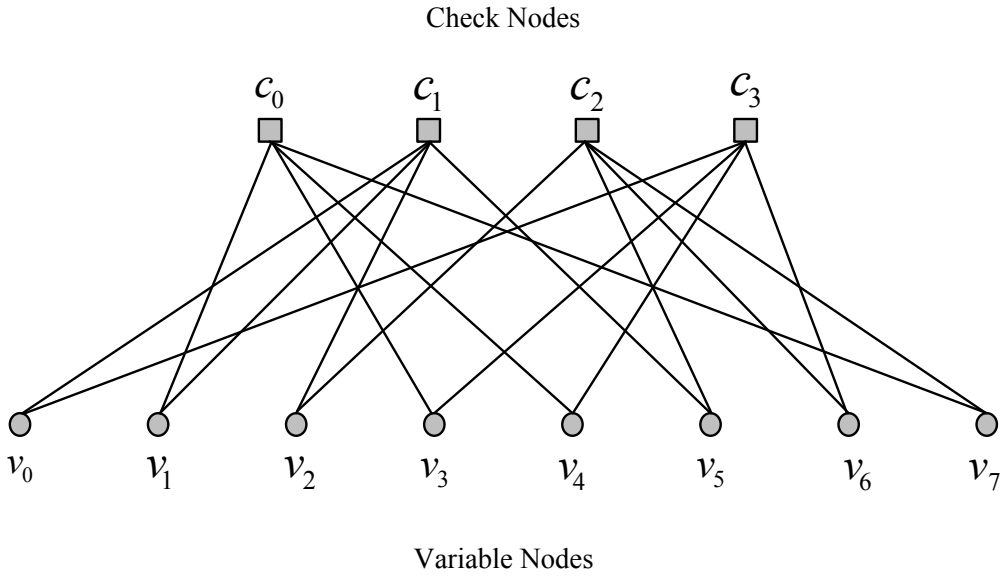

Figure 2-12 Graphical Representation of LDPC Codes

Gallagher's codes were characterized by a parity check matrix in which each row has exactly n_r and each column has exactly n_c non-zero elements, where n_r and n_c are small positive integers. As the block length gets large, the code can be described by a sparse matrix, or equivalently by sparsely connected graph [73] whose structure is given implicitly by the definition of the code. This crucial innovation involved the design of the code such that the decoding problem can be broken down into a set of smaller (but interdependent) sub-problems. Each of these sub-problems is solved individually by some processing nodes, taking into consideration probabilistic feedback from neighbouring nodes in its decision. In order to avoid the nodes' complexity to grow with the block length, the number of adjacent nodes must be independent of the codeword size.

LDPC codes were largely forgotten for about 30 years after their discovery, until the invention of sparse graphs [73] and iterative decoding based turbo codes by Claude Berrou, Alain Glavieux [74] and Punya Thitimajshima in 1993. This sparked a revived interest in the design of more powerful coding schemes and LDPC codes were finally rediscovered by MacKay and Neal some years later [75]. Since then, it has been a major research topic in

coding theory, resulting in various refinements and improvements. LDPC codes will be employed in this work in order to boost the performance of the sphere detector.

2.8.2 MIMO channel capacity

The main goal of a MIMO system is to increase the capacity of the wireless communication system. The capacity of the MIMO system is linked to the mutual information between the transmitter and the receiver. For a MIMO system with a fixed channel matrix **H** which is perfectly known at the receiver, the mutual information between transmitter and receiver can be described by equation (2-14)[33],[70], [76]:

$$\boldsymbol{I}(\mathbf{x};\mathbf{y}) = H(\mathbf{y}|\mathbf{x}) = H(\mathbf{y}) - H(\mathbf{n})$$

$$= \log_2 \det\left(\pi e \boldsymbol{\psi}_{\mathbf{yy}}\right) - \log_2 \det\left(\pi e \boldsymbol{\psi}_{\mathbf{nn}}\right) = \log_2 \det\left(\boldsymbol{\psi}_{\mathbf{yy}} \boldsymbol{\psi}_{\mathbf{nn}}^{-1}\right)$$

$$= \log_2 \det\left((\boldsymbol{\psi}_{\mathbf{nn}} + \mathbf{H}\boldsymbol{\psi}_{\mathbf{xx}}\mathbf{H}^{\mathbf{H}})\boldsymbol{\psi}_{\mathbf{nn}}^{-1}\right) = \log_2 \det\left(\mathbf{I}_{N_R} + \mathbf{H}\boldsymbol{\psi}_{\mathbf{xx}}\mathbf{H}^{\mathbf{H}}\boldsymbol{\psi}_{\mathbf{xx}}^{-1}\right). \quad (2\text{-}14)$$

where $\boldsymbol{\psi}_{\mathbf{yy}}$ is the receive covariance matrix and $\mathbf{I}_{N_R}$is the identity matrix. The channel capacity of a MIMO system for a given channel matrix **H** can be achieved by maximizing the mutual information $\boldsymbol{I}(\mathbf{x};\mathbf{y})$ over the possible choices of input distributions $p(\mathbf{x})$, subject to the transmit power constraint $\mathrm{tr}\{\boldsymbol{\psi}_{\mathbf{xx}}\} \leq E_s$ [70]. Assuming the availability of perfect *CSI* at the transmitter, the MIMO channel can be regarded as a set of several parallel *SISO* channels by using **SVD** at both the transmitter and receiver. Multiplying the received signal with the conjugate transpose of the left singular vectors $\mathbf{U}^{\mathbf{H}}$ yields:

$$\tilde{\mathbf{y}} = \mathbf{U}^{\mathbf{H}}\boldsymbol{y} = \mathbf{U}^{\mathbf{H}}(\mathbf{U}\sum\mathbf{V}^{\mathbf{H}})\mathbf{x} + \mathbf{U}^{\mathbf{H}}\boldsymbol{n} = \mathbf{I}\sum\mathbf{V}^{\mathbf{H}}\mathbf{x} + \tilde{\mathbf{n}} \quad (2\text{-}15)$$

This operation does not affect the mutual information as it is invertible and thus leads to:

$$\boldsymbol{I}(\mathbf{x};\tilde{\mathbf{y}}) = \log_2 \det\left(\mathbf{U}^{\mathbf{H}}\boldsymbol{\psi}_{\mathbf{yy}}\mathbf{U}\mathbf{U}\boldsymbol{\psi}_{\mathbf{nn}}^{-1}\mathbf{U}^{\mathbf{H}}\right) = \log_2 \det\left(\boldsymbol{\psi}_{\mathbf{yy}}\boldsymbol{\psi}_{\mathbf{xx}}^{-1}\right) = I(\mathbf{x};\mathbf{y})$$

$$= \log_2 \det\left(\mathbf{I}_{N_T} + \mathbf{V}^{\mathbf{H}}\boldsymbol{\psi}_{\mathbf{xx}}\mathbf{V}\boldsymbol{\Sigma}^{H}\mathbf{U}^{\mathbf{H}}\boldsymbol{\psi}_{\mathbf{nn}}^{-1}\mathbf{U}\boldsymbol{\Sigma}\right) \quad (2\text{-}16)$$

For simplicity the assumption made is that $\boldsymbol{\psi}_{\mathbf{nn}} = N_0\mathbf{I}_{N_R}$, i.e., $\boldsymbol{\psi}_{\mathbf{nn}}$ is made up of independent identically distributed noise samples at the receiver. $\boldsymbol{\psi}_{\mathbf{nn}}$ will be referred to as *spatially white noise* in this scenario. The last terms in (2-16) then become $1/N_0\boldsymbol{\Sigma}^{\mathbf{H}}\boldsymbol{\Sigma}$, which is diagonal. To maximise the mutual information, $\boldsymbol{\psi}_{\mathbf{xx}}$ is chosen such that $\widetilde{\boldsymbol{\psi}}_{\mathbf{xx}} = \mathbf{V}^{\mathbf{H}}\boldsymbol{\psi}_{\mathbf{xx}}\mathbf{V}$ is diagonal as well [33] and that the transmit power constraint is met with equality ($tr\{\boldsymbol{\psi}_{\mathbf{xx}}\} = E_s$). This can be achieved by using the matrix of right singular vectors $\mathbf{V}$ for precoding at the transmitter, which leaves the transmit power unchanged. *Spatially coloured noise*($\boldsymbol{\psi}_{\mathbf{nn}} \neq N_0\mathbf{I}_{N_R}$) is comprehensively covered in [77].

The Closed loop MIMO channel capacity

The capacity of a MIMO system can be improved by exploiting the channel state information available to the transmitter through a closed-loop signalling system. The closed loop MIMO channel capacity and the spatially white receiver noise can thus be expressed as follows:

$$C_{\mathrm{MIMO}}^{\mathrm{CL}}(\mathbf{H}) = \log_2 \det\left(\mathbf{I}_{N_t} + \widetilde{\boldsymbol{\psi}}_{\mathbf{xx}}\boldsymbol{\Sigma}^{\mathbf{H}}\mathbf{U}^{\mathbf{H}}\boldsymbol{\psi}_{\mathbf{nn}}^{-\mathbf{1}}\mathbf{U}\boldsymbol{\Sigma}\right) = \sum_{k=1}^{\boldsymbol{\Sigma}} \log_2\left(1 + \sigma_{k,k}^2 \frac{[\widetilde{\boldsymbol{\psi}}_{\mathrm{x,x}}]_{k,k}}{N_0}\right) \qquad (2\text{-}17)$$

where $\boldsymbol{\Sigma}$ is the number of non-zero eigenvalues of the Gram matrix $\mathbf{H}^{\mathrm{H}}\mathbf{H}$. The capacity can be maximized by using iterative water-filling [33] to determine the diagonal entries of $\widetilde{\boldsymbol{\psi}}_{\mathbf{xx}}$, subject to the transmit power constraint tr $\{\widetilde{\boldsymbol{\psi}}_{\mathbf{xx}}\} = E_s$.

The Open loop MIMO channel capacity

Consider now the open loop case where no CSI is available at the transmitter. The optimal transmit covariance matrix is given by $\widetilde{\boldsymbol{\psi}}_{\mathbf{xx}} = E_S/N_t\mathbf{I}_{N_t}$ [33]. By using similar derivations as for closed-loop case, the open-loop capacity can be shown to be:

$$C_{\mathrm{MIMO}}^{\mathrm{OL}}(\mathbf{H}) = \log_2 \det\left(\mathbf{I}_{N_t} + \frac{E_S}{N_t}\boldsymbol{\Sigma}\boldsymbol{\Sigma}^{\mathbf{H}}\mathbf{U}^{\mathbf{H}}\boldsymbol{\psi}_{\mathbf{nn}}^{-\mathbf{1}}\mathbf{U}\right) = \sum_{k=1}^{E} \log_2\left(1 + \sigma_{k,k}^2 \frac{E_S/N_t}{N_0}\right) \qquad (2\text{-}18)$$

where the last equality is again for the case of spatially white receiver noise.

It can be clearly seen that the expressions for the closed-loop and open-loop case are very similar in the sense that both $\boldsymbol{\Sigma}$ parallel data streams can be simultaneously transmitted in parallel, thus resulting in improved spectral efficiency compared to SISO systems since the MIMO capacity scales as $C_{\mathrm{MIMO}}(\mathbf{H}) \propto \boldsymbol{\Sigma}.\mathrm{Log}_2(\mathrm{SNR})$ in the limit for high SNR. The only difference lies in the power allocation: systems exploiting CSI at the transmitter can achieve capacity gains whenever the optimal transmit power allocation deviates from a uniform distribution. This is the case for the low to medium SNR regime/or when the (average) eigenvalue spread is high.

The Outage and Ergodic MIMO channel capacity

Consider now the case where **H** is not fixed, but a random variable as will be the case for essentially all practical applicants. In this case, the channel capacity will not only depend on the SNR, but will also depend on the channel statistics, in contrast to the AWGN case. More specifically, it will be a function of the number of observed realizations of **H** and the distribution of the singular values of **H**. The terms *MIMO Outage Capacity (MOC)* will be used to denote the scenario whenever transmission takes place over a certain fixed number N_s of independent realizations **H**. The outage capacity $C_{MOC}(N_s, P_e)$ is the maximum rate at which communication is possible with a probability of transmission error no higher than P_e:

$$C_{MOC}(N_s, P_e) = \left\{R: \Pr\left(\frac{1}{N_s}\sum_{n=1}^{N_s} C_{\mathrm{MIMO}}(\mathbf{H}_n) < R\right) \leq P_e\right\} \tag{2-19}$$

Likewise, the terms *Ergodic MIMO Capacity* (EMC) will be used to denote the scenario where the transmission interval is long enough to observe the full channel statistics. At rates up to C_{EMC}, communication will be possible with vanishing probability of error as the length of the transmission interval tends to infinity. The probability of errors is strictly greater than zero at higher rates. The ergodic capacity can be expressed as:

$$C_{EMC} = \lim_{N_s \to \infty} C_{MOC}(N_s, 0) = \varepsilon\{C_{\mathrm{MIMO}}(\mathbf{H})\} \tag{2-20}$$

Closed form expressions for C_{EMC} has already been derived by Telatar [33] under the assumption of uncorrelated fading and perfect CSI at the receiver but no CSI at the transmitter. These were recently extended to the case of correlation at transmitter and/or receiver by Kiessling [77]. Telatar [33] also derived outage capacity results for the case of a single antenna at transmitter or receiver, i.e., for *SIMO* and *MISO* systems. The case of multiple antennas at transmitter and receiver was later addressed by Foschini and Gans [78]. In practice, the channel state information, i.e., the realization of **H** has to be learned by the receiver. The pilot overhead required to estimate all $N_t.N_r$ sub-channels lowers the potential gains of MIMO systems. This issue was first studied by Marzetta and Hochwald [79]. They showed that as the channel's coherence time becomes shorter, there will be no further capacity gain from increasing the number of transmit antenna beyond a critical point. The capacity of MIMO schemes using training based channel estimation was derived by Hassibi and Hochwald [80].

2.8.3 MIMO System Setup and Assumptions

The following system setup will be assumed throughout this thesis unless stated otherwise. MIMO signals will be transmitted in blocks of data over MIMO channels. MIMO transmission will be achieved by employing N_t antennas at the transmitter and N_r antennas at the receiver. An information source produces stream of bits $\mathbf{x} \in \chi^{N_t}$ of independent identically distributed (i.i.d.) information bits which will be subsequently encoded using LDPC codes of code rate $R_C = {}^{K}/_{N}$. The coded bits will then be interleaved resulting in the generation of the code word $\boldsymbol{e} \in \mathcal{C} \subset \mathbb{F}_2^{[K\times 1]}$ which is then divided into $N_{\mathbb{C}}$ blocks c_f, of $N_t \times L$ bits. L denotes the number of bits per modulated symbol resulting in $\mathbf{M} = 2^L$ different constellation points and f denotes time-frequency index. It will also be assumed that $f \in \{1, \ldots, N_{\mathbb{C}}\}$ specifies the time-frequency band used for transmission. Each vector c_f is finally mapped onto a vector transmit symbol $\mathbf{x} \in \mathbb{C}^{[N_t X\ 1]}$ whose components x_t are taken

from some complex signal $\mathbb{C}$. The analysis of the MIMO detectors will focus on non-selective or flat fading MIMO channels unless otherwise specified. It will also be assumed that transmitter and receiver are perfectly synchronized in time and frequency. After matched filtering and sampling at the receiver, the transmission at f can be represented by the following equivalent discrete-time complex-valued baseband model:

$$\boldsymbol{y}_f = \mathbf{H}_f \mathbf{x}_f + \mathbf{n}_f \tag{2-21}$$

where $y_f \in \mathbb{C}^{[N_r \times 1]}$ is the received signal, $\mathbf{H}_f \in \mathbb{C}$ (N_r x N_t) is the channel matrix, and $\mathbf{n}_f \in \mathbb{C}^{[N_r \times 1]}$ is the receiver noise. The entries of $\mathbf{y}_f$, $\mathbf{H}_f$ and $\mathbf{n}_f$ are zero-mean, circularly symmetric complex Gaussian random variables, and the entries $h_{i,j}$ of $\mathbf{H}_f$ are normalized to have unit variance. The average energy per transmit symbol $\mathbf{x}_f$ will be denoted by E_s. The corresponding average energy per bit will be denoted by E_b. The double-sided power spectral density of the complex noise (N_o/ 2 per real dimension) will be denoted by N_o. The Nyquist rate sampling of the real and imaginary parts of the received signal will be assumed, such that the signalling rate T_S and the sampling bandwidth $B = 1/T_S$. The signal-to-noise ratio is thus given by SNR = E_S/N_o. Furthermore, the covariance will be defined by $\sigma^2 = N_t N_o/E_S$. Unless stated otherwise, the transmit power will be assumed to be uniformly distributed over the transmit antennas ($\boldsymbol{\varphi}_{xx} = E_S/N_t \boldsymbol{I}_{N_t}$) and the noise to be spatially white ($\boldsymbol{\varphi}_{nn} = N_o \boldsymbol{I}_{N_r}$).

The state-of-the art Forward Error Correction (FEC) schemes namely LDPC codes will be employed for the purpose of performance evaluations in this thesis. A very high diversity scenario, where the codeword is transmitted over a large number of independent channel realizations will be considered. Binary Phase Shifting Keying (BPSK) and **M**-ary *Quadrature Amplitude Modulation (***M**-QAM*)* [66] constellations for transmission will be employed.

2.8.4 MIMO System description

Consider a symmetric MIMO system with N_t transmit and $N_r = N_t$ receive antennas. The transmitted vector symbols $\mathbf{x} = \left[x_1, x_2, \dots, x_{N_t}\right]^T$ drawn from a modulation constellation $\mathbf{A} = \left[a_1, a_2, \dots, a_{N_t}\right]$ at each instant are transmitted from each of the N_t transmit antennas. At the receiver, various detection schemes will be used to detect the received vector $\mathbf{y} \in \mathbb{C}^{[N_r \times 1]} = \left[y_1, y_2, \dots, y_{N_r}\right]^T$. For simplicity, the received signal will be expressed by the following linear model:

$$\mathbf{y} = \mathbf{Hx} + \mathbf{n} \tag{2-22}$$

where $\mathbf{n} \in \mathbb{C}^{[N_r \times 1]}$ is some Additive White Gaussian Noise (AWGN). $\mathbf{H} \in \mathbb{C}^{[N_r \times N_t]}$ is the lattice generating matrix whose entries describe the coupling between the j^{th} transmit and the i^{th}receive antenna. The components of **x, H** and **n** will be chosen to be zero-mean, circularly symmetric, complex Gaussian random variables.

Furthermore, the entries of **H** are normalized such that $E\left\{\left|h_{i,j}\right|^2\right\} = 1$, that is, each sub-channel is passive. The magnitudes $\left|h_{i,j}\right|$ follow a Rayleigh distribution, while the phases $\angle \mathrm{h}_{i,j}$ are uniformly distributed. Using a **QR** Decomposition, the channel matrix will be decomposed into the unitary matrices $\mathbf{Q} \in \mathbb{C}^{[N_r \times N_r]}$ and the upper triangular matrix $\mathbf{R} \in \mathbb{C}^{[N_t \times N_t]}$ composed of real, non-negative singular values. Let $\boldsymbol{\varphi}_{\mathbf{xx}} = \mathcal{E}\{\mathbf{x}\mathbf{x}^{\mathrm{H}}\}$ and $\boldsymbol{\varphi}_{\mathbf{nn}} = \mathcal{E}\{\mathbf{n}\mathbf{n}^{\mathrm{H}}\}$ denote the respective transmit and noise covariance matrix. $\boldsymbol{\varphi}_{\mathbf{nn}}$ must be positive definite and $tr\{\boldsymbol{\varphi}_{\mathbf{nn}}\} = N_r N_o$. With **n** and **x** independent, the covariance of the received signal **y** is thus given by $\boldsymbol{\varphi}_{\mathbf{yy}} = \boldsymbol{\varphi}_{\mathbf{xx}} \mathbf{H}^{\boldsymbol{H}} + \boldsymbol{\varphi}_{\mathbf{nn}}$ while the signal-to-noise ratio (SNR) per receive antenna is given by E_S/N_o. The overall task of the MIMO detector is to detect the most likely vector **x** that was transmitted based on prior knowledge of **y**, **H** and the statistics of **n**.

2.8.5 Equivalent Real-Valued MIMO System Model

The N_t-dimentional complex-valued system model described by equation (2-22) can be decomposed into an equivalent $2N_t$-dimentional real-valued system model. The premise behind the decomposition process is to separate real and complex variables. This is done by decomposing all complex variables into their real and imaginary parts and reads:

$$\begin{bmatrix} \Re\{\mathbf{y}_f^c\} \\ \Im\{\mathbf{y}_f^c\} \end{bmatrix} = \begin{bmatrix} \Re\{\mathbf{H}_f^c\} & -\Im\{\mathbf{H}_f^c\} \\ \Im\{\mathbf{H}_f^c\} & \Re\{\mathbf{H}_f^c\} \end{bmatrix} \begin{bmatrix} \Re\{\mathbf{x}_f^c\} \\ \Im\{\mathbf{x}_f^c\} \end{bmatrix} + \begin{bmatrix} \Re\{\mathbf{n}_f^c\} \\ \Im\{\mathbf{n}_f^c\} \end{bmatrix} \tag{2-23}$$

where $\boldsymbol{y}_f \in \mathbb{R}^{[N_{2r} \times 1]}$, $\mathbf{x}_f \in X = A^{[N_L \times 1]}$, $\mathbf{H}_f \in \mathbb{R}^{[N_{2r} \times N_L]}$, and $\mathbf{n}_f \in \mathbb{R}^{[N_{2r} \times 1]}$ with $N_{2r} = 2N_r$ and $N_L = 2N_t \times \Re\{\boldsymbol{y}_f^c\}$ and $\Im\{\boldsymbol{y}_f^c\}$ denote the real and imaginary parts of the complex signal $\boldsymbol{y}$ respectively. By introducing the **QR** decomposition, the estimate $\hat{\mathbf{x}}$ of the transmitted vector for such a MIMO system will be described by the equation:

$$\hat{\mathbf{x}} = \arg \min_{\mathbf{x} \in \chi} \|\hat{\boldsymbol{y}} - \mathbf{R}\mathbf{x}\|^2 \tag{2-24}$$

where $\hat{\boldsymbol{y}} = \mathbf{Q}^{\boldsymbol{H}}\boldsymbol{y}$, $\mathbf{H} = \mathbf{QR}$, $\mathbf{Q}$ is a unitary matrix and $\mathbf{R}$ is an upper triangular matrix as in Section 2.8.4. The different N_l components of $\mathbf{x}_f$ in the matrix $\mathbf{R}$ will be referred to as the *layers* of the transmit signal. The corresponding covariance matrices of the real valued signal and noise are both symmetric and described by:

$$\boldsymbol{\varphi}_{\mathbf{xx}} = \frac{1}{2}\begin{bmatrix} \Re\{\boldsymbol{\varphi}_{\mathbf{xx}}^c\} & -\Im\{\boldsymbol{\varphi}_{\mathbf{xx}}^c\} \\ \Im\{\boldsymbol{\varphi}_{\mathbf{xx}}^c\} & \Re\{\boldsymbol{\varphi}_{\mathbf{xx}}^c\} \end{bmatrix} \text{ and } \boldsymbol{\varphi}_{\mathbf{nn}} = \frac{1}{2}\begin{bmatrix} \Re\{\boldsymbol{\varphi}_{\mathbf{nn}}^c\} & -\Im\{\boldsymbol{\varphi}_{\mathbf{nn}}^c\} \\ \Im\{\boldsymbol{\varphi}_{\mathbf{nn}}^c\} & \Re\{\boldsymbol{\varphi}_{\mathbf{nn}}^c\} \end{bmatrix} \tag{2-25}$$

Since the components of $\mathbf{x}_f^c$ are taken from square **M**-QAM constellations, the entries of x_f can be equivalently drawn from A-ary *Amplitude Shift Keying (ASK)* constellations and can be written as $\mathbf{x} = a(k + ½) \in A$ where $k \in \{-A/2, \ldots, A/2-1\}$, $A = \sqrt{\mathbf{M}}$ and $a = \sqrt{\frac{6}{\mathbf{M}-1}}$ is the normalisation factor [64]. The transmit signal can hence be interpreted as a shifted finite *lattice* with orthonormal basis vectors, while the noiseless received signal can be seen as a subset of points belonging to a skewed infinite lattice defined by the *lattice generator matrix*

H. The task of all detection algorithms discussed in this thesis is to find the lattice point **Hx** with minimum or the shortest Euclidean distance to the received vector **y**, that is, to solve what is known as the *Integer Least Squares (ILS)* or *Closest Lattice Point Search (CLPS)* problem [16].

3. MIMO Detection Strategies

3.1 Introduction

The introduction of Multiple-Input Multiple-Output (MIMO) systems has opened up a new dimension for relieving the scarce radio frequency spectrum. It has been demonstrated that multiple antenna systems provide very promising gain in capacity without increasing spectrum and transmit power consumption, and at the same time less sensitive to fading channels [7]-[8]. However, the transmission of wireless signals over interference MIMO channels poses more serious challenges not previously present in the more traditional Additive White Gaussian Noise (AWGN) channels. In order to approach Shannon's capacity limit over MIMO channels, propagation impairment mitigation techniques need to be incorporated in channel coding and detection techniques.

The subject of signal detection for MIMO systems has become one of the major research topics in recent years [4]-[18]. Several detection techniques have been proposed in the literature. These include linear detectors such as the Zero Forcing (ZF), Minimum Mean Square estimation (MMSE) and non-linear detectors such as the Vertical Bell Labs Space Time (V-BLAST) methods [5]-[10]. The Maximum Likelihood (ML) is optimum in the sense that it minimizes the overall error probability and has been shown to be efficient in MIMO transmission setups where few transmit antennas and smaller constellations are employed [7].

However, the major drawback of the ML is its increased computational complexity (due to exhaustive search process) which renders it impractical for real-time implementation, particularly where a large number antennas and large constellation sizes are involved. Although the ML decoding algorithm is prohibitively complex for most practical applications, the theoretical analysis of the ML decoding allows performance prediction of suboptimal detection strategies. That is, it can be employed as a yardstick through which the

performance of other detectors can be measured against. Whilst the extent to which these detection schemes trade off performance with complexity varies, it will be assumed that they all share the idea that the effect of the channel matrix should be explicitly cancelled so that the receiver can effectively treat the MIMO channel as an AWGN channel.

In this chapter, MIMO detection schemes which include ML detector, linear and non-linear suboptimal detectors and the Lattice Reduction Aided Detection (LRAD) scheme are presented. The theoretical background of the ML and its variants is introduced in the first part of this chapter. This will be followed by a survey of suboptimal detection schemes based on the ZF, the MMSE, Successive Interference Cancellation (SIC) and the VBLAST in the second part of this chapter. Low Density Parity Check (LDPC) codes are proposed to reverse the performance offset introduced by the suboptimal detectors particularly the SIC where it will be used to stop error propagation. The third part of this chapter covers the LRAD scheme. The LRAD is proposed to transform the infinity ML lattice to finite LRAD lattice, with the main goal of reducing the complexity of the ML. It will be shown in Chapter 6 through simulation results that complexity reduction will be achieved at the expense of marginal performance degradation. The last part of this chapter introduces tree search based detection algorithms, which are the main focus of this thesis.

3.2 The ML Detector

For any given MIMO channel, the task of the receiver is to detect the transmitted signal $\mathbf{x}$ from the received signal $\mathbf{y} = \mathbf{Hx} + \mathbf{n}$. That is, the detector detects the most likely vector $\mathbf{x}$ that was transmitted based on prior knowledge of $\mathbf{y}$, $\mathbf{H}$, and the noise statistics $\mathbf{n}$. The received vector $\mathbf{y}$ is considered as a perturbed lattice point due to the Gaussian noise $\mathbf{n}$. The optimum ML detector makes decisions based on maximizing the posteriori probabilities, and hence minimizing the probability of an erroneous receiver decision on which message was

transmitted. This decision criterion is called maximum a posteriori (MAP) and is based on Bayes' decision rule which is given by [82]:

$$\mathbf{x} := \underset{\mathbf{x}\in\boldsymbol{\chi}}{arg\,max}\ P(\mathbf{y_m}|\mathbf{x_m}) = \underset{\mathbf{x}\in\boldsymbol{\chi}}{arg\,max}\frac{\boldsymbol{p(\mathbf{y_m}|\mathbf{x_m}).P(\mathbf{x})}}{\boldsymbol{p(\mathbf{y_m})}} = \underset{\mathbf{x}\in\boldsymbol{\chi}}{arg\,max}\, p\big((\mathbf{y_m}|\mathbf{x_m}).P(\mathrm{x}_m)\big) \quad (3\text{-}1)$$

where $p(\mathbf{y}_m|\mathbf{x}_m)$ is the conditional probability density function (p.d.f) of detecting the received (observed) signal vector ($\mathbf{y}$) given that $\mathbf{x}_m$ was transmitted, $P(\mathbf{y_m}|\mathbf{x_m})$ is the a priori probability (APP) of the m^{th}signal being transmitted give that $\mathbf{y_m}$was received, $m = 1,2,3,\dots,\mathbf{M}$ is the number of signals transmitted, $p(\mathbf{y})$ is the p.d.f of the received vector ($\mathbf{y}$) and can be stated as [82]:

$$p(\mathbf{y}) = \sum_{m=1}^{M} p(\mathbf{y}_m|\mathbf{x}_m).P(\mathbf{x}_m) \quad (3\text{-}2)$$

It can be clearly seen in equation (3-1) that the decision rule based on finding the signal that maximizes $P(\mathbf{y}_m|\mathbf{x}_m)$ is equivalent to finding the signal that maximizes $p(\mathbf{y}_m|\mathbf{x}_m)$. The conditional p.d.f $p(\mathbf{y}_m|\mathbf{x}_m)$ is called the likelihood function and the decision criterion based on maximizing $p(\mathbf{y}_m|\mathbf{x}_m)$ over the $\mathbf{M}$ signals (basis vector) is called the ML criterion [66]. Computations of $P(\mathbf{x}_m)$ can be simplified by working with natural logarithms. This translates the ML criterion to the detection problem that minimizes the Euclidean distance $d(\mathbf{x}_m, \mathbf{y})$from the received vector where:

$$d(\mathbf{x}_m, \mathbf{y}_m) = \sum_{k=1}^{N}\big(\mathbf{y}_k - \mathbf{x}_{m,k}\big)^2 \quad (3\text{-}3)$$

where $k = 1, 2, 3 \cdots N$ is the message size of the received signal. This is sometimes termed the minimum distance detection [66]. The ML criterion can be represented by two detection algorithms: Maximum Likelihood Sequence Detector and the MAP Detector.

3.2.1 Maximum Likelihood Sequence Detection

The Maximum Likelihood Sequence Detector (MLSD) yields the most likely transmitted sequence $\mathbf{x}$ by maximizing the APP, $P(\mathbf{x}|\mathbf{y})$, that $\mathbf{x}$ was transmitted given that $\mathbf{y}$ was received,

where **y** extends over the whole message, i.e., where the observed symbols are interdependent over the signal interval. The assumption made is that all possible transmitted sequences are equiprobably [21] and that the transmitted signal has memory [66].

Consider a symmetric MIMO system with N_t transmit and N_r receive antennas, where $N_t = N_r = N_c$. If the noise vector n_c in the complex-valued model consists of circularly symmetric complex Gaussian i.i.d. samples with covariance matrix $\varepsilon[n_c, n_c^T] = \sigma_{n,c}^2\mathbf{I}$, where **I** is the identity matrix, then the covariance matrix of the corresponding real noise vector $n = [\Re\{n_c^T\} - \Im\{n_c^T\}]^T$ is given as the $2N_c = N$-dimensional matrix $\varepsilon[nn^T] = \sigma_n^2\mathbf{I}$ with $\sigma_n^2 = \frac{1}{2}\sigma_{n,c}^2$ and real Gaussian per component. Given that the N-dimensional lattice generating matrix **H** and the transmitted vector $\mathbf{x}^{(m)} = \{x_1^m, x_2^m, \cdots, x_K^m\}$ are known where $k = 1,2,3, \ldots, K$ is the message size, the p.d.f of the received MIMO signal **y** can be, according to Bayes' decision rule, equivalently written as [6]:

$$p(\boldsymbol{y}|\mathrm{H}, \mathbf{x}) = \frac{1}{\left(2\pi\sigma_{\mathrm{n}}^2\right)^{N/2}} exp\left(-\frac{\|\mathbf{y}-\mathrm{H}\mathbf{x}\|^2}{2\sigma_{\mathrm{n}}^2}\right) \tag{3-4}$$

Therefore, the estimate for the transmitted vector can be approximated to:

$$\hat{\mathbf{x}} = arg\, max_{\mathbf{x}\in\boldsymbol{\chi}}\, p(\boldsymbol{y}|\mathrm{H}, \mathbf{x}) \tag{3-5}$$

where $\boldsymbol{\chi} \subset \mathbb{Z}^{2N}$ is an infinity lattice field and $\mathbb{Z}$ is the set of infinity integers. By substituting $\boldsymbol{p}(\boldsymbol{y}|\mathrm{H}, \mathbf{x})$ in (3-4) with (3-5), (3-5) can be written as:

$$\hat{\mathbf{x}} = arg\, max_{\mathbf{x}\in\boldsymbol{\chi}} \left\{ \frac{1}{\left(\boldsymbol{2\pi\sigma_n^2}\right)^{N/2}} exp\left(-\frac{\|\mathbf{y}-\mathbf{H}\mathbf{x}\|^2}{2\sigma_n^2}\right) \right\} \tag{3-6}$$

It can be clearly seen in (3-6) that the decision rule based on finding the signal that maximizes $p(\boldsymbol{y}|\mathrm{H}, \mathbf{x})$ is equivalent to finding the signal that minimizes $\|\mathbf{y} - \mathrm{H}\mathbf{x}\|^2$ in (3-6). Therefore, (3-6) can be retransformed to distance detection problem by working with natural logarithms. This translates the ML criterion to the detection problem that minimizes the

Euclidean distance $d(\mathbf{x}_m, \mathbf{y})$ from the received vector which is sometimes termed the minimum distance detection [66] and can be expressed as:

$$\hat{\mathbf{x}} = arg\, min_{\mathbf{x}\in\boldsymbol{\chi}} \|\mathbf{y} - \mathrm{H}\mathbf{x}\|^2 \tag{3-7}$$

where $d(\mathbf{x}_m, \mathbf{y}) \geq \|\mathbf{y} - \mathrm{H}\mathbf{x}\|^2$. (3-7) can be equivalently written as:

$$d\left(\mathbf{y}, \mathbf{x}^{(m)}\right) = \sum_{k=1}^{K} \left(\mathbf{y}_k - \mathbf{x}_k^{(m)}\right)^2 \tag{3-8}$$

The ML estimate is referred to as the Log Likelihood Ratio (LLR) in this case. The MLSD for $\mathbf{x}$ given $\mathbf{y}$ can generally be expressed as [83]:

$$\hat{\mathbf{x}} = arg\, min_{\mathbf{x}(c)\in\boldsymbol{\chi}}\, p(\mathbf{y}_m|\mathrm{H}, \mathbf{x}_m) \tag{3-9}$$

(3-9) can be expressed as:

$$\hat{\mathbf{x}} = arg\, min_{\mathbf{x}(c)\in\boldsymbol{\chi}} \frac{1}{\left(2\pi\sigma_n^2\right)^{N/2}} exp\left(\frac{\|\mathbf{y}-\mathrm{H}\mathbf{x}\|^2}{2\sigma_n^2}\right) \tag{3-10}$$

where $\boldsymbol{\chi}$ is the infinity search space.

3.2.2 The MAP Detector

The MAP detection algorithm was developed by Abend and Fritchman in 1970 for channels with Inter-Symbol Interference (ISI), and with memory. Unlike the MLSD which makes decisions based on the Euclidean distance, the MAP makes symbol-by-symbol decisions based on the computation of the APP for each detected symbol [66]. Thus, the detector is optimum in the sense that it minimizes the probability of symbol error. This scheme is generally referred to as the ML detector.

The problem with MAP approach is that there are 2^{NK} [26], [40] possible vectors in the search space. This calls for an exhaustive or brute-force search whose computational complexity increases exponentially with the message sizes *N*, and number of users, *K* in a multiuser system such as Code Division Multiple Access (CDMA). The complexity of the

MAP detector also increases with the number of constellation points in multi-level signalling systems and the number of transmit antennas in MIMO systems. Searching over all possible transmit signals $\mathbf{x} \in \boldsymbol{\chi}$ in the vector space $\boldsymbol{\chi}$ is not clearly an efficient way of solving the ML detection problem. Several near-optimal detection algorithms which reduce the computational cost of the ML detector have been proposed in the literature. These include the Fano detection algorithm [84], M-algorithm, Sequential detection algorithms, LRAD and the SD. These powerful detectors solve the detection problem by constructing a subset search list $\mathcal{L} \subset \boldsymbol{\chi}$ of size $|\mathcal{L}|$ which contains only a fraction of the elements in the vector space $\boldsymbol{\chi}$. The subset search list $\mathcal{L}$ should contain the ML estimate and the counter-hypotheses, i.e., the elements in the subset search list that are complementary to the required ML estimate.

3.2.3 Analytical Results of the ML Detector

The ML detector performs optimum signal detection. It compares the received signal with all possible transmitted signal vectors which have been altered by channel matrix **H** or perturbed by noise. The ML estimates transmit symbol vector **x** according to the maximum likelihood rule. Assuming equal power allocation for all transmit antennas and perfect channel state information (CSI) (the channel matrix **H** is perfectly known at the receiver), the ML detector can yield superior performance compared to any other detection schemes studied in the literature. Figure 3-1 shows an example of analytical (theoretical) results for a symmetric $(N_t = N_r = N)$ QPSK-ML-MIMO system generated using MATLAB for different number of transmit antenna configurations (N=1, N=2, N=4, N=6 and N=8). For a 4x4 MIMO configuration (N=4), the ML detector yields a BER of approximately 2×10^{-6} at 25dB.

The results in Figure 3-1 also confirm the benefits of MIMO systems. As can be seen in Figure 3-1, the diversity performance improves significantly as the number of receive antennas, N increases from N=1 to N=8. These analytical results confirm that probability of

error P_e(BER) for given MIMO system configuration decreases significantly with the exponent of SNR as discussed in Section 2.5.

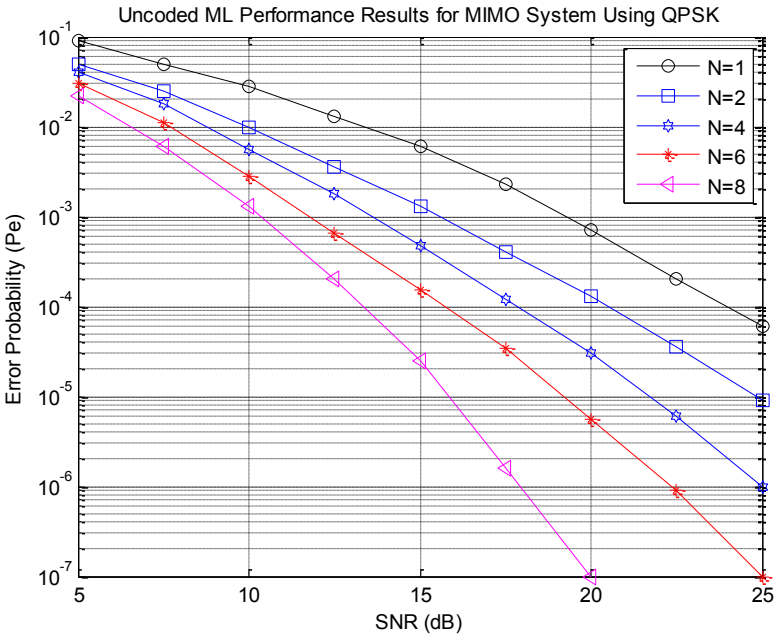

Figure 3-1 Simulation Results For ML

That is, the diversity gain of a MIMO system increases with increasing number of receive antennas and the two quantities are related by $D_{MAX} = N_t \times N_r$.

3.2.4 Summary of ML Detection Schemes

From the analytical results, it has been shown that the performance of the MIMO system improves with an increase in the number of transmit and receive antennas. However, the complexity of the ML detector increases with the number of transmits antennas and the modulation-order or signal constellation size. As with all modulation techniques, the performance of the ML deteriorates with increase in the modulation order. Although the ML show undesirable features, it cannot be written off from the field of wireless communications as it is used as a yard stick through which other detection schemes are measured against.

3.3 Linear Detectors

3.3.1 The Zero-Forcing Detector

A straightforward solution to the MIMO detection problem is to suppress the interference among the layers, i.e. the received data blocks. The Zero-Forcing (ZF) detector [85] solves the unconstrained least-squares problem by multiplying the received signal by the Moor-Penrose pseudo-inverse $\mathbf{H}^{\dagger}$ of the channel matrix to obtain (3-1). Since the entries of $\hat{\mathbf{x}}$ are not necessarily integers, they can be rounded off to the closest integer, a process referred to as slicing [21] or quantisation, to obtain:

$$\hat{\mathbf{x}}_B=[\mathbf{H}^{\dagger}\mathbf{y}]\boldsymbol{\chi}^m \tag{3-11}$$

where $\hat{\mathbf{x}}_B$ is the Babai estimate and $\boldsymbol{\chi}^{\boldsymbol{m}}$ is the set of all constellation or lattice points. This strategy is also referred to as decorrelating detector and is attractive where performance degradation due to noise enhancement can be accepted in order to achieve very low receiver complexity [85]. The advantage of this detector is that it eliminates interference completely. Unlike the ML detector whose computational complexity per symbol rises exponentially with the number of users, the decorrelating detector has a linear complexity per symbol. The receiver filter matrix $\mathbf{G}_{ZF}$ can be defined as:

$$\mathbf{G}_{ZF} = (\mathbf{H}^H\mathbf{H})^{-1}\mathbf{H}^H = \mathbf{H}^{\dagger} \tag{3-12}$$

where $\mathbf{H}^H\mathbf{H} = \mathbf{G}$ is the Gram matrix and $\mathbf{H}^H$ is the Hermitian transpose of the channel matrix $\mathbf{H}$.

Multiplying the (3-12) with the received signal $\mathbf{y} = \mathbf{Hx} + \mathbf{n}$ yields:

$$\tilde{\mathbf{y}} = \mathbf{G}_{ZF}\mathbf{y} = \mathbf{G}_{ZF}\mathbf{Hx} + \mathbf{G}_{ZF}\mathbf{n} = \boldsymbol{\varpi}\mathbf{x} + \tilde{\mathbf{n}} \tag{3-13}$$

where $\boldsymbol{\varpi}$ is the residual interference among the layers, $\tilde{\mathbf{n}}$ is the correlated noise at the ZF detector output. Figure 3-2 shows the block diagram of the ZF linear equalizer. The Log likelihood Ratio (LLR) for each of the layers can be calculated as:

$$L_p(c_{l,i}|\tilde{y}) \approx \quad max_{\mathbf{x}_l \in \boldsymbol{\chi}_{l,i}^{+1}} \left\{ -\beta_l \frac{|\tilde{\mathbf{y}}_l - \mathbf{x}_l|^2}{[\boldsymbol{\varphi}_{\mathbf{xx}}]_{l,l}} + \sum_{n=1}^{N_b} \frac{c_{l,n} L_a(c_{l,n})}{2} \right\} - \underset{\mathbf{x} \in \boldsymbol{\chi}_{l,i}^{-1}}{max} \{\cdots\} \qquad (3\text{-}14)$$

where β_l is the Signal-to-Interference-and Noise Ratio (SINR) on layer l, at the output of the filter $\mathbf{G}_{ZF}$, $\boldsymbol{\varphi}_{\mathbf{xx}}$ is the covariance matrix for the transmit vector $\mathbf{x}$ and $\boldsymbol{\chi}_{l,i}^{+1}$ is the set of all constellation points for which the i^{th} bit in layer l is $c_{l,i} = \pm 1$.

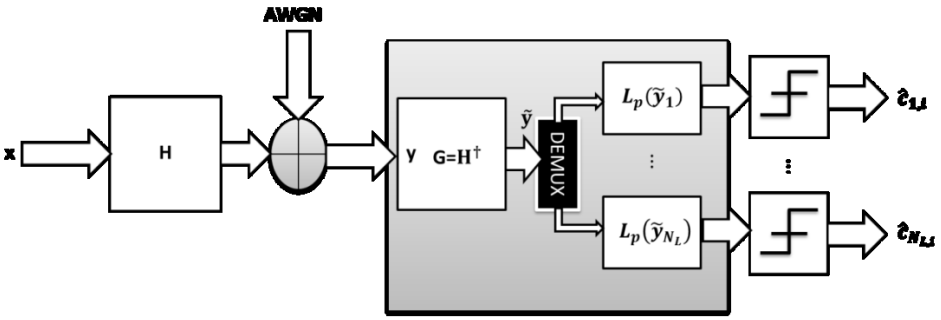

Figure 3-2 Block diagram of a Zero-Forcing Equalizer

It is however important noting that the complexity of de-mapping is significantly reduced at the expense of noise enhancement and a reduction of the spatial diversity. This drawback can be partially solved by the Minimum Mean Squared Error (MMSE) detector.

3.3.2 The Minimum Mean Squared Error Detector

The ZF linear based equalization shows poor performance particularly in symmetrical MIMO setups ($N_t = N_r$), where the signal-to-interference-noise-ratio (SINR) is exponentially distributed and the system suffers frequently from strong noise enhancement. This problem can be alleviated by taking the receiver noise into account in the design of the MMSE detector.

The MMSE detector can be considered as the decorrelating detector which takes background noise into account and utilize the knowledge of received signal energies to improve detection.

Unlike the ZF detector, the MMSE detector was designed to suppress noise enhancement and at the same time eliminate the residual interference amongst the signal layers. The linear mapping which incorporates noise minimizes the mean-squared error between the actual data and the soft output of the conventional detector by applying a partial or modified inverse of the correlation matrix see [26]. The MMSE filter matrix can be modelled as:

$$\mathbf{G}_{MMSE} := (\mathbf{H}^H \mathbf{\Phi}_{\mathbf{nn}}^{-1} \mathbf{H} + \mathbf{\Phi}_{\mathbf{xx}}^{-1})^{-1} \mathbf{H}^H \mathbf{\Phi}_{nn}^{-1} = (\mathbf{H}^H \mathbf{H} + \sigma^2 \mathbf{I})^{-1} \mathbf{H}^H \tag{3-15}$$

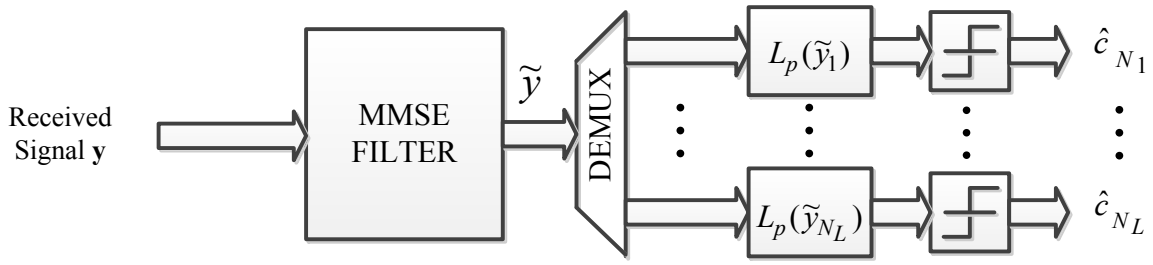

Figure 3-3 Block diagram of an MMSE Filter

Figure 3-3 shows the block diagram of an MMSE Filter. The MMSE detector has been proposed for centralized receivers in AWGN and known fading channels [26]. The amount of modification increases with increase in the background noise. It provides better Bit-Error Rate (BER) than the ZF detector, but however, the performance of the MMSE detector approaches that of the ZF detector as the noise goes to zero, see [26].

The reduction of noise enhancement can be achieved at the expense of increased interference between layers. In addition to this problem, the diagonal elements of $\boldsymbol{\varpi}$ are not necessarily unit ($\boldsymbol{\varpi} \neq \mathbf{I}$). The estimator is said to be biased in this case. This will cause decision errors in multi-level signalling techniques. However, this drawback can be overcome by the use of an unbiased MMSE filter, where $\mathbf{G}_{UB-MMSE} := \mathbf{\Theta G}_{MMSE}$ with $\mathbf{\Theta} = diag\left(1/\lambda_{1,1}, \cdots \lambda_{N_L,N_L}\right)$.

Another important disadvantage of this detector is that, unlike the ZF detector, it requires estimation of the received amplitudes. Like the ZF detector, the MMSE detector faces a huge task of implementing matrix inversion. For more information about this detector, see [26].

3.3.4 Results and Discussion of Linear Detection Schemes

Performance results for linear detection for a 2×2 MIMO system in uncorrelated AWGN channels are presented in Figure 3-4. Both uncoded and LDPC coded ZF- MMSE-MIMO transmissions are considered using BPSK and 4-QAM modulation schemes. The respective modulation schemes are respective representatives for low and high spectral efficiency regimes at simulation level.

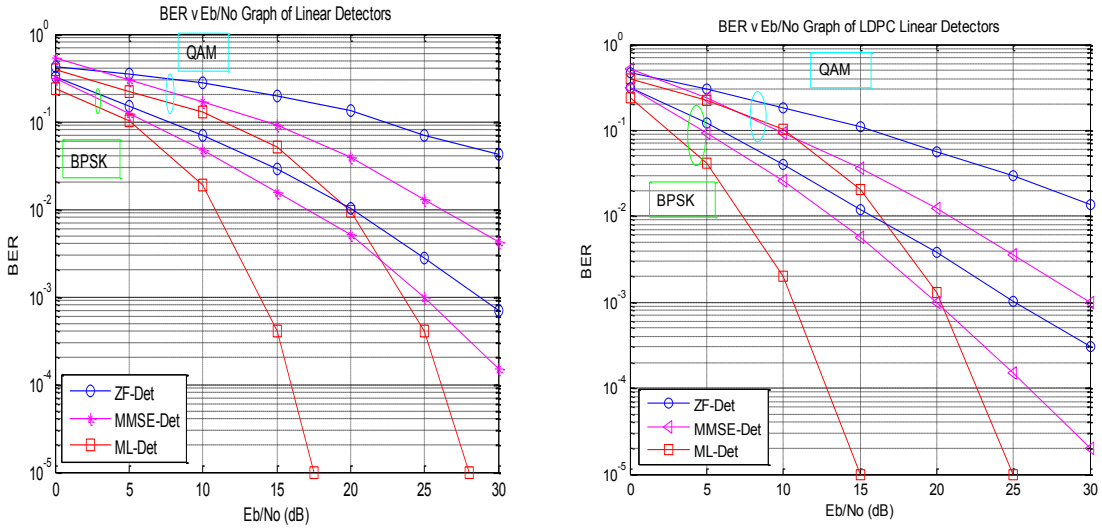

Figure 3-4 Simulation Results for coded and uncoded ZF and MMSE Detection

The uncoded ZF linear based equalization shows poor performance in an AWGN channel. The poor performance can be attributed to strong noise enhancement, which often results from ill-conditioned channel matrix **H**. It can be clearly seen that the problem can be alleviated by applying the MMSE filter which takes the receiver noise into account, though at the expense of increased interference between the received signal layers. The MMSE yields a performance gain of about 10dB over the ZF and is evident particularly in symmetrical MIMO systems where the probability of having a rank-deficient realization of the channel matrix is high.

Encoding the MMSE-MIMO signal with the state-of-the art LDPC coding scheme has the effect of reducing the SNR required by the MMSE for the case of 4-QAM to achieve a BER of 1×10^{-2} by 5dB, i.e., a coding gain of 5dB thereby boosting the performance of linear

detectors. However, coding has the effect of reducing the capacity of the MIMO system. Therefore, a trade-off between capacity, performance and complexity has to be made in practical MIMO systems. Furthermore, the performances of both coded and uncoded ZF and MMSE decreases with increase in modulation order. The offset between both schemes goes down from around 5dB in case of BPSK to below 1dB for 4-QAM.

3.3.5 Summary of Linear Detection

Linear detection has been identified as the simplest detection method which offers several advantages including the following:

Low complexity: Unlike the ML detector whose complexity per transmitted symbol is exponential, the complexity of linear detection per transmitted symbol is linear. The detection of MIMO signal using linear detection only involves vector-matrix multiplication and computation of individual LLRs for each received symbol in each transmitted layer.

High quality of the soft output: The loss in mutual information is mainly due to the strong noise enhancement since the SINR on different layers can be precisely characterized. It has also been proved that the generation of soft output can be the major challenge for other detection schemes [86]. Further to this, the difference in performance between MMSE based linear detection and ML detection is typically below 1dB at BERs around 1×10^{-1}. In high diversity environment, where powerful coding schemes can be employed over deep channels fades, linear detection can therefore be a promising alternative to more advanced detection techniques [87].

However, linear detection techniques suffer from major setbacks. The main setbacks include the following:

Increased pre-processing complexity: Computation of the filter matrix requires calculation of the inverse of a matrix first. This can result in increased pre-processing complexity compared to tree search schemes.

Noise enhancement: The performance of linear detection depends crucially on the average eigenvalue spread of the channel and on the nature of the channel matrix, that is, whether the channel matrix is well-conditioned or ill-conditioned. Therefore, linear detectors show very poor performance in symmetric MIMO setups and in the presence of correlation at the transmitter and receiver. It promotes the use of advanced detection techniques in such environments, with the evident SNR gains at low target error rates, due to the high diversity order.

Lower benefit from priori information: There is little or no gain from using feedback from the decoder, since this information is not used to reduce the interference among layers. This is in contrast to the non-linear detection techniques where priori information can be used to improve detection on a layer by layer basis as in the case of the VBLAST and/or the OSIC detectors. The use of linear detectors should therefore be restricted to the first iteration in an iterative detection-decoding setup. More powerful detection algorithms can thereafter be employed in all following iterations [88].

3.4 Non-Linear Detectors

The major drawback of the MMSE detector is its inability to reduce interference between layers effectively. Thus, different detection techniques [6], [89] based on interference cancellation have been developed. This class of detectors estimate the Multiple Access Interference (MAI) and multipath induced interference and subtract out the estimates from the congregate signal. This strategy is also known as nulling and cancelling or matrix Decision Feedback Equalization (DFE) [6]. There are two major variants of this technique: Parallel Interference Cancellation (PIC) and Successive Interference Cancellation (SIC) [26].

PIC schemes use a linear filter to obtain an initial estimate for the transmitted data. Subsequently, N_L different filters are used in parallel, each subtracting out the contribution of all but a single layer L from the received signal.

Hard or soft estimates [90] can be used in interference cancellation process and performance very close to channel capacity can be achieved in scatter-rich or high diversity environments. However, in scenarios where space is the main source of diversity and/or high correlation is present, there will be a substantial offset in performance to more powerful detection schemes.

3.4.1 Successive Interference Cancellation Detector

The Successive Interference Cancellation (SIC) is a form of non-linear detection strategy in which signals are detected in order of perceived reliability [26]. Detection takes place on a layer-by-layer basis, with the interference from already detected layers removed from the received signal before detecting the next layer, see Figure 3-4. This can be done by using a set of linear filters, as originally proposed, or based on **QR** Decomposition (QRD) of the channel matrix, i.e., $\mathbf{H} = \mathbf{QR}$, where $\mathbf{Q}$ is a unitary matrix and $\mathbf{R}$ an upper triangular matrix. Both approaches are equivalent. Multiplying the received signal with $\mathbf{Q}^T$ yields:

$$\tilde{\mathbf{y}} = \mathbf{Q}^T\mathbf{y} = \mathbf{Q}^T\mathbf{H}\mathbf{x} + \mathbf{Q}^T\mathbf{n} = \mathbf{Q}^T\mathbf{Q}\mathbf{R}\mathbf{x} + \tilde{\mathbf{n}} = \mathbf{R}\mathbf{x} + \tilde{\mathbf{n}} \tag{3-16}$$

where $\tilde{\mathbf{n}}$ is the modified receiver noise which is still white after multiplication with the unitary matrix $\mathbf{Q}^T$. Exploiting the upper triangular structure of $\mathbf{R}$, the LLRs for each layer can now be determined by a back- substitution process [87]-[88]:

$$L(c_{l,i}|\tilde{\mathbf{y}}, [\mathbf{x}]_{N_L}^{l+1}) \approx max_{\mathbf{x}_l \in \mathcal{A}_i^{+1}} \left\{ -\frac{|r_{l,l}|^2}{N_0} \left\| \frac{\tilde{y}_l}{r_{l,l}} - \sum_{k=l+1}^{N_L} \frac{r_{l,k}}{r_{l,l}} \mathbf{x}_k - \mathbf{x}_l \right\|^2 + \sum_{n=1}^{N_b} \frac{c_{l,n} L_a(c_{l,n})}{2} \right\} \tag{3-17}$$

where $c_{k,i}$ is the i^{th} bit in layer k, $c_{l,n}$ is the corresponding n^{th} bit in layer l and N_b is the total number of bits in a codeword. The estimate $\mathbf{x}_k$ for the signal on layer k is obtained by

taking hard decisions on the bits $c_{k,i}$ and the subsequent mapping to the corresponding modulation symbol.

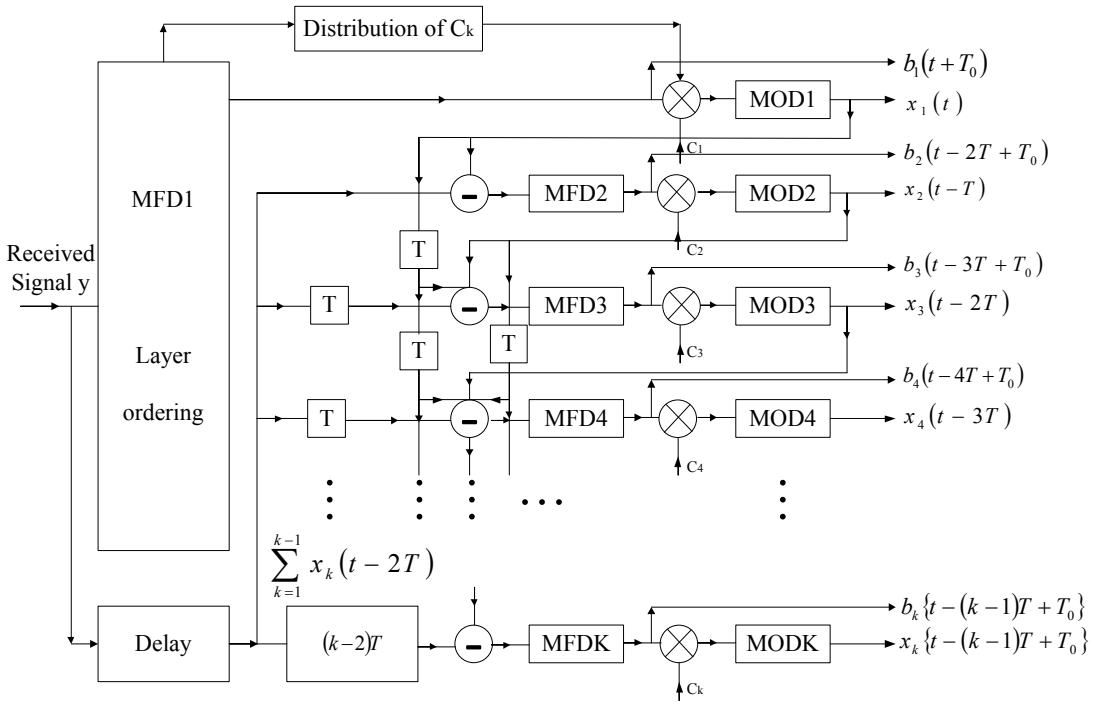

Figure 3-5 Block Diagram of a Successive Interference cancellation Detector

However, the computed LLRs are only correct if no decision error has occurred in previously detected layers. The effects of error propagation can be minimized by detecting the reliably received signals first and by sorting the layers in decreasing order of the post-equalization SINR. This strategy is commonly referred to as Ordered Successive Interference Cancellation (OSIC) [27], [91] and achieves the best performance when using the MMSE criterion for layer ordering [92].

The interference cancellation process operates on equivalent systems where the rows of **x** and the columns of **H** have been appropriately permuted. For QRD-based SIC, the layer ordering can either be done before the matrix decomposition or by using a greedy algorithm during the matrix decomposition which is known as Sorted **QR** Decomposition (SQRD) [93]. In order to obtain the optimal ordering, a so-called Post-Sorting-Algorithm (PSA) needs to be executed.

3.4.2 Vertical Bell Labs Layered Space-Time Detector

The Vertical Bell Labs Layered Space-Time (V-BLAST) is a class of non-linear detectors that offers better performance with only modest increase in complexity. It was the brainchild of Foschini [7] and was specifically designed to detect spatially multiplexed MIMO signals. The V-BLAST strategy is based on successive interference cancellation. The concept behind this strategy is to use an appropriate (space-time) encoding scheme at the transmitter in order to achieve good performance at the receiver by using the so-called Ordered Successive Interference cancellation (OSIC) [27], or simply the Successive Interference cancellation (SIC) detector. Examples of appropriate encoding schemes at the transmitter include Space Time Coding (STC), Space Time Block Coding (STBC) and Space Time Turbo Codes (STTC) [94].

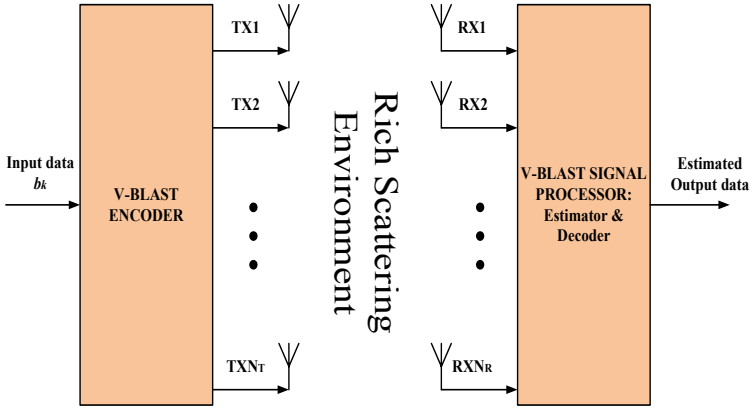

Figure 3-6 Block Diagram of the VBLAST Detector

Figure 3-6 shows the block diagram of the VBLAST detector. The input data stream to the transmitter of a MIMO system is de-multiplexed into N_t sub-streams, where N_t is the number of transmit antennas in a symmetric ($N_t = N_r$) MIMO system. The sub-streams are separately encoded (and/or interleaved) and modulated. These data streams are then mapped one-by-one or layer-by-layer onto the MIMO transmit antennas for transmission. In such a system, however, a great challenge is posed in designing an efficient detector because of the interference among the transmit antennas [95].

The detection process of the simplest V-BLAST scheme involves two main operations namely (a) nulling (interference suppression) and (b) sorting (or layer ordering) and cancelling. The first interference suppression operation nulls out interference by projecting the received vector onto the null subspace (perpendicular subspace) of the subspace spanned by the interfering signals. This stage involves orthogonalization of the channel matrix as $\mathbf{H} = \mathbf{QR}$, where $\mathbf{Q}$ is a unitary orthogonal matrix and $\mathbf{R}$ is the upper triangular matrix. The received signal $\mathbf{y} = \mathbf{Hx} + \mathbf{n}$ is then pre-processed to obtain (3-18).

$$\tilde{\mathbf{y}} = \mathbf{Q}^T\mathbf{y} = \mathbf{Q}^T\mathbf{Hx} + \mathbf{Q}^T\mathbf{n} = \mathbf{Q}^T\mathbf{QRx} + \tilde{\mathbf{n}} = \mathbf{Rx} + \tilde{\mathbf{n}} \tag{3-18}$$

where $\mathbf{Q}^T\mathbf{QRx} = \mathbf{Rx}$ and $\mathbf{Q}^T\mathbf{Q} = \mathbf{I}$, with $\mathbf{I}$ being the identity matrix.

The second operation involves ordering of the received signals in decreasing amplitudes and then finally cancelling the received signal with the largest amplitude first. The contribution of the detected signal is subtracted from the received vector in this way. This process is repeated until when the received signal with the least amplitude is detected. Note that the received signal with the largest amplitude does not benefit from the cancellation process. On the other hand, the received signal with the least amplitude see much reduced interference which translates to a huge benefit for the weakest signal. With a suitable combination of detectors, e.g., the serial connection of the V-BLAST and MMSE detector, with the MMSE serving as an input to the V-BLAST, spectacular spectral efficiencies of the order of 82bits/Hz can be achieved. This translates to data rates of 820 Mbits/s for a 10MHz bandwidth system - a significant leap towards achieving very high data rates compared to current wireless systems. In addition to these advantages, uncoded data can be transmitted independently in multiple antenna systems, meaning that there is no redundancy and there is no correlation among antennas [96].

The major drawback of the V-BLAST detection scheme is that the error at the first stage of this detector propagates throughout all detection stages, resulting in a system which is far

from near-optimal [15]. This is a very important issue in uncoded systems where error correction is not used, thus the error rate of the V-BLAST is dominated by the first stage. This disadvantage can however be overcome by performing nulling and cancelling from the "*strongest" to the "weakest*" signal as proposed in [7]. Regardless of their disadvantages, the above heuristic methods all require $O(mn^2)$ [21] computations, essentially because they all first solve the unconstrained least-squares problem.

3.4.3 Results of Non-Linear Detection Schemes

Performance results for both linear and non-linear detection schemes for a 2×2 MIMO system in uncorrelated fading channels are presented in Figure 3-7. Only uncoded VBLAST and MMSE-SIC MIMO transmissions are considered using BPSK and 4-QAM modulation schemes in this section. Again, the respective modulation schemes are representatives for low and high spectral efficiency regimes at simulation level. There is a clear gain in performance of the non-linear detection scheme over all linear detection schemes particularly when lower order modulation schemes are employed. The MMSE-SIC and the VBLAST benefit substantially from the reduced error probability on the first layer arising from the cancellation of the strongest signal, and MMSE-SIC achieves a performance within 1-3dB of ML in the low SNR regime of interest.

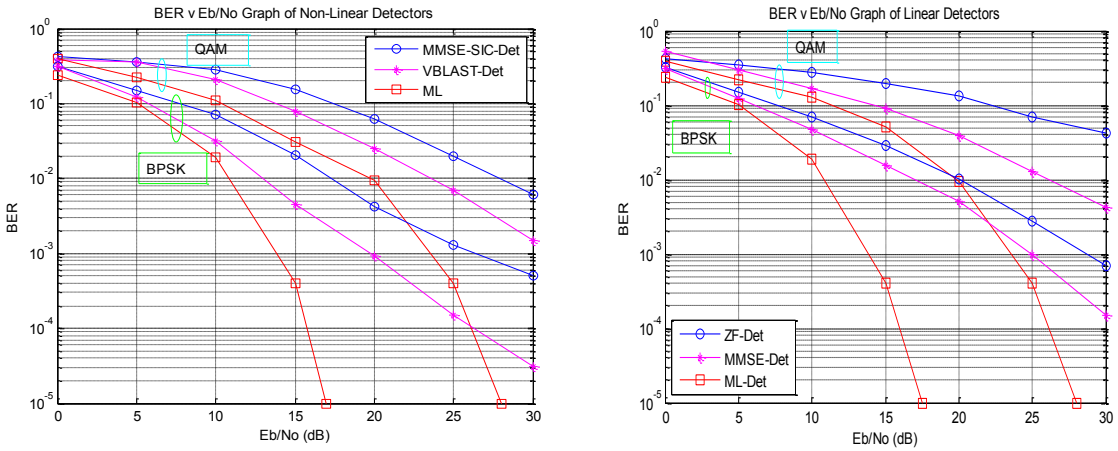

(a) Non-Linear Detectors (b) Linear Detectors

Figure 3-7 Performance Results for Linear Versus Non-Linear detectors

However, the MMSE-SIC detection scheme approaches the performance of linear detectors as the modulation order is increased. The reason being the increased level of ISI, thus, MMSE-SIC-based detection schemes are preferable to linear detection mainly if low BERs are targeted in cases where lower modulation schemes are employed. Figure 3-7(a) clearly shows that the VBLAST detection schemes yields performance improvements compared to the MMSE-SIC detection scheme. The performance gain is attributed to the coding gain (arising from STBC of STC coding) introduced at the transmitter. However, the drawback of the VBLAST detection is the increased complexity of the detector which increases with the number of transmit or receive antennas.

While MMSE-SIC consistently outperforms linear detection schemes, for uncoded transmission setup, this is not necessarily the case for coded transmission. The challenge lies in incorporating the effects of error propagation in the calculation of the LLRs. Under the assumption of perfect cancellation, performance of the MMSE-SIC detector can be severely degraded, unless the channel decoder can be used to enhance the reliability of the estimates [97]. However, this problem can be addressed by subtracting soft estimates from the received signal and use their variance to assess the expected residual noise after the cancellation step, though at increased computational cost [97] and the performance is still inferior to simple linear detection for a number of application scenarios of interest [89]. Another drawback of the SIC detector is that it suffers from a high processing delay. This is a major challenge to applications that are less tolerant to high processing delays, such as cellular systems. One way to deal with stringent delay requirement is to limit the number of cancellations. Processing delay is one of the issues to be considered in the future work.

3.4.4 Summary of Non-Linear Detection Schemes

SIC based detection techniques have several advantages which include the following:

Low detection complexity for Hard-SIC: The detection as well as the pre-processing complexity is comparable to that of linear detection schemes, if **SQRD** based hard-SIC is used. These heuristic methods require $O(mn^2)$ [21] computations, essentially because they all first solve the unconstrained least-squares problem. However, the performance will only be satisfactory if the decoder can be included in the interference cancellation stage.

Attractive for iterative detection-decoding: SIC based detection schemes can achieve good performance once feedback of sufficient quality becomes available from the decoder. It may hence be used in the later stages of iterative detection-decoding [88], [97], where it is also possible to reduce the complexity of Soft-SIC [98].

However, the following challenges are encountered in the use of non-linear detectors:

Capacity loss: If a V-BLAST transmit strategy is employed, the resulting loss in transmit diversity leads to a reduction in the achievable data rate [67]. SIC based detection schemes are highly suboptimal, due to error propagation in the first detector-decoder iteration [97] and due to a suboptimal rate allocation strategy in the last iterations where the first layers can be perfectly cancelled. In both cases, the scheme will be unable to operate close to channel capacity.

Channel-dependent optimal transmit strategy: If the channel is flat and quasi-static fading, the transmitter should be using equal rate allocation and layer ordering at the receiver [27]. In a high diversity environment on the other hand, the layer capacities depend only on the number of interfering layers. The optimal strategy in this case is not to order the layers at the receiver but adjust the rates on the different layers based on the average SINRs of the layers [100]. The transmitter must hence have knowledge of the channel statistics in order to choose an appropriate transmit strategy. In environments with a limited amount of diversity, equal rate allocation at the transmitter and an "average" layer ordering for all time-frequency bands [101] can be used, but this will result in a loss in achievable data rates, as discussed above.

Error Propagation: The errors at the first stage of the SIC detectors propagate throughout all detection stages, resulting in a system which is far from near-optimal. This is a very important issue in uncoded systems where error correction is not used, thus the error rate of the V-BLAST is dominated by the first stage. This disadvantage can however be overcome by performing nulling and cancelling from the "strongest" to the "weakest" signal as proposed in [7].

Propagation Delay: Non-Linear detectors suffer from high processing delays. This is a major challenge to applications that are less tolerant to high processing delays, such as cellular systems.

3.5 Lattice Reduction Techniques

Lattice reduction technique was first proposed for MIMO detection in [6]. For an overview of Lattice Reduction Aided Detection (LRAD) schemes, see, [6], [14], [16]. The heuristic methods discussed above are exact only if the columns of **H** are perfectly linearly independent and orthogonal. Practically, the columns of **H** are rarely orthogonal due to the orthogonality defect, $\boldsymbol{\zeta}(\mathbf{H})$ of the channel matrix [6] which is associated with the strong noise enhancements caused by the linear filters. This gives rise to significant performance degradation. The orthogonality defect is given by [6]:

$$\zeta(\mathbf{H}) = \frac{\prod_{l=1}^{N_L} \|h_l\|}{det(\mathbf{H})} \geq 1 \tag{3-19}$$

The equality sign applies if the columns of **H** are perfectly orthogonal. **H** can be diagonalized by a unitary transformation on the left, and so, slicing the unconstrained least-squares solution yields the exact solution.

Orthogonalizing the columns of **H** via a **QR** decomposition, or otherwise, generally destroys the lattice structure [18]. The reason being that if **x** has integer entries, then, **Hx** does not need to have integer entries. One method that attempts to alleviate this is *lattice reduction.* The

concept behind these methods is to find an invertible $m \times m$ matrix, such that $\mathbf{T}$ and $\mathbf{T}-\mathbf{1}$ have integer entries thereby preserving the lattice structure and such that the channel matrix is as "orthogonal as possible." Having found such a $\mathbf{T}$, rather than solve the original ML detection problem, the integer least-squares problem can be solved as follows [18]:

$$min_{\mathrm{t}\in\mathbb{Z}^{\mathrm{m}}}\|\mathbf{x}-\mathbf{Gt}\|^2 \tag{3-20}$$

To illustrate the lattice reduction aided techniques, consider components of the transmitted signal:

$$\mathbf{x} = a\left(\mathbf{z}+\frac{1}{2}\mathbf{1}_{N_L}\right) \tag{3-21}$$

The noiseless received signal can be interpreted as a subset of points in infinity shifted lattice generated by $\mathbf{H}$:

$$\mathbf{Hx} = \mathbf{H}a\left(\mathbf{z}+\frac{1}{2}\mathbf{1}_{N_L}\right) = a\left(\mathbf{Hz}+\frac{1}{2}\mathbf{H1}_{N_L}\right),\ \mathbf{z}\in\mathbb{Z}^{N_L} \tag{3-22}$$

where $\mathbf{1}_{N_L}$is an all-ones column vector with N_L elements and $\mathbf{z}+\frac{1}{2}\mathbf{1}_{N_L}$

The columns of $\mathbf{H}$ are in this context referred to as the lattice basis vectors. The target of lattice reduction techniques is now to find a new basis $\bar{\mathbf{H}}$ which spans the same lattice but whose columns are nearly orthogonal. This is equivalent to finding an appropriate unimodular matrix $\mathbf{T}$ such that $\bar{\mathbf{H}} = \mathbf{HT}$ has minimal orthogonality defect. An example for such a lattice basis reduction algorithm is the Lenstra-Lenstra-Lovasz (LLL) algorithm. This equivalent transmission model is based on the lattice channel matrix $\bar{\mathbf{H}}$:

$$\mathbf{Hx}+\mathbf{n} = \mathbf{HTT}^{-1}\mathbf{x}+\mathbf{n} = \bar{\mathbf{H}}\bar{\mathbf{x}}+\mathbf{n} \tag{3-23}$$

where $\bar{\mathbf{x}} = \mathbf{T}^{-1}\mathbf{x}$. Introducing $\bar{\mathbf{z}} = \mathbf{T}^{-1}\mathbf{z}$ leads to (3-24):

$$\bar{\mathbf{x}} = \mathbf{T}^{-1}\mathbf{x} = a\left(\mathbf{T}^{-1}\mathbf{z}+\frac{1}{2}\mathbf{T}^{-1}\mathbf{1}_{N_L}\right) = a\left(\bar{\mathbf{z}}+\frac{1}{2}\mathbf{T}^{-1}\mathbf{1}_{N_L}\right) \tag{3-24}$$

Using the two equations above, standard MIMO detection techniques can then be used to obtain the estimate $\hat{\mathbf{z}}$ of the transmit signal in the equivalent transformed lattice, which is then transformed back to establish an estimate in the original transmit vector: $\hat{\mathbf{x}} = \mathbf{T}\hat{\mathbf{z}}$.

Taking the case of the ZF linear detector with the filter matrix $\bar{\mathbf{G}} = \bar{\mathbf{H}}^{\dagger}$as an example, see Figure 3-8, the noise-reduced signal becomes $\bar{\bar{\mathbf{y}}} = \bar{\mathbf{G}}\mathbf{y} = \bar{\mathbf{x}} + \bar{\mathbf{G}}\mathbf{n}$. The noise enhancement is substantially reduced since the basis vectors forming the lattice reduced channel matrix $\bar{\mathbf{H}}$ are much closer to being orthogonal, i.e. $\zeta(\bar{\mathbf{H}}) \ll \zeta(\mathbf{H})$. The estimate $\hat{\mathbf{x}}$ is obtained by appropriate scaling and shifting after quantization of the filter output.

Since the quantization step is done in the equivalent lattice disregarding the finiteness of the original signal lattice, an additional bounding operation is required after transformation of the estimate back into the original signal space [6]. Lattice reduction itself is NP-hard. A common heuristic is the LLL [102] algorithm. Permitting a gross oversimplification, the LLL can be regarded as Gram-Schmidt over integers. Figure 3-8 shows the block diagram of an LRAD.

While lattice reduction may lead to some improvement in the solution of integer least-squares problem over the infinite lattice, it is not useful for finite lattice which is a subset of an infinite lattice.

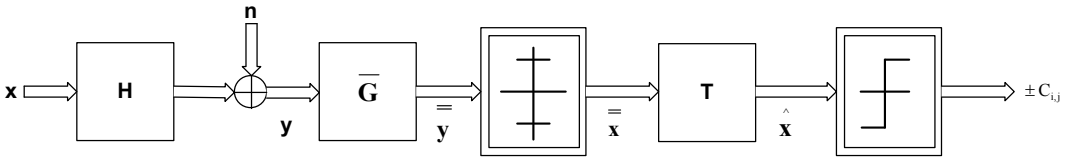

Figure 3-8 Block diagram of an LRAD

The reason is that the lattice transforming matrix **T** often destroys the properties of subset. The main disadvantages are the following:

High preprocessing complexity: The LLL algorithm typically used for lattice basis reduction is of considerable complexity [6]. This can be a limiting factor in scenarios with low channel coherence times.

Low quality soft output: It is difficult to generate LLRs of high quality at the output of the detector. Lattice reduction is therefore mainly attractive when very low raw BERs are targeted (e.g. in combination with high-rate channel coding) or in environments with low time and frequency diversity.

3.5.1 Performance Results and Discussion

The performance results for both linear and non-linear detection schemes using the LLL-algorithm are presented in Figure 3-9. The reduced lattice basis can be achieved by introducing the LLL algorithm.

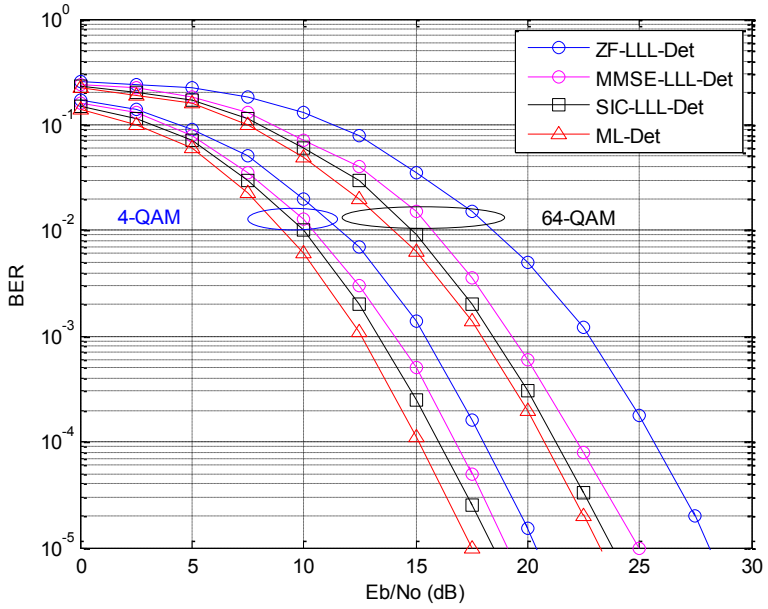

Figure 3-9 LRAD performance results for 4-QAM and 64-QAM 4x4 MIMO setup

This allows achieving BER performance within 5dB of the ML for all antenna setups and modulation schemes employed. The SIC-LLL achieves performance within 1dB of ML for all antenna setups. The worst case 64-QAM, 4x4 MIMO ZF-LLL performance is within roughly 2dB to about 5dB of the ML performance for all SNR ranges.

Figure 3-10 shows the effect of equipping the transmitter with more antennas. Increasing the number of the antennas results in an increase in diversity gain as explained in Chapter 2. The LLL-SIC detector yields performance gain of about 4dB at a BER of about 10^{-5} for the case of 4-QAM transmission. As expected, the performance of the LRAD detector deteriorates with increase in constellation size for both MIMO setups in Figure 3-9 and Figure 3-10.

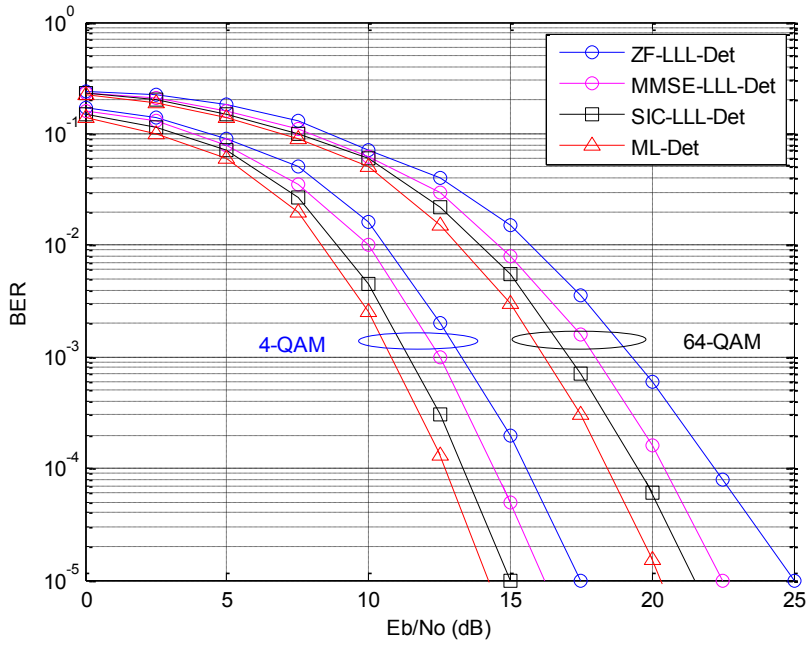

Figure 3-10 LRAD performance results for4-QAM and 64-QAM 4x6 MIMO setup

Whilst hard output results are very promising, achieving good soft output is a major challenge for lattice reduction aided detection techniques, as the lattice generated by the reduced basis is partially modified. This problem can be alleviated by using a number of points in the vicinity of the quantised lattice point $\hat{\mathbf{z}}$ and transform them back into the original signal space. However, some of these points may eventually be mapped onto the same signal point. Thus, the magnitudes of the LLRs cannot be estimated in this scenario. The slight gains obtained by this approach typically do not justify the invested effort. An alternative solution to the problem is to generate a list of possible transmit signals, each with one bit fixed to a certain value.

3.5.2 Summary of the LRAD detection Schemes

The LRAD advantages include high quality hard output. The LLL-SIC achieves high quality hard output with BER performance within 1 dB of ML in the whole BER range, for all considered antenna setups and constellation sizes. The detection complexity of the LRAD is approximately double that of the original linear or (Hard-) SIC based detection schemes due to the shifting operations and additional vector-matrix multiplication required for transforming the estimate back into the original signal space. However, the LRAD detection complexity is several magnitudes lower than the ML as will be proved in Chapter 6.

Nevertheless, the LRAD has disadvantages which include high processing complexity which arises due to the LLL algorithm. The LLL algorithm is typically used for lattice basis reduction and can introduce significant complexity. This can be a limiting factor in scenarios with low channel coherence times. Low quality soft output: as discussed above, it is difficult to generate LLR of high quality at the output of the detector. Lattice reduction is therefore mainly attractive when very low raw BERs are targeted (e.g., in combination with high-rate channel coding) or in environments with low time and frequency diversity.

3.6 Introduction to tree search based detection schemes

Several tree search based detection algorithms have been proposed in the literature [13], [16], [18]. The Fincke and Pohst algorithm [13] was developed for finding the closest lattice points. It was later extended to *sphere decoding* algorithm for MIMO systems by Hassibi and Vikalo [18]. Instead of performing a brute-force search in the entire search space, the *Sphere Decoding* algorithm recursively searches for the closest lattice points inside a hyper-sphere centred at the query point $\mathbf{y}$. However, the main challenge of the SD is the choice of the initial radius. The SD is very sensitive to the initial radius of the sphere. For a full discussion of the SD, see Chapter 4.

Schnorr and Euchner introduced an enumeration strategy [103] to improve Fincke and Pohst's decoding algorithm [13]. This strategy involves enumerating the lattice points inside the hyper-sphere in an order of increasing distance from the components of integer point corresponding to **y**. The *Closest Lattice Point Search Algorithm* developed by Agrell et. al. generalizes the Schnorr and Euchner's algorithm for decoding of any MIMO system [16]. This technique ignores the determination of the initial sphere radius as the search algorithm makes use of a special ordering. Chan and Lee [104] introduced a hybrid version of the ordering in Schnorr-Euchner and the Fincke and Pohst's sphere decoding algorithm while, Kannan developed an alternative version to the Fincke and Pohst's based SD decoding algorithm [105]. Unlike the SD, the Kannan's algorithm recursively searches the entire lattice points inside a rectangular parallelepiped, centred at the query point **y** with its edges along the Gram-Schmidt vectors of a proper basis of the lattice. The Finite signal sets and stack algorithms are considered in [92].

The SD is a typical example of the quasi-optimal detection schemes which constructs a subset search list. It confines the search list in a hyper-sphere of radius R_0. Attention will be restricted to the sphere detector characterized by the depth-first-search algorithm (see Section 3.6.3) throughout this work as it is the main topic of this research. Before the discussion is extended to the sphere detector, some basic terminologies used in sphere detector and its variants are presented in the next section.

3.6.1 Basic Sphere Detection Terminology

The basic definitions of terms which will be frequently used in detection schemes and the subsequent description of tree search based detection algorithms discussed in the rest of this work are presented in this section. Figure 3-8 is used for illustrating tree based detection algorithms.

Node refers to a point in the tree. Each node is uniquely defined by the path which connects it to the root of the tree and has associated an accumulated path metric.

Root node is the node from which the tree emanates. It resides in the virtual layer $N_L + 1$ and has path length and path metric 0.

Ancestor/Grandparent refers to the root node from which all parent nodes and their children or grandchild nodes emanate from.

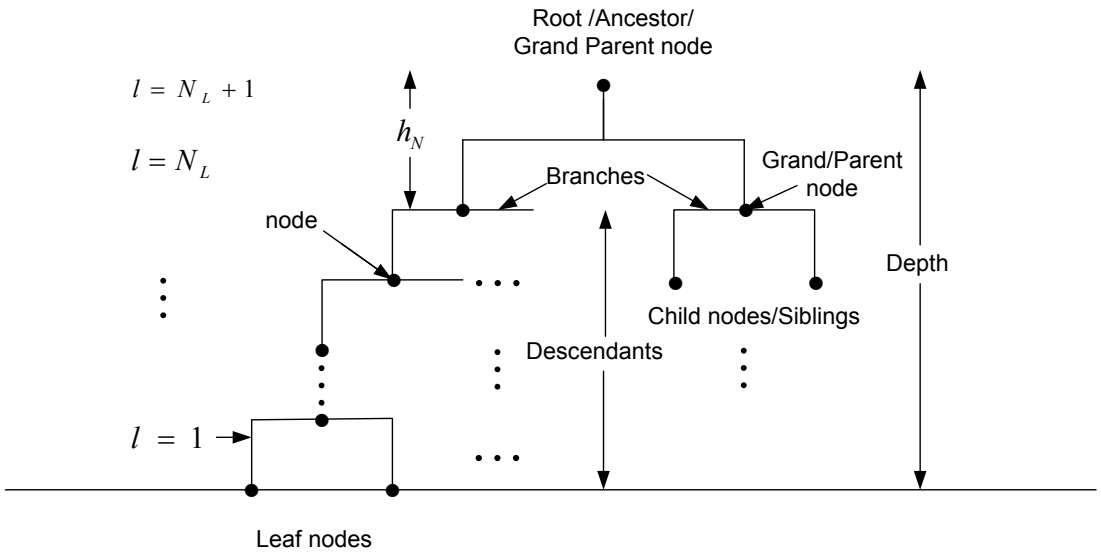

Figure 3-11 Tree search diagram illustrating sphere detection terminologies

Parent node is a node at layer l, to which a child node at layer $l - 1$ is directly connected to; all nodes except the root node have a unique parent node.

Child node is a node which is directly connected to a parent node in layer l and is located in layer $l - 1$. All nodes except leaf nodes can have child nodes.

Siblings are children with the same parent, i.e., these are nodes which originate from the same parent node.

Leaf node, also referred to as lattice point, is a node in layer 1. The associated path has length N_L and its path metric is equal to the metric $\mu(\mathbf{x})$ of the corresponding hypothesis on

the transmit signal **x**. Nodes which have no child nodes but are not located in layer 1 are not referred to as leaf nodes in this terminology.

Descendants refer to all nodes and their children or grandchildren that emanate from the root node. Note that every node is a root node as far as its child nodes are concerned. Also note that all parent, child and grandchild nodes are descendant nodes as far as the root node is concerned.

Branch is an edge in the tree which connects a parent node to its child node. It has associated with it a metric increment, or branch metric $\boldsymbol{\mu_l}$.

Internal nodes are nodes which are not leaf nodes. This includes the root node.

Node Extension denotes the process of adding to the tree one or multiple child nodes of a node. Due to the involved calculation of branch metrics, it is typically the computationally most expensive part of the tree search.

Layer: the term layer is used to describe each coded or uncoded block of transmitted (or received) data.

Depth is the number of layers between the root node and the leaf nodes.

Height is the maximum level of any node in a tree.

Binary Tree is an ordered tree with all nodes having at most two children.

Enumeration strategy: in the context of sphere decoding, this term is used to describe the order in which the child nodes are added to the parent node in the node extension (tree search) process and can have a major impact on the complexity of the search.

NP-Complete (Non-deterministic polynomial-time complete) is a class of decision problems where a given solution can be verified, but there is no efficient way of locating that solution. Computational time increases rapidly with the problem size.

NP-hard (Non-deterministic polynomial-time hard): In communications parlance, this is a class of decision problems whose computational complexity is exponential with the problem size, i.e., they are decision problems that are informally "at least as hard as the hardest problems in non-deterministic polynomial time hard signals.

Complexity: In the context of sphere decoding, it generally refers to the number of computations or operation executed during tree search, that is, the number of additions, subtraction, multiplications or divisions. The number of operations varies with the length of the input bits and the initial radius of the hyper-sphere. The amount of execution time of the sphere detection algorithm rises polynomially or exponentially with number of operations, particularly in low SNR regimes, thus giving rise to NP-hard and NP-complete decision problems.

Soft Decisions are multilevel or symbol based decisions. But in soft decision, decoded received samples from the channel pass directly to the detector.

Hard Decisions are two level or binary based decisions and is the final decision. Hard decoding is simpler than soft but soft decoding has a better performance compared to hard decision. Hard/Soft decoding is common in convolutional codes.

Optimal is a term used to describe received/detected signals which are exact or almost exact copies of the transmitted signals.

3.6.2 Tree Search Based Detection Schemes

The task of the MIMO detector is to generate the soft output for each bit i of each transmit signal component x_i. The l^{th} component of the transmit signal will be referred to as layer l throughout this work. If the soft output is calculated based on the maxLogAPP approach, the i^{th} log likelihood ratio (LLR) in layer l can be expressed as the difference between two metrics $\boldsymbol{\mu}(\mathbf{x}_{l,i}^{+1})$ and $\boldsymbol{\mu}(\mathbf{x}_{l,i}^{-1})$:

$$L_p(c_{l,i}|\mathbf{y}) = max_{x_{l,i}^{+1} \in \mathcal{A}_{l,i}^{+1}}\{\mu(\mathbf{x}_{l,i}^{+1})\} - max_{x_{l,i}^{-1} \in \mathcal{A}_{l,i}^{-1}}\{\mu(\mathbf{x}_{l,i}^{-1})\} \quad (3\text{-}25)$$

where $\boldsymbol{\mu}(\mathbf{x}_{l,i}^{+1})$ is the magnitude of the i^{th} signal $\mathbf{x}_{l,i}^{+1}$ located in layer l and $\boldsymbol{\mu}(\mathbf{x}_{l,i}^{-1})$ is the magnitude of the complement of $\boldsymbol{\mu}(\mathbf{x}_{l,i}^{+1})$. This corresponds to the hypotheses that $\mu(\mathbf{x}_{l,i}^{+1})$ or $\mu(\mathbf{x}_{l,i}^{-1})$ was transmitted, respectively. $\boldsymbol{\mathcal{A}}_{l,i}^{\pm 1}$ denotes the set of symbols $\mathbf{x}(\boldsymbol{c}) \in \boldsymbol{\mathcal{A}}$ for which $c_{l,i} = \pm 1$. The dependency of the metrics $\mu_l(\mathbf{x})$ on c is implicit. These metrics are defined as [106]:

$$\mu_l(\mathbf{x}) = -\frac{1}{N_0}\|\mathbf{y} - \mathbf{H}\mathbf{x}\|^2 + \sum_{l=1}^{N_L}\sum_{i=1}^{N_b} In(\Pr(c_{l,i})) - In(Pr(\mathbf{y})) \quad (3\text{-}26)$$

where N_b is the total number of bits in a codeword. The MAP estimate $\hat{\mathbf{x}}^{MAP}$ is the hypothesis which maximizes the metric $(\mathbf{x})$ over all possible choices of $\mathbf{x} \in \boldsymbol{\mathcal{A}}$. The corresponding bit vector is $\hat{c}^{MAP} \in \{-1, 1\}$. The maxLogAPP detection problem may thus also be stated in the form [103]:

$$L_p(c_{l,i}|\mathbf{y}) = \hat{c}_{l,i}^{MAP}(\mu(\hat{x}^{MAP}) - max_{\boldsymbol{x} \in \boldsymbol{\mathcal{A}}_{l,i}^{-MAP}}\{\mu(\mathbf{x})\} \quad (3\text{-}27)$$

where $\boldsymbol{\mathcal{A}}_{l,i}^{-MAP}$ is the set of all potential counter-hypotheses to the MAP estimate for layer l and bit position i. Counter-hypothesis refers to any symbol $\mathbf{x}(c) \in \boldsymbol{\mathcal{A}}$ with a bit value complementary to that of the MAP estimate at the considered layer l and bit position $i, c_{l,i} = -\hat{c}_{l,i}^{MAP}$. Clearly, the sign of the LLR for any bit $c_{l,i}$ is equivalent to the sign of $\hat{c}_{l,i}^{MAP}$ while its magnitude, and hence the reliability of the bit, is given by the difference between the metric of the MAP estimation and the metric of the best counter-hypotheses. Solving the maxLogAPP detection problem is thus equivalent to finding the MAP estimate and $N_L \times N_b$ counter-hypotheses.

In order to allow constructing the subset search list $\boldsymbol{\mathcal{L}} \subset \boldsymbol{\mathcal{A}}$ efficiently based on a tree search, the Euclidean distance part of the metric $(\mathbf{x})$ has to be reformulated such that it can be calculated using a back substitution process. This can be achieved by using the **QR-**

decomposition of the channel matrix for a MIMO system. Due to the upper triangular structure of **R**, the metric for any transmit signal **x** can now be written as sum of per-layer metric increments.

3.6.3 Classification of Tree Search Algorithms

Decoding algorithms which aim at maximizing a certain metric during a tree search can be categorized into three main classes: Metric First Search (MFS), Breadth First Search (BFS) and Depth First Search (DFS).

The Metric First Search keeps an (ordered) list of several nodes during the search while at the same time extending the node which currently has the largest path metric by its child nodes. The search stops when a predefined number of leaf nodes have been found or the number of list entries exceeds a certain limit. This approach is also known as Sequential Detection.

The Breadth First Search, also known as the K-Best algorithm, keeps a list of the best K nodes in the same layer of the decision tree, where K is the number of the best hypotheses (nodes) visited during the detection process. Unlike the MFS, the BFS constructs the tree on a layer-by-layer basis, i.e. it enumerates all siblings within the same layer before moving to the next layer. At each tree extension step, siblings of all parent nodes currently in the list are generated and sorted according to their path metrics. A certain predefined number of the nodes with largest metric are written back to the list and used for the next extension process. This algorithm is preferable in terms of hardware implementation since it has fixed complexity and memory usage. The BFS algorithm can achieve optimal solution by making K as large as the number of nodes over a layer, though at increased complexity. However, the main disadvantage of the breadth-first search algorithms is that the performance of MIMO in terms of BER is degraded, especially when the number of candidate symbols kept at each level, is small [20]. Moreover, although they provide constant throughput, the latency of decoding the received data is still quite long [20].

The Depth First Search is a strategy which considers only a single node at a time. The algorithm extends this single node vertically from the top layer to the bottom layer until the path metric falls below a certain threshold. It then back-tracks to previously considered layers and extends the tree in a different direction. Leaf nodes found during the search may be stored in a list, to enable the calculation of soft output. When the Schnorr-Euchner Enumeration Strategy is applied, the DFS algorithm allows solving the ML detection problem with a complexity far below the brute-force search. However, the computational complexity of the DFS algorithm is variable and high particularly in the low SNR region. The DFS will be described in detail in Chapter 5, where it is employed as an example of the Sphere Detection algorithm.

4. Sphere Decoding

4.1 Introduction

Sphere Decoding (SD) was originally discovered by Finke and Pohst [12] in 1985 as a strategy for solving the Closest Lattice Point Problem (CLPP) or Shortest Vector Problem (SVP) [107]. It was later adapted to solve other engineering and technological problems including communications, cryptography, Global Positioning Systems (GPS) [21], geodesy and land surveying [108]. The SD was first used in communications for soft decoding of the Golay code by Viterbo and Bigleri in 1993 [99]. Currently, it has emerged as the most powerful and promising means of finding the Maximum Likelihood (ML) solution to the detection problem for Multiple-Input Multiple-Output (MIMO) digital communication systems such as Orthogonal Frequency Division Multiplexing-MIMO (OFDM-MIMO) broadband systems. Unlike the ML detector whose complexity rises exponentially with the number of transmit and receive antennas, the complexity of the SD is polynomial for both finite and infinite lattices which makes real-time implementation of the ML detector practical.

The complexity of sphere decoding depends on the initial radius R_0 of the hyper-sphere which in turn determines the number of lattice points inside the hyper-sphere. To avoid the exponential complexity of the ML problem, the search for the closest lattice point is restricted to include only vector constellation points that fall within a certain search sphere or subset search list $\mathcal{L}$. This approach allows for finding the ML solution with only polynomial complexity, for sufficiently high SNR regimes [21].

In this chapter, a new framework for efficient ML solution using the SD characterized by the Depth-First-Search (DFS) algorithm and the traditional Successive Interference Cancellation

(SIC) strategy is proposed. Orthogonalisation of the channel matrix **H** using the Sorted **QR** Decomposition (SQRD) method is proposed to reduce the complexity. The use of SQRD will enable the generation of an upper triangular structure which will enable the detection of the most reliably received signals first. This will be achieved by sorting/ordering the received vector into an upper triangular structure, with the most reliable signal in the N^{th} layer. The advantage of the proposed method is that SQRD combines layer ordering into the matrix decomposition step at negligible overhead, and at the same time yields an optimised initial radius leading to increased efficiency of the proposed SD. The proposed strategy is also compatible with sequential tree-search detectors, as well as auxiliary preprocessing schemes such as the Minimum Mean Squared Error (MMSE), Vertical Bell Layered Space-Time (VBLAST) and Lattice Reduction Aided Detection (LRAD). These strategies will improve the reliability of the received signals and also serve as comparison techniques. Low Density Parity Check (LDPC) codes will be employed to stop error propagation in the SIC block.

4.2 The Sphere Detection Concepts

The basic principle of the SD is to search for the closest point among all the lattice points confined in a hyper-sphere of radius R_0 centered at the query or received point, where each codeword is represented by a lattice point in a lattice field. That is, it searches for the transmitted vector signal set that minimizes the Euclidean distance with respect to the received signal vector. This requires testing the Euclidean distance between each lattice point and the given central query point to determine whether it is smaller than the radius R_0 of the hyper-sphere or not [109]. The received vector is not however arbitrary, but is rather an unknown lattice point that has been perturbed by an additive noise vector whose statistical properties are known [21].

The SD enumerates all lattice points inside a hyper-sphere centred at a given received vector using either the Finke-Pohst (FP) or the Schnorr-Euchner (SE) enumeration strategies [17], [110]. It keeps track of only a single node of the tree at any given time. Figure 4-1 illustrates the principle of sphere detection where the empty circle is the received lattice point and the red circle is the Closest Lattice Point (CLP). The search criteria is based on calculating the minimum and maximum bounds for each point and scale increasingly all points until all lattice points are calculated, starting with initial radius R_0.

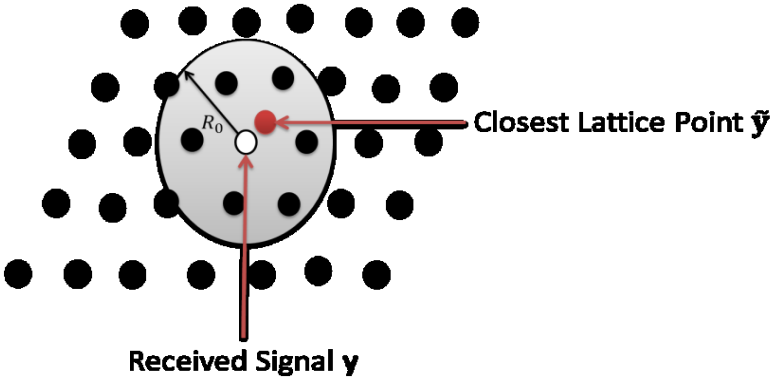

Figure 4-1 Geometrical representation of sphere detection algorithm

If no point is found inside the hyper-sphere, then the algorithm increases the radius of the sphere and restart again. This only arises when the chosen initial radius R_0 is less than the distance between the received signal (empty circle) and the CLP (red circle). It is important noting that choosing a large sphere radius leads to a sphere containing a very high number of hypotheses and counter-hypotheses, also referred to as candidates, and hence to high detection complexity. The problem which needs to be solved here is the so-called integer-least squares problem:

$$\hat{\mathbf{x}} = \boldsymbol{arg\,min}_{\mathbf{x}\in\mathcal{L}\subset\mathcal{A}}\|\mathbf{y}-\mathbf{H}\mathbf{x}\|^2 \tag{4-1}$$

This requires finding an optimal initial radius R_0, which only includes very few points inside the sphere or search space, ideally a single point. The distance between the query point and the lattice point in question is given by:

$$R_0^2 \geq \|\mathbf{y} - \mathbf{Hx}\|^2 \tag{4-2}$$

It will be shown later that this problem can be solved using a combination of the SIC-based QR decomposition and the tree based DFS detection algorithm.

4.3 Design Description

4.3.1 System Model

This thesis focuses on coded MIMO signals that have been transmitted over a MIMO channel using N_t transmit antennas and N_r receive antennas where $N_r \geq N_t$. Uncoded MIMO signals will also be investigated using this system model: a potential option for boosting system capacity as it avoids transmission of redundant bits. At the transmitter, the transmit vector $\mathbf{x}$ is transmitted over a MIMO channel. The received signal $\mathbf{y}$, can be modelled by (4-3):

$$\mathbf{y} = \mathbf{Hx} + \mathbf{n} \tag{4-3}$$

where $\mathbf{x} \in \boldsymbol{\mathcal{A}}^{N_r} = \left[x_1, x_2, \ldots, x_{N_t}\right]^T$ denotes the transmitted vector, $\mathbf{n} = \left[n_1, n_2, \ldots, n_{N_r}\right]^T$ is the vector for independent and identically distributed (i.i.d) (uncorrelated), circularly symmetric, complex Gaussian noise samples and $\mathbf{H}$ denotes the $N_r \times N_t$ channel matrix whose entries $h_{j,i}$ describe the coupling between the i^{th} transmit antenna and the j^{th} receive antenna, and $[\cdot]^T$ is the transpose operator. Figure 4-2 shows a typical MIMO system model described above. The block diagram in Figure 4-2 can be described as follows. The data streams are de-multiplexed at the transmitter into N_t parallel data streams (*layers*). The parallel data streams are then encoded by a terminated LDPC encoder before being bitwise interleaved by the bit interleaver π_i.

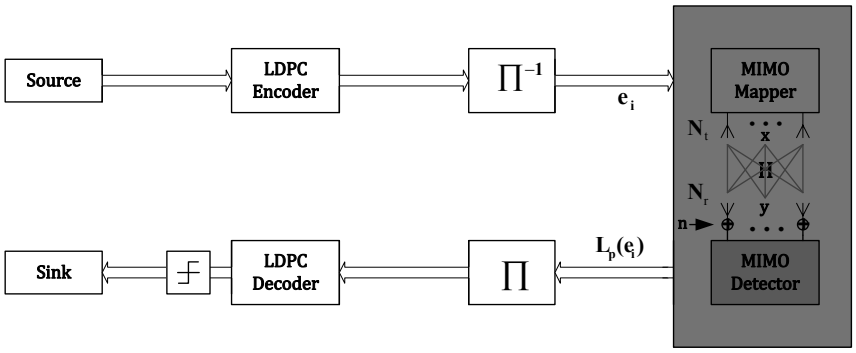

Figure 4-2 Block diagram of a complete MIMO System

The interleaved bits are then mapped to **M**-QAM symbols using the mapping function **M**. After mapping the symbols, the resulting transmit vector $\mathbf{x} = [x_1, x_2, \cdots, x_{N_t}]^T$ is mixed with the $N_t \times N_r$ channel matrix **H** before adding the $N_r \times 1$ noise vector $\mathbf{n} = [n_1, n_2, \cdots, n_{N_r}]^T$ to yield the received signal $\mathbf{y} = [y_1, y_2, \cdots, y_{N_t}]^T$. For a 4 × 4MIMO system, the components of the received signals can be analysed as follows:

$$y_1 = h_{1,1}x_1 + h_{1,2}x_2 + h_{1,3}x_3 + h_{1,4}x_4 + n_1 \tag{4-4}$$

$$y_2 = h_{2,1}x_1 + h_{2,2}x_2 + h_{2,3}x_3 + h_{2,4}x_4 + n_2 \tag{4-5}$$

$$y_3 = h_{3,1}x_1 + h_{3,2}x_2 + h_{3,3}x_3 + h_{3,4}x_4 + n_3 \tag{4-6}$$

$$y_4 = h_{4,1}x_1 + h_{4,2}x_2 + h_{4,3}x_3 + h_{4,4}x_4 + n_4 \tag{4-7}$$

The detection problem is to find the transmitted vector $\hat{\mathbf{x}}$ belonging to the set of all possible transmitted vector symbols $\boldsymbol{\mathcal{A}}$ which minimizes the Euclidean norm with respect to the received vector **y**, that is;

$$\hat{\mathbf{x}} = arg\, min_{\mathbf{x}\in\boldsymbol{\mathcal{A}}} \|\mathbf{y} - \mathbf{H}\mathbf{x}\|^2 \tag{4-8}$$

where $\hat{\mathbf{x}}$ is the estimate for the transmitted vector $\mathbf{x}$. This system model represents the original ML detection problem, which is computationally expensive. Since the closest lattice point in infinity lattice is also the closest point in a hyper-sphere of radius R_0, the ML detection problem can be reduced to a sphere detection problem in (4-1) which has been repeated in (4-9) for convenience:

$$\hat{\mathbf{x}} = arg\, min_{\mathbf{x}\in\mathcal{L}\subset\mathcal{A}} \|\mathbf{y} - \mathbf{H}\mathbf{x}\|^2 \tag{4-9}$$

where the search space is restricted to the subset search list $\mathcal{L}$. Furthermore $\mathbf{H}$ is a non-orthogonal random variable. Orthogonalisation of the channel matrix $\mathbf{H}$ using the Sorted $\mathbf{QR}$ Decomposition (SQRD) method is utilised in order to obtain an upper triangular structure which will enable the detection of the most reliably received signals first. The concept of sorting signals implies coupling the output of the OSIC detector to the input of the SD. Starting the detection process with the most reliably received signals increases the performance of schemes with fixed or upper bounded complexity [111] and reduces the complexity for schemes with variable complexity [92], [103]. Matrix decomposition enables the sorting/ordering of the received vector in an upper triangular structure, with the most reliable signal in the N^{th} layer. To achieve this, SQRD will be employed as it combines layer ordering into the matrix decomposition step at negligible overhead [93].

4.3.2 Tree representation of sphere decoding

The SD detector proposed in this Chapter is based on the Depth First Search (DFS) algorithm. A tree search representation will be used to illustrate how the proposed algorithm walks over the tree throughout the design. The sphere detection problem will be reformulated into a tree search problem by performing $\mathbf{QR}$ decomposition on the channel matrix, $\mathbf{H}$ [4]. This allows for the construction of an OSIC based subset search list $\mathcal{L}$ which minimizes the number of visited lattice points, thus reducing the complexity of the SD significantly.

4.3.3 OSIC-based QR Decomposition

The **QR** decomposition, also known as **QR** -factorization [21] is the decomposition of a matrix into an orthogonal matrix and an upper triangular matrix. It is normally used to solve integer least square (ILS) problems. The main advantage of decomposing the channel matrix is that a near-optimal solution can be achieved in low SNR regimes without enhancing noise as is the case in linear equalizers. That is, it orthogonalises the channel matrix **H**. The problem size can also be significantly reduced by breaking the problem into a number of sub-problems which are handy and easy to solve [21] and can lead to a much reduced complex system. This is done by establishing a valid range for each signal point as will be shown in Section 4.3.4. In this Chapter, OSIC-based **QR** decomposition will be employed to introduce performance and to reduce the complexity of the SD as follows:

$$\mathbf{H} = \mathbf{Q}\begin{bmatrix}\mathbf{R}\\ \mathbf{0}\end{bmatrix} = [\mathbf{Q_1}\ \ \mathbf{Q_2}]\begin{bmatrix}\mathbf{R}\\ \mathbf{0}\end{bmatrix} \tag{4-10}$$

where $\mathbf{R}$ is an $N_t \times N_t$ upper triangular matrix, $\mathbf{0}$ is a $(N_r - N_t) \times N_t$ zero matrix and $\mathbf{Q} = [\mathbf{Q}_1\ \ \mathbf{Q}_2]$ (for rectangular matrix) is an $N_r \times N_r$ orthogonal matrix with $\mathbf{Q_1}$ and $\mathbf{Q_2}$, are the first N_t and $N_r - N_t$ unitary orthogonal columns of $\mathbf{Q}$ respectively. By substituting (4-10) into (4-2) and multiplying with $\mathbf{Q}^H$, the Hermitian Transpose of $\mathbf{Q}$ results in (4-11):

$$R_0^2 \geq \left\|\mathbf{y} - [\mathbf{Q}_1\ \ \mathbf{Q}_2]\begin{bmatrix}\mathbf{R}\\ \mathbf{0}\end{bmatrix}\mathbf{x}\right\|^2 = \left\|\begin{bmatrix}\mathbf{Q}_1^H\\ \mathbf{Q}_2^H\end{bmatrix}\mathbf{y} - \begin{bmatrix}\mathbf{R}\\ \mathbf{0}\end{bmatrix}\mathbf{x}\right\|^2 = \|\mathbf{Q}_1^H\mathbf{y} - \mathbf{Rx}\|^2 + \|\mathbf{Q}_2^H\mathbf{y}\|^2 \tag{4-11}$$

(4-11) can be rewritten as:

$$R_0^2 - \|\mathbf{Q}_2^H\mathbf{y}\|^2 \geq \|\mathbf{Q}_1^H\mathbf{y} - \mathbf{Rx}\|^2 \tag{4-12}$$

where $\mathbf{Q}_1^H$ and $\mathbf{Q_2^H}$ are the respective Hermitian Transposition matrices for $\mathbf{Q}_1$ and $\mathbf{Q}_2$. Let $\tilde{\mathbf{y}} = \mathbf{Q}_1^H\mathbf{y}$ and $R_{SD}^2 = R_0^2 - \|\mathbf{Q}_2^H\mathbf{y}\|^2$, (5-12) can be written as:

$$R_{SD}^2 \geq \|\tilde{\mathbf{y}} - \mathbf{R}\mathbf{x}\|^2 \tag{4-13}$$

where R_{SD} is the new sphere radius conditioned on the initial radius R_0 and $\tilde{\mathbf{y}}$ is the estimate for the received signal $\mathbf{y}$. It can be seen from (4-13) that orthogonalising $\mathbf{H}$ yields a nice and handy upper triangular structure which permit OSIC detection of MIMO signals with low SNR regimes without enhancing noise in a tree search structure. This can be improved by sorting the upper triangular layers in decreasing order of the post-equalization SINR. This point will be illustrated clearly by means of an example in Section 4.3.5.

4.3.4 Upper and Lower Bound Sphere Radius

The DFS-based SD keeps track of only a single node of the tree at any given time. Provided that the search radius is large enough such that the hyper-sphere is not empty (i.e., contains at least a lattice point), the ML solution is clearly located inside the sphere and the hard output from the SD will be optimal in the ML sense. The condition which guarantees the existence of at least a single lattice point inside the hyper-sphere of radius R_{SD} centred at the received signal $\mathbf{y}$ can be obtained by applying the constraint:

$$R_{SD}^2 \geq \|\tilde{\mathbf{y}} - \mathbf{R}\mathbf{x}\|^2 = \sum_{i=1}^{N_L}\left(\tilde{\mathbf{y}}_i - \sum_{j=i}^{N_L} r_{j,i}\mathbf{x}_{i-l+1}\right)^2 = \sum_{l=1}^{N_L} d_l \tag{4-14}$$

where i is the number of columns in $\mathbf{R}$ and number rows in vectors $\tilde{\mathbf{y}}$ and $\mathbf{x}$. $j = l = 1, 2, 3, \cdots, N_L - 1, N_L$ is the number rows in $\mathbf{R}$. Clearly, the distance d_l of a lattice point from the received signal in layer l, should be greater than zero so that the cumulative sum of the distance metric increases in a positive sense as R_{SD}. Thus, the constraint on the overall per-layer distance can be applied as:

$$\left(\tilde{\mathbf{y}}_i - \sum_{j=i}^{N_L} r_{j,i}\mathbf{x}_{i-l+1}\right)^2 \leq R_{SD}^2 - \sum_{i=l+1}^{N_L} d_i = R_l^2\left([\mathbf{x}]_{N_l}^{l+1}\right) \tag{4-15}$$

where $R_l^2\left([\mathbf{x}]_{N_l}^{l+1}\right)$ is the remaining radius at the layer l if $[\mathbf{x}]_{N_l}^{l+1}$ has been used as a partial estimate for the transmit signal spanning layers $l+1$ through N_L. Expanding the left hand side of (4-15) backwards, starting from the $N_l = N_1$ layer to the first layer, yields [21]:

$$R_{SD}^2 \geq \left(\tilde{\mathbf{y}}_{N_l} - r_{N_l,N_l}\mathbf{x}_{N_l}\right)^2 + \left(\tilde{\mathbf{y}}_{N_l-1} - r_{N_l-1,N_l}\mathbf{x}_{N_l} - r_{N_l-1,N_l-1}\mathbf{x}_{N_l-1}\right)^2 + \cdots \tag{4-16}$$

Since the N_L^{th} row of the upper triangular matrix has a single non-zero term, the necessary condition for $\mathbf{Hx}$ to lie in a hyper-sphere can be obtained by considering the N_L^{th} term of the above expansion which is:

$$R_{SD}^2 \geq \left(\tilde{\mathbf{y}}_{N_L} - r_{N_L,N_L}\mathbf{x}_{N_L}\right)^2 \tag{4-17}$$

This leads to the constraint which determines the range of valid signal points. This condition is equivalent to $\mathbf{x}_{N_L}$ belonging to the interval [21]:

$$\left\lceil \frac{-R_{SD}+\tilde{\mathbf{y}}_{N_L}}{r_{N_L,N_L}} \right\rceil \leq x_{N_L} \leq \left\lfloor \frac{R_{SD}+\tilde{\mathbf{y}}_{N_L}}{r_{N_L,N_L}} \right\rfloor \tag{4-18}$$

Likewise, the $\mathbf{x}_{N_L-1)}$ term belongs to the interval:

$$\left\lceil \frac{-R_{SD}'_{N_L-1}+\tilde{\mathbf{y}}_{N_L-1|N_L}}{r_{N_L-1,N_L-1}} \right\rceil \leq x_{N_{L-1}} \leq \left\lfloor \frac{R_{SD}'_{N_L-1}+\tilde{\mathbf{y}}_{N_L-1|N_L}}{r_{N_L-1,N_L-1}} \right\rfloor \tag{4-19}$$

where $\tilde{\mathbf{y}}_{N_L-1|N_L}$ is the received signal conditioned to the already estimated symbol x_{N_l} and R'_{SD} is the new radius conditioned to initial radius R_{SD} . $\lceil\cdot\rceil$ and $\lfloor\cdot\rfloor$ denote the rounding up and rounding down (quantisation) operations respectively. The SD starts the tree search at layer N_L by applying the above constraints in (4-18) and (4-19). This iterative process can be repeated until when $x_{(1)}$ is found.The lower bound radius $R_{LSD} = \left\lceil \frac{-R_{SD}'_{L-1}+\tilde{\mathbf{y}}_{L-1|N_L}}{r_{N_L-1,N_L-1}} \right\rceil$ and upper bound radius $R_{USD} = \left\lfloor \frac{R_{SD}'_{N_L-1}+\tilde{\mathbf{y}}_{N_L-1|N_L}}{r_{N_L-1,N_L-1}} \right\rfloor$ of the SD can be estimated by the lower and

the upper limits of the inequality in (4-15) respectively. Due to rounding errors introduced by floating-point computations, the two radii contain errors [109]. Underestimation of R_{LSD} leads to decoding failure, on the other hand, overestimating R_{USD} leads to excessive computational burden. The distance d_{ML} between the ML lattice point and the received lattice point is proposed to overcome this hurdle.

4.3.5 The Depth Tree Search Algorithm

Now, consider a vector space $\mathcal{A}$ with N_L elements representing lattice points in an M-ary tree with N_L layers and k nodes per layer. The number of nodes per layer k increase down the tree from the root node to the leaf nodes. The DFS algorithm can be illustrated by a tree structure rooted at layer N_L with all branches emanating from each parent node in the tree until the leaf nodes are reached.

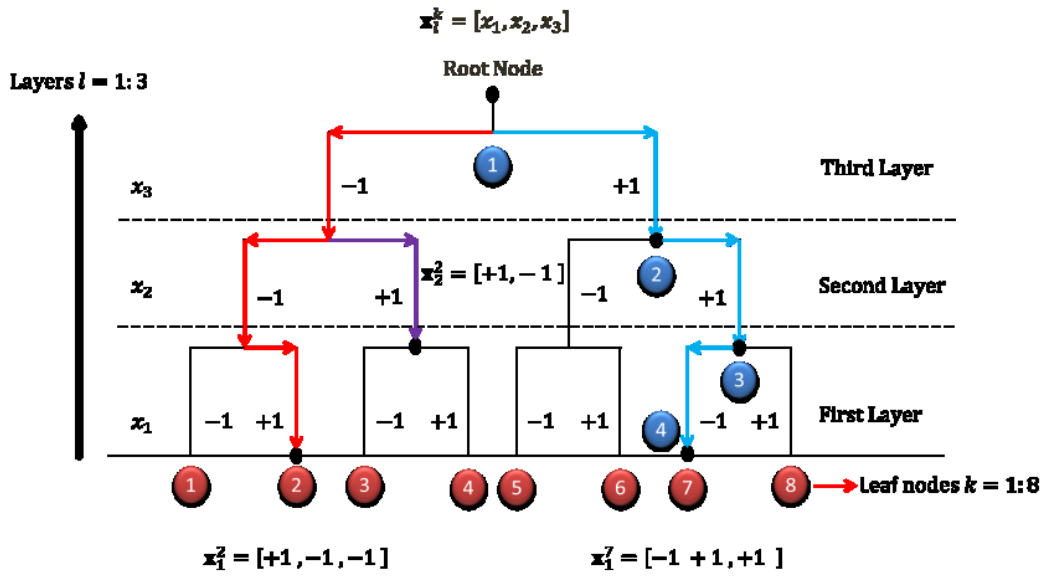

Figure 4-3 BPSK Binary Tree representation of sphere detection algorithm

Figure 4-3 shows how the process of sphere decoding can be represented by a binary tree of depth or height of $N_L + 1$, where $N_L = 3$, i.e., the algorithm walks through 4 nodes down from the root node to the leaf nodes; say from node 1 through to node 4 in blue circles. Note

that the binary tree represented in Figure 4-3 is up-side down and is a 2-ary tree (**M**=2) for Binary Phase Shift Keying (BPSK) signalling system.

Table 4.1 shows all the possible hypothesis and counter hypothesis that can be tracked from Figure 4-3.

Note that the number of entries in each hypothesis and/or counter hypothesis increases with each layer as the algorithm traverses the tree from the root node to the leaf nodes, i.e., from layer $l = 3$ down to $l = 1$. The candidates are drawn from the set $\mathbf{M} = \{-1, 1\}$ which resides in the generated lattice field and have been mapped using BPSK modulation schemes. The elements in set **M** correspond to 1 or 0 respectively.

Table 4-1 Hypothesis and counter hypothesis in the generated lattice field

Nodes	**Layers**		
	$l = 1$	$l = 2$	$l = 3$
$\boldsymbol{k = 1}$	$\mathbf{x} = [-1, -1, -1]$	$\mathbf{x} = [-1, -1]$	$\mathbf{x} = [-1]$
$\boldsymbol{k = 2}$	$\mathbf{x} = [+1, -1, -1]$	$\mathbf{x} = [+1, -1]$	$\mathbf{x} = [+1]$
$\boldsymbol{k = 3}$	$\mathbf{x} = [-1, +1, -1]$	$\mathbf{x} = [-1, +1]$	-
$\boldsymbol{k = 4}$	$\mathbf{x} = [+1, +1, -1]$	$\mathbf{x} = [+1, +1]$	-
$\boldsymbol{k = 5}$	$\mathbf{x} = [-1, -1, +1]$	-	-
$\boldsymbol{k = 6}$	$\mathbf{x} = [+1, -1, +1]$	-	-
$\boldsymbol{k = 7}$	$\mathbf{x} = [-1, +1, +1]$	-	-
$\boldsymbol{k = 8}$	$\mathbf{x} = [+1, +1, +1]$	-	-

The DFS algorithm based on the tree search in Figure 4-3 can now be described as follows: First, let $\mathbf{x}_l^{(k)} = \left[x_{1,l}^{(k)}, x_{2,l}^{(k)}, \cdots, x_{(N_L - l+1),l}^{(k)}\right]^T$ be a vector at the k^{th} node in the l^{th} layer of the tree, where $1 \leq k \leq M^{(N_L - l+1)}$ and $1 \leq l \leq N_L$. Then, a symbol vector $\mathbf{x} \in \boldsymbol{\mathcal{A}}^{N_L}$ can be represented by $x_1^{(k)}$ in the first layer of the tree at the k^{th} node. Let the Partial Euclidean Distance (PED) d_l of an $(N_L - l + 1)$-dimensional vector be $\mathbf{u_l} = \left[u_1, u_2, \cdots, u_{N_L - l+1}\right]^T$:

$$d_l = \sum_{i=1}^{N_L}\left(y_i - \sum_{i=j}^{N_L} r_{j,i}u_{i-l+1}\right)^2 \quad (4\text{-}20)$$

where j is the number of rows and i is the number of columns of r.The tree search is confined by the boundaries defined in (4-18) and repeated in (4-21) for convenience:

$$\left\lceil \frac{-R_{SD}+\tilde{y}_{N_L}}{r_{N_L,N_L}} \right\rceil \leq x_{N_L} \leq \left\lfloor \frac{R_{SD}+\tilde{y}_{N_L}}{r_{N_L,N_L}} \right\rfloor \quad (4\text{-}21)$$

The FP enumeration strategy starts at the $N_L{}^{th}$ layer, obtains the first estimate for $x_{N_{(L-1)}}$and then the algorithm proceeds to the next layer in the natural reverse order of the layers. It is clearly advantageous to exploit the upper triangular structure of r by first calculating the PED d_l for x_l among $\{x_j\}_{j=1}^{N_L}$ since the component y_l contains only x_l but not any other components, $\{x_j\}_{j=1}^{N_L-1}$, see example below in this section for clarity. The enumeration process is repeated until either no constellation point lies inside the remaining radius or a leaf node is found in layer $l = 1$. If the leaf node is found, the sphere detector goes back to the previous layer ($l = 2$)and selects the next signal point according to the enumeration strategy employed. For example in the case of BPSK where the search list in the hyper-sphere is $\boldsymbol{\mathcal{L}} \epsilon\{-1,1\}$, if the algorithm selects the signal point $x_2 = -1$ on its way **down** the tree and compute a sphere radius $R_{SD} = r_{2a}$based on this choice, it will select point $x_2 = 1$ on its way **up** the tree, compute a new radius $R_{SD} = r_{2b}$and compare the two radii r_{2a} and r_{2b}. Of two radii, the smaller radius represents the leaf node with a smaller Euclidean distance to the received signal **y**, i.e., the closest lattice point. The signal point corresponding to the smaller radius will be used as an improved estimate for the transmit signal x_2. The algorithm continues up and down in this zigzag fashion and stops once no further points lie inside the sphere radius and layer N_L is reached again, i.e., when the algorithm completes a cycle from layer N_L to $N_1$and back again to N_L.

To improve the efficiency of the algorithms, all nodes with distances larger than d_l (a parameter no smaller than $\hat{d} = \left\| \underline{\mathbf{y}} - \mathbf{R}\underline{\hat{\mathbf{x}}} \right\|^2$), can be pruned or discarded after computing the entire node distances at the ${N_l}^{th}$ layer, i.e., all nodes (and their descendants or child and grandchild nodes) outside the sphere will be discarded. If a node is discarded, the node and all its descendants will not be considered any more. Next, all the sibling node distances at the $(N_L - 1)^{th}$ layer stemming from parent nodes not discarded at the ${N_L}^{th}$ layer will be computed. If a node at the $(N_L - 1)^{th}$ layer has a distance larger than d_{N_L-1}, a parameter satisfying $\hat{d} \leq d_{N_L-1} \leq d_{N_L}$, it will be discarded. The vector selected at the first layer is the ML solution $\hat{\mathbf{x}}$.

From the above explanation, it can be seen that the decoding process sometimes goes up a level and sometimes goes down a level, but in different branches each time. It goes through the tree, except the root node, and performs Depth-First Searching. As an example of the Depth First Search sphere detection algorithm, consider three inputs Binary Phase Shifting Keying (BPSK) vector $\mathbf{x}$ with levels $\boldsymbol{\mathcal{L}} \epsilon\{-1,1\}$ mixed and transmitted according to the channel matrix:

$$\mathbf{H} = \begin{bmatrix} -0.97 & -0.09 & -0.29 \\ -1.51 & -1.68 & -1.13 \\ 1.41 & 1.14 & 0.4 \end{bmatrix} \tag{4-22}$$

The resulting received signal is:

$$\mathbf{y} = \begin{bmatrix} 0.747 \\ 2.49 \\ -2.40 \end{bmatrix} \tag{4-23}$$

The optimal solution $\hat{\mathbf{x}}$ to the detection problem is given by:

$$\hat{\mathbf{x}} = arg\, min_{\mathbf{x} \in \boldsymbol{\mathcal{L}} \subset \boldsymbol{\mathcal{A}}} \|\mathbf{y} - \mathbf{H}\mathbf{x}\|^2 \tag{4-24}$$

This solution can be obtained by decomposing or orthogonalizing the channel matrix **H** as follows:

$$\mathbf{H} = \mathbf{QR} = \begin{bmatrix} -0.425 & 0.839 & 0.341 \\ -0.662 & -0.545 & 0.515 \\ 0.618 & 0.007 & 0.786 \end{bmatrix} \begin{bmatrix} 2.2823 & 1.8540 & 1.1180 \\ 0 & 0.8323 & 0.3698 \\ 0 & 0 & -0.3666 \end{bmatrix} \tag{4-25}$$

$$\Longrightarrow \mathbf{Q}^H = \begin{bmatrix} -0.4250 & -0.662 & 0.618 \\ 0.8386 & -0.5447 & -0.0065 \\ 0.3408 & 0.5153 & 0.7863 \end{bmatrix} \tag{4-26}$$

The sphere detection algorithm searches for all bit sequences for which:

$$\|\mathbf{y} - \mathbf{Hx}\|^2 \leq R_0^2 \tag{4-27}$$

where R_0 is the search radius and for convenience, it is equal to 1 in this example. Combining (4-25) and (4-27) and then multiplying by $\mathbf{Q}^H$ yields:

$$\|\mathbf{Q}^H\mathbf{y} - \mathbf{Q}^H\mathbf{QRx}\|^2 = \|\hat{\mathbf{y}} - \mathbf{R}\hat{\mathbf{x}}\|^2 \leq R_0 \tag{4-28}$$

where:

$$\hat{\mathbf{y}} = \mathbf{Q}^H\mathbf{y} = \begin{bmatrix} -0.4250 & -0.662 & 0.618 \\ 0.8386 & -0.5447 & -0.0065 \\ 0.3408 & 0.5153 & 0.7863 \end{bmatrix} \begin{bmatrix} 0.747 \\ 2.49 \\ -2.40 \end{bmatrix} = \begin{bmatrix} -3.4475 \\ -0.7144 \\ -0.3494 \end{bmatrix} \tag{4-29}$$

$$\hat{\mathbf{x}} = \mathbf{Q}^H\mathbf{Qx} = \mathbf{I}.\mathbf{x} \tag{4-30}$$

$$\mathbf{Q}^H\mathbf{Q} = \mathbf{I} = \begin{bmatrix} 1 & 0 & 0 \\ 0 & 1 & 0 \\ 0 & 0 & 1 \end{bmatrix} \tag{4-31}$$

Equation (4-28) can be rewritten as:

$$\left\| \begin{bmatrix} -3.4475 \\ -0.7144 \\ -0.3494 \end{bmatrix} - \begin{bmatrix} 2.2823 & 1.8540 & 1.1180 \\ 0 & 0.8323 & 0.3698 \\ 0 & 0 & -0.3666 \end{bmatrix} \begin{bmatrix} \hat{x}_1 \\ \hat{x}_2 \\ \hat{x}_3 \end{bmatrix} \right\|^2 \leq 1 \tag{4-32}$$

with $R_0 = 1, \hat{\mathbf{x}} = [\hat{x}_1, \hat{x}_2, \hat{x}_3]^T, \hat{\mathbf{y}} = [-3.4475, -0.7144, -0.3494]^T$ and **R** equal to the upper triangular coefficient 3-by-3 matrix. Here, note the advantage of orthogonalising the channel matrix **H** using **QR** decomposition which yields a nice and handy upper triangular structure in equation (4-32). This enables the commencement of OSIC detection process on a layer-by-layer basis starting with the third layer $\hat{x}_3$ which represents the root of the tree according to the above example. It can be clearly seen that the N_L^{th} layer ($l = 3$), represented by the third row of the upper triangular structure, has only a *single non-zero element* with the other two elements equal to zero, i.e., $r_{3,1} = 0$ and $r_{3,2} = 0$: *a simplified structure*. The advantage of starting detection process on the N_L^{th} layer (at the root node) becomes clear in this example.

Overall, the sphere detection problem is concerned with finding the vector $\hat{\mathbf{x}} = [\hat{x}_1, \hat{x}_2, \hat{x}_3]^T$ (according to the above example) which satisfies the above inequality in (4-27), given **H** and **y**. Equation (4-27), which is an ILS problem, looks very simple at first sight. It is however a complicated problem which requires a sophisticated algorithm to produce a reliable solution particularly in multi-level signalling systems. Solving this problem involves testing each element in the vector $\hat{\mathbf{x}}$. First, starting with R_0, and ignoring $\hat{x}_1$ and $\hat{x}_2$ for the time being, $\hat{x}_3$ is computed. Next, ignoring $\hat{x}_1$ this time $\hat{x}_2$ is computed using search radius R_{SD} conditioned to the initial radius R_0. This process continues provided that the condition in (4-27) is satisfied until when all the points in the search space are visited or when a failure/erasure is declared. When a failure is declared, the algorithm restarts again with a larger radius. In practical communications systems, the search space contains many lattice points, which explains why the computational complexity of the ML detector increases with the number of visited points. Binary inputs where $\hat{x}_1, \hat{x}_2, \hat{x}_3$ can only take either -1 or 1 have been used in this example.

$$\mathbf{x}_l^{\mathbf{k}} = [x_1, \cdots, x_N]^T$$

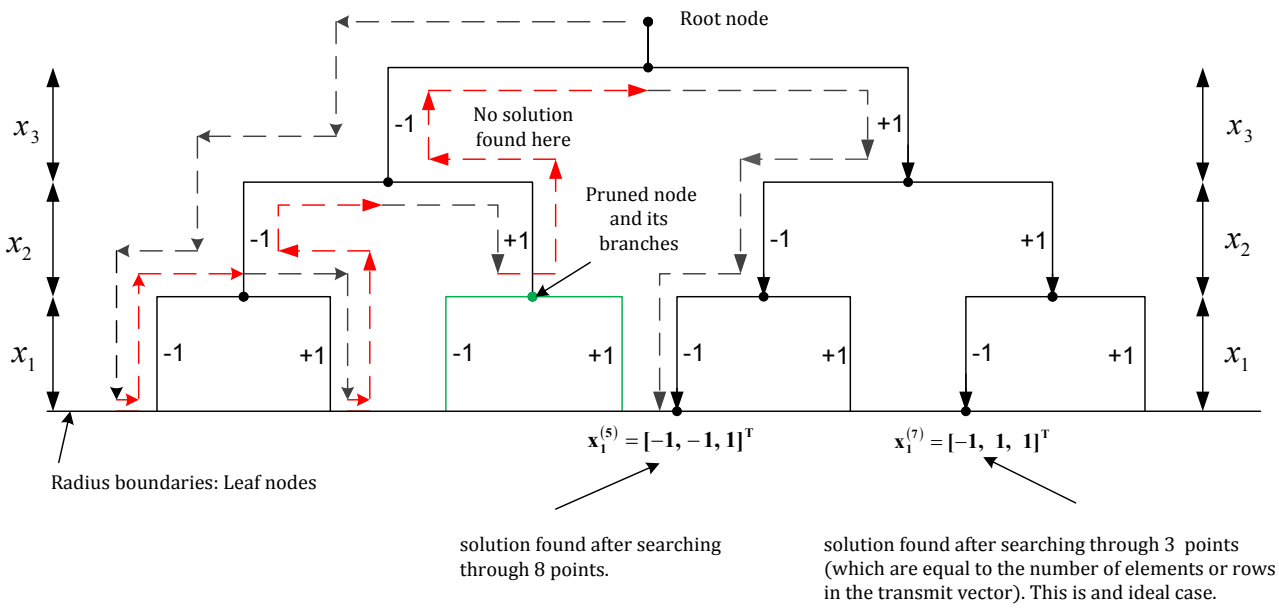

Figure 4-4 Binary Tree diagram illustrating Pruning and Depth-First-Search algorithm

Now, the rest of the depth search algorithm works as flows: Given that the element $r_{3,3}$ or $\hat{x}_3 = -1$ then:

$$\|-0.3494 + 0.3666\hat{x}_3\|^2 = \|-0.3494 + 0.3666.(-1)\|^2 \leq 1 \text{ or } 0.0716 \leq 1 \qquad (4\text{-}33)$$

This means that $\hat{x}_3 = -1$ can be a possible solution to the detection problem. However, it can only be concluded that -1 is a solution for $\hat{x}_3$ after testing all values (-1 or 1) for $\hat{x}_1$ and $\hat{x}_2$ (and for $\hat{x}_3 = 1$) which satisfy the inequality in (4-27), i.e., the values of $\hat{x}_1, \hat{x}_2, \hat{x}_3$ that jointly satisfy (4-27) with the least distance from the received point. Equation (4-33) gives the cost function of $\hat{x}_3$ as 0.0172. Figure 4-4 illustrates how the sphere decoding algorithm in this example walks through the proposed binary tree. The red arrows indicate backtracking where the computed Partial Euclidian Distance (PED) is greater than the proposed initial radius whereas the nodes and branches highlighted in green indicate the pruned or discarded nodes and their subsequent descendants. The dotted arrows highlighted in grey and the black

continuous arrows represent all the nodes whose PED satisfied the condition imposed by (4-28).

If there are more than one set of vectors that satisfy the condition in (4-27), then the one with the minimum Euclidean distance d from the received vector is chosen as the best possible or ML candidate according to Figure 4-5, i.e., the solution is $\mathbf{x_1^5} = [-1, -1, 1]^T$ where $d = d_1$ since $d_1 < d_2$. Note also that the tree is upside-down, with the root on top of the tree.

Note that two-level (binary or BPSK) signalling or modulation scheme have been used in this example. However, multi-level signalling schemes such as QAM, 16-QAM, 64QAM, 8PSK, 16PSK, etc., can be used instead.

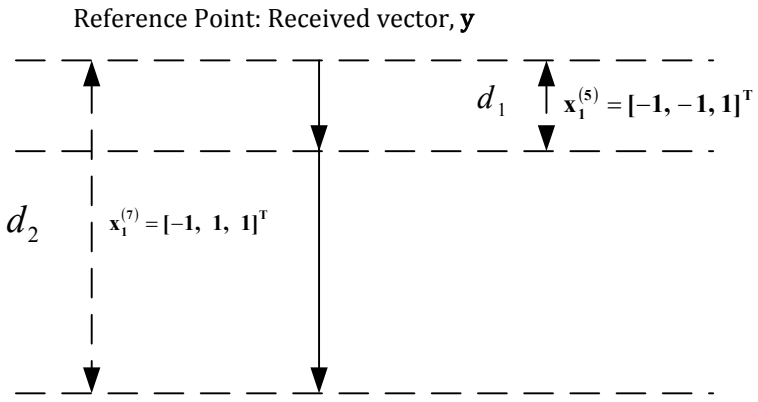

Figure 4-5 Illustration of selection of the best candidate in sphere detection

Multi-level signalling techniques increase the number of constellation or lattice points, thus increasing the complexity of the sphere detector significantly and at the same time reducing the reliability of the received signals. However the complexity of the sphere detector can be reduced by employing the Schonner-Euchner enumeration strategy and tree pruning.

Further to this, the selection of the best candidate proposed in Figure 4-5 is based on fixed initial sphere radius. Since fixed initial sphere radius is not the most efficient method of solving the sphere detection problem, the extended MMSE adaptive initial sphere radius is

proposed to avoid a scenario where the tree search ends up with more than one set of candidates satisfying the condition in (4-27) where a single candidate is required.

4.4 Optimization Techniques

The order in which the child nodes are added to the parent node in the extension process has a major impact on the complexity of the tree search detection schemes. Firstly, the enumeration strategy will influence the number of nodes visited during the search for some of the schemes. Secondly, efficient enumeration strategies avoid calculating branch metrics for paths which are subsequently discarded. Many of the proposed schemes have been developed in the context of the sphere detection. However, it will be shown that they are also applicable to other tree search schemes.

4.4.1 Finke-Pohst Enumeration Strategy

Let $z_l = \tilde{\mathbf{y}}_l - \sum_{n=l+1}^{N_l} r_{l,n}\mathbf{x}_n$ be the interference reduced signal at layer l in the tree search, and let $s_a, \cdots, s_b \in \boldsymbol{\mathcal{A}}$ be the set of possible choices for $\mathbf{x}_l$ in this layer, i.e., the set of potential child nodes, with $s_a < \cdots < s_b$.Then the Finke-Pohst enumeration [12] can be defined as the strategy which considers the possible choices s_i in the natural order, starting with s_a until when s_b is found. Figure 4-6 illustrates the Finke-Pohst enumeration strategy where four signal points are considered. It enumerates the symbols starting from s_1 through to s_4 in the natural order.

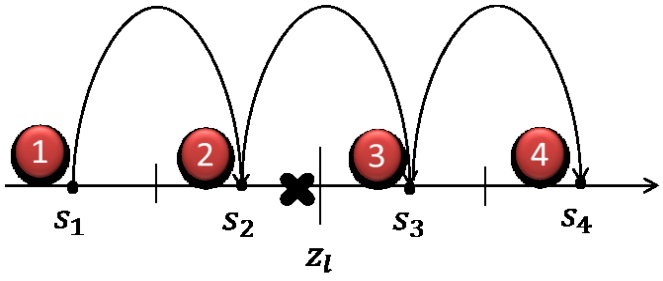

Figure 4-6 Illustration of the Finke-Pohst Enumeration Strategy

4.4.2 Schnorr-Euchner Enumeration Strategy

Alternatively, the points can be ordered in ascending order of their Euclidean distance. Hence, they will be enumerated in a zigzag manner starting from the signal point closest to z_l, which is, s_2 as shown in Figure 4-7. It then proceeds on to the next closest point to z_l i.e., s_3, through to s_1 and finally to s_4. This strategy was originally developed by Schnorr and Euchner [103] and has later been reinvented in [104], [112]. Schnorr-Euchner enumeration is intuitively preferred over the Finke-Pohst enumeration, as it effectively implements a largest branch metric first enumeration strategy for Euclidean distance part of the metric and also avoids having to explicitly calculate the branch metrics for all considered signal points to obtain the correct order of enumeration [16], [113]-[115].

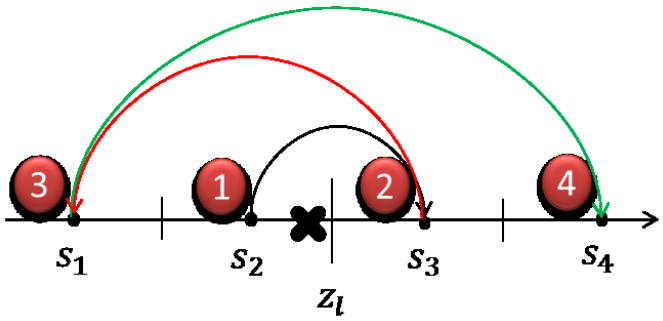

Figure 4-7 Illustration Schnorr-Euchner Enumeration Strategy

From the definition of the branch metrics, it also becomes clear that implementing such a strategy will then require the explicit calculation of the branch metrics for all considered constellation points, at least for the case of multi-level modulation.

4.4.3 Tree Pruning

The tree search complexity can be further reduced by pruning branches from the tree for which it can be assured that they do not contain any leaf nodes inside the current sphere radius. This can be done by establishing a lower bound on the branch metrics which are required to reach a leaf node from the currently considered node. If this lower bound exceeds

the remaining search radius, any nodes lying in the considered branch can be excluded from the search without sacrificing optimality in the ML sense. This permits reduction of the number of visited nodes in the low SNR regime at the expense of the effort invested in determining the lower bounds, which involve using convex relaxation of semi-definite programming method [116]-[117].

On the other hand, branches from the tree which are unlikely to contain leaf nodes can be pruned. This approach can result in some loss in performance. The sphere radius is adapted such that it increases as the algorithm explores paths of higher length, motivated by the fact that paths of higher length have also larger accumulated Euclidean distance. A reasonable choice for the radius adaptation rule is obtained by considering the per-layer distance metric of the ML solution.

4.5 Simulation Setup of the Proposed Sphere Detector

The proposed SD (PSD) controls the initial radius to ensure that no decoding failure occurs and that only a few number of lattice points are visited thus avoiding exhaustive search. It keeps track of the ML radius d_{ML}, the upper bound R_{UB} and lower bound R_{LB} radii of the conventional SD (CSD). If d_{ML} is smaller than R_{LB}, the initial radius of the PSD is given by d_{ML}. However if d_{ML} is larger than R_{LB}, the initial radius of the PSD is given by the average of d_{ML} and R_{LB}, otherwise is the initial radius of the PSD is given by the average of d_{ML} and R_{UB}.

MIMO signals are transmitted in blocks of data over uncorrelated flat fading MIMO channels. A random information source is used to generate a stream of independent and identically distributed (i.i.d.) information bits which are subsequently encoded using Low Density Parity Check codes of a code rate $R_C = {}^{K}/_{N} = 1/2$, where K is the number of

information bits and $N\ (=2K)$ is the sum of the information bits and parity check (redundant) bits. Note that the redundant bits constitute twice the information bits. The bit streams are then interleaved and divided into N_t blocks (sub-streams) of bits. The bit steams are mapped into L bits, where L denotes the number of bits per modulated symbol, resulting in $\mathbf{M} = 2^L$ different constellation points. 4-QAM and 64-QAM modulation schemes are applied on each sub stream as representatives for the respective low and high spectral efficiency regimes. The constellation points are finally mapped onto a vector transmit symbol $\mathbf{x} \in \mathbb{C}^{[N_t X\ 1]}$ whose components x_t are taken from some complex signal $\mathbb{C}$. It is also assumed that transmitter and receiver are perfectly synchronized in time and frequency.

At the receiver, the proposed SD is used to detect the most likely vector $\mathbf{x}$ that was transmitted based on prior knowledge of $\boldsymbol{y}$, $\mathbf{H}$, and the statistics of noise $\mathbf{n}$ where $\boldsymbol{y} \in \mathbb{C}^{[N_r \times 1]}$ is the received signal, $\mathbf{H} \in \mathbb{C}\ (N_r \text{ x } N_t)$ is the channel matrix, and $\mathbf{n} \in \mathbb{C}^{[N_r \times 1]}$ is the receiver noise, the entries of $\boldsymbol{y}$, $\mathbf{H}$ and $\mathbf{n}$ are zero-mean, circularly symmetric complex Gaussian random variables, and the entries $h_{i,j}$ of $\mathbf{H}$ are normalized to have unit variance. The average energy per transmit symbol is denoted by E_s. The corresponding average energy per bit is denoted by E_b while the double-sided power spectral density of the complex noise (N_O/ 2 per real dimension) is denoted by N_o. The signal-to-noise ratio is thus given by SNR = $\boldsymbol{E_S/N_O}$.

4.6 Performance Results and Discussion

The BER performance of the proposed PSD is evaluated by comparing it with the ML and conventional CSD and MMSE-SIC detection scheme. Figure 4-8 (a) shows the performance results for uncoded 4x4 MIMO systems with 4-QAM and 64-QAM transmission setups. The simulations compare the performance of the PSD detector characterised by the DFS algorithm, with the ML, CSD and the MMSE-SIC detectors. It can be clearly seen that the

PSD approaches the ML performance to within 1dB in the whole SNR regime for both case of 4-QAM and 64-Qam transmission setups. The results in Figure 4-8 (a) show that the PSD scheme achieves performance improvement of about 3dB at a BER of 10^{-3} for the case of the 4-QAM compared to the performance of the suboptimal MMSE-SIC detection schemes. The MMSE-SIC detection schemes show poor performance as the modulation order increases. It can also be seen that the performance of the MMSE-SIC detector gets worse compared to both the ML and the SD as the SNR increases. The poor performance can be attributed to interference and/or strong noise enhancement, which often results from ill-conditioned channel matrix **H** and error propagation which occurs in the SIC simulation block.

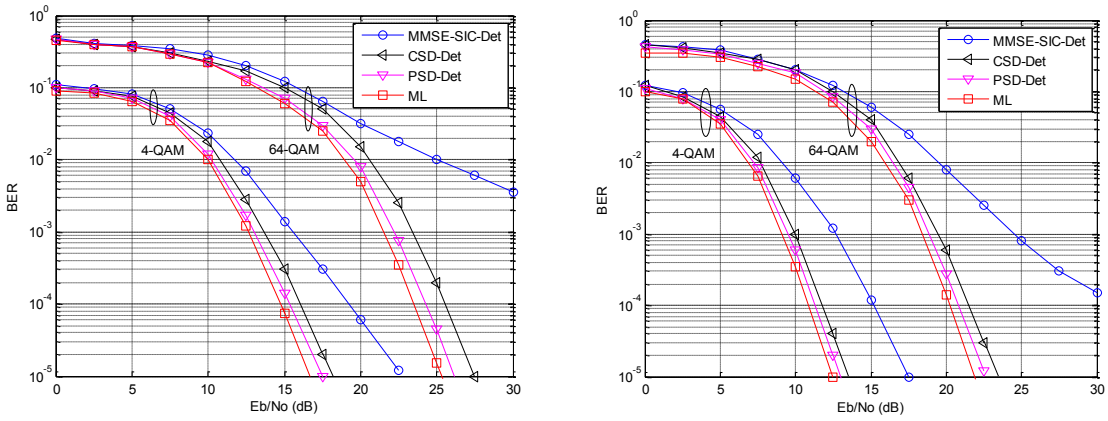

(a) Uncoded 4x4 MIMO System Setup **(b) Uncoded 4x6 MIMO System Setup**

Figure 4-8 Performance comparison for 4x4 and 4x6 MIMO Setup for the proposed SD

Another possible reason for poor performance attributed to the modulation order. As the modulation order increases, the Euclidean distance between adjacent lattice points decreases. These lattice points gradually overlap, resulting in a phenomenon called Inter-Symbol-Interference (ISI). The overall effect is increased complexity. However, higher order modulation schemes can be attractive in applications where the goal is to achieve high data rates. The CSD complexity can be reduced by employing pre-processing schemes which include ZF, MMSE, MMSE-SIC or ZF-SIC while the performance can be boosted by

employing optimisation techniques such as tree pruning, Schnorr-Enumeration strategies and powerful coding schemes.

Figure 4-8 (b) shows the effect of equipping the transmitter with more antennas. As can be clearly seen in Figure 4-8 (b), the PSD benefits substantially from reduced error probability by equipping the transmitter with more antennas (6 transmit antennas in this case compared to 4 antennas in Figure 4-8 (a). By increasing the number of antennas to 6, the BER performance of the PSD at 10^{-3} improves by about 3dB. It has already been proved that equipping both the transmitter and the receiver with more antennas can result in significant increase in performance [7]. However, this is achieved at the expense of increased computational complexity of the detector.

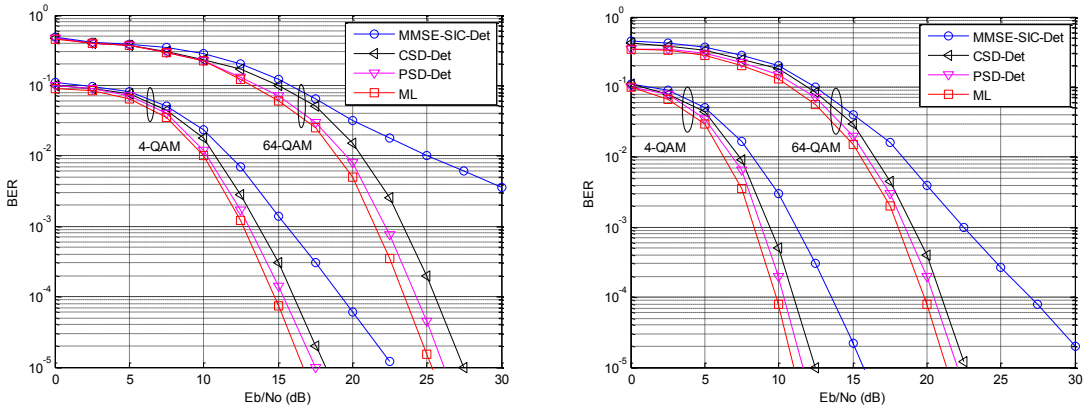

(a) Uncoded 4x4 MIMO System Setup (b) Coded 4x4 MIMO System Setup

Figure 4-9 Performance comparison for coded and uncoded 4x4 MIMO setup for the proposed SD

Figure 4-9 shows the BER results for an uncoded 4x4 MIMO and a ½ rate LDPC coded 4x4 MIMO setups where 4-QAM and 64-QAM modulation schemes were applied on each sub stream. The introduction of the state-of-the-art LDPC coding scheme results in substantial performance improvements for all the detection schemes. Thus the LDPC coding schemes are attractive in applications where low BER is the main target, though the performance gain is achieved at the expense of high complexity. It can also be clearly seen that low order

modulation schemes perform better than higher order modulation schemes at the cost of bandwidth inefficiency.

4.7 Summary of the Sphere Decoder Results

Performance improvement of the PSD can be achieved by employing the Schnorr-Euchner sphere detector which successively refines the search radius as new leaf nodes are found inside the sphere. Although the PSD can achieve optimal performance with much lower complexity compared to the ML detector, the computational complexity of the PSD schemes is variable and still high particularly in the low SNR region. The average complexity of the CSD can be significantly reduced by employing MMSE based pre-processing and SIC layer ordering. This also substantially reduces variations in the tree search complexity. Both average and worst case complexity can be further reduced in the low SNR regimes by combining MMSE-SIC pre-processing with tree pruning. The average complexity is then largely independent of the operating SNR. The topic of complexity analysis will be dealt with in Chapter 6. It is important noting that the tree search complexity increases as the target error rate is decreased. ML performance can be retained by using MMSE-SQRD pre-processing and by using tree pruning.

4.8 Conclusion

A tree search MIMO SD detector based on the DFS algorithm was proposed in this chapter. The PSD can be used to estimate the ML solution. However, this is achieved at the detriment of the NP-hard complexity of the sphere decoder. This problem can be alleviated by splitting the SD computational complexity into a preprocessing step, though at the expense of negligible performance loss. MMSE-SIC pre-processing with layer ordering is essential to achieve a favourable performance-complexity trade-off. This can be achieved by employing QR Decomposition. In addition to the MMSE-SIC pre-processing, efficient enumeration

method such as Schnorr-Euchner enumeration can be used to substantially speed-up the tree search process. The average complexity is largely independent of the SNR. This complexity of the SD is dependent on the selection of the initial sphere radius. This aspect is addressed in Chapter 5 whiles the complexity analysis is discussed in Chapter 6. Nevertheless, the simulation results presented in this chapter are consistent with theory.

5. Initial Radius Selection

5.1 Introduction

The Sphere Decoder (SD) was introduced to perform Maximum Likelihood (ML) detection in real-time MIMO digital wireless communication systems [17]. Unlike the ML detector whose complexity rises exponentially with the number of transmit and receive antennas, the complexity of the SD is polynomial for both finite and infinite lattices which makes real-time implementation of the ML detector practical [24]. To avoid the exponential complexity of the ML problem, the search for the closest lattice point is restricted to include only vector constellation points that fall within a certain search sphere or subset search list $\mathcal{L}$. However, the major technical challenge of the SD detection technique is the determination of an optimal initial search radius R_0. The choice of the initial radius for the SD has a significant impact on the complexity and the performance of the SD. The selection of the initial radius is NP-hard itself particularly in MIMO setups where large signal constellations or many transmit and receive antennas are employed. If the chosen initial radius R_0 is too small, no lattice point is found inside the hyper-sphere, hence the SD algorithm has to declare an erasure or increase the search radius and restart again. This does not only imply that many nodes in the tree are searched twice, but the original problem of choosing the initial radius of the sphere still remains unresolved - this translate to a wastage of computational resources and thus increasing the detection complexity. Furthermore, when an erasure is declared, the SD cannot guarantee the optimal BER performance [118]-[120].

Conversely, choosing a large initial sphere radius leads to a sphere containing a very high number of lattice points, also referred to as candidates, thus leading to high detection

complexity. Research in the SD based detection schemes has shifted towards finding an optimal initial radius which reduces the search operations [19], [21], [106], [120]-[127].

Currently, there is no well-established technique for computing the initial search radius. However, several techniques for computing the initial radius have been proposed in the literature [21], [111]. A fixed sphere radius based on a scaled version of the mean random variable $r_c^2 = \alpha n\sigma^2$ (see section 5.4), is suggested in [21]. The adaptive radius approach starts with $R_0 = \infty$, sets the new radius to the Euclidean distance of any new leaf node found inside the current sphere radius and stops once no more leaf nodes are found inside the sphere instead of keeping the search radius fixed [111]. The distance between the lattice point mapped by Minimum Mean Squared Error (MMSE) solution and the received signal is proposed initial radius in [118], [111]. The MMSE radius guarantees the existence of at least a single lattice point in the hyper-sphere, thus avoiding decoding failure. The MMSE utilizes the result of **QR** decomposition to obtain a suboptimal solution and selects the distance between the received signal and the lattice point mapped by the suboptimal solution as R_0. However, the determination of the number of lattice points inside the sphere remains a mystery.

In this Chapter, a simple Schnorr-Euchner SD (SE-SD) with a new Extended Minimum Mean Squared Error (EMMSE) radius is proposed. The initial radius proposed in this thesis is based on variable parameter α and the new scaled variance of the noise σ_n. The proposed initial radius also depends on the noise power spectral density N_0, number of transmit antennas N_t and the energy per transmitted symbol E_s. First, the total noise power spectral density is computed at the receiver by multiplying the noise spectral density of each symbol by the number of antennas at the transmitter. The new version of the SNR is then calculated by dividing the energy per symbol by the total noise power spectral density. The variable

parameter α is then computed using the probability of the existence of a lattice point inside a sphere (see Section 5.4). Using the variable parameter α, a new noise covariance matrix which incorporates the number of transmit antennas, the energy of the transmitted symbols and the channel matrix is calculated by multiplying by the variable parameter α and the square-root of the new SNR.

The new covariance matrix is then incorporated into the EMMSE model to reduce the impact of noise superimposed on MIMO signals (see Section 5.4). The EMMSE radius is finally found by computing the distance between the sphere centre and an improved EMMSE estimate. This distance can be fine-tuned by varying the variable parameter α to adjust the number of visited lattice points in the hyper-sphere. To further reduce the complexity of the SD, the proposed method utilizes the result of **QR** decomposition which is inherent in the SE-SD proposed in the previous chapter, thus no extra processing is required. The proposed method does not only reduce the complexity of the SD, but also improves the bit error rate performance of the SD, particularly at low SNR.

The rest of this chapter is organised as follows. First, different initial radius techniques proposed in the literature are presented. This will be followed by the design description of the proposed initial sphere radius. Second, the feasibility of the proposed method will be demonstrated by comparing the proposed initial radius with conventional SD radius and with other methods proposed in the literature. Finally, performance and complexity results are presented for the case of hard output detection for different initial radius methods.

5.2 Selection of Initial Sphere Radius

One of the major challenges posed by the Sphere Detection technique is the selection of the initial sphere radius [21]. It has also been difficult to predict the number of lattice points inside the sphere. Researchers are currently faced with the determination of the initial sphere

radius. The determination of the initial sphere radius has so far proved hard to address. However, a natural candidate for the sphere radius is the smallest radius that guarantees the existence of a lattice point inside the sphere for any received vector. Several sphere radius selection criteria based on fixed search radius [19], [21], [119]-[121] and adaptive search radius [104] have been proposed.

The conventional SD (CSD) initial radius is based on the noise variance σ^2 and is given in [121], [18] as $r^2 = \alpha n\sigma^2$, where $n = 2\max(N_t, N_r)$, $\alpha > 1$ is an experience based figure. This choice of the initial radius is based on the statistical properties of noise to avoid NP-hard problems associated with a channel matrix-based initial radius. An important advantage of a noise variance-based radius compared to an initial radius based on the channel matrix **H** is the reduction of the computational complexity [18]. Complexity aspects of the CSD will be dealt with in detail in Chapter 6.

Qiao proposed a deterministic method for selecting an initial hyper-sphere radius for communication applications [19]. Another option of sphere radius proposed in [21], [122] is the distance between the Babai estimate and the vector **Hx**, i.e. $R_B = \|\mathbf{y} - \mathbf{H}\hat{\mathbf{x}}_{\boldsymbol{B}}\|$, where $\hat{\mathbf{x}}_{\boldsymbol{B}}$ is the Babai estimate for the transmit vector **x**.The Babai radius R_B guarantees the existence of at least one lattice point inside the sphere, thus avoiding decoding failure. However, this method does not specify the number (whether few or too many) of lattice points inside the sphere [21]. In addition to this problem, the Babai method may produce a too small radius due to the rounding errors in floating-point computation and cause sphere decoding failure [108], that is, declaration of an erasure. Thus, the selection of the initial radius remains a challenge to the CSD detection problem. The target goal of the selection of an optimal initial radius is to reduce the complexity of the CSD. If an optimal radius (the radius of a sphere

with a single point) is obtained, then the MIMO detection problem would be completely solved. A brief overview of the fixed and adaptive radius is provided in the next sections.

5.2.1 Fixed Radius Search

One way of determining a reasonable choice of R_0 in order to find the ML solution only is to consider the distance d_{ML} between the ML solution and the received signal point. Since the ML solution is the point which minimizes the Euclidean distance to the received signal, d_{ML} is the upper bounded by the distance between the noisy received signal $\mathbf{Hx}$ and $\mathbf{y}$, respectively:

$$d_{ML}^2 = min_{\mathbf{x}_{i\in\chi}}\|\mathbf{y}-\mathbf{H}\mathbf{x}_i\|^2 = \|\mathbf{y}-\mathbf{H}\hat{\mathbf{x}}^{ML}\|^2 = \|\mathbf{H}(\mathbf{x}-\hat{\mathbf{x}}^{ML})+\mathbf{n}\|^2 = d_x^2 \quad (5\text{-}1)$$

where $\mathbf{y} = \mathbf{Hx} + \mathbf{n}$ and $\mathbf{x}_i$ is the i^{th} component in the vector $\mathbf{x}$. Observe that $d_x = \|\mathbf{y} - \mathbf{Hx}_i\|$ is chi-square distributed with N_{2r} degrees of freedom. Different authors [121], [18] suggest choosing the sphere radius to be a scaled version of the mean random variable, $R_0^2 = kN_rN_o$. The constant $k(P_{ML})$ is chosen such that the sphere contains ML solution with probability of at least P_{ML} [21]:

$$P_{ML} = \Pr(d_{ML} < R_0) \geq \Pr(d_x < R_0) = \int_0^{kN_rN_0,} \frac{\xi^{N_r-1}}{N_0^{N_r}\Gamma(N_r)} e^{-\frac{\xi}{N_0}} d\xi \quad (5\text{-}2)$$

The structure of the involved lattice (i.e., the realization of **H** and the signal set employed at the transmitter) is not taken into account when fixing the search radius based in (5-1). Since the number of nodes inside the sphere does depend on the lattice structure [18], [124], following this approach will not necessarily minimize the complexity of the tree search.

Alternatively, the search radius may be determined based on the Euclidean distance of an initial estimate of **x,** which can, for example, be obtained by linear detection [119]. This approach avoids running the search multiple times, as the distance of the ML solution is a

lower bound on the distance of any estimate on the transmit signal. However, the number of lattice points found may still be very large, and the additional overhead for determining the estimate must be invested.

The abovementioned approaches consider only the problem of finding ML solution and show large fluctuations in the number of nodes visited during the tree search. Both problems have been addressed in [125] where the knowledge about the lattice structure is used to establish an estimate of the number of leaf nodes found inside a sphere of the given radius. The radius can be successively refined based on this information, until a certain desired number of leaf nodes are found. The variance in the number of visited nodes can be substantially reduced by applying this technique. The number of visited nodes is independent of the chosen enumeration strategy for this approach.

5.2.2 Adaptive Radius Search

An elegant and efficient way to solve the radius determination problem is obtained by a small extension of the sphere detection algorithm [106]. Instead of keeping the search radius fixed, it is set to the Euclidean distance of any new leaf node found inside the current sphere radius [106], [103]. The search may thus be started with $R_0 = \infty$ and stops once no more leaf nodes are found inside the sphere.

The number of nodes visited when using this approach depends crucially on the choice of the enumeration strategy. It may in principle also be used with a Fincke-Pohst enumeration strategy. However, the sphere detector has to be started again from the root node every time the radius has been updated, such that many nodes will be visited multiple times [113]. Moreover, the number of found nodes is very high since this enumeration strategy always starts from the constellations point which is farthest away from the interference reduced signal. Both drawbacks are avoided by employing the Schnorr-Euchner enumeration strategy.

The first leaf node found will be the Babai point which is in many cases very close to the ML solution. Furthermore, the SD will not have to be restarted after the search radius has been tightened. Thus, very low detection complexity can be achieved with this scheme. This approach will be referred to as Schnorr-Euchner Sphere Detector (SE-SD) throughout this thesis.

5.2.3 System Model

A system model provided in Section 4.3.1 will be repeated in this section for convenience. The received signal vector transmitted over a MIMO system with N_t transmit antennas and N_r receive antennas is given by:

$$\mathbf{y} = \mathbf{H}\mathbf{x} + \mathbf{n} \tag{5-3}$$

where $\mathbf{x} \in \mathbb{C}^{N_t} = \left[x_1, x_2, \dots, x_{N_t}\right]^T$ and $\mathbf{y} \in \mathbb{C}^{N_r} = \left[y_1, y_2, \dots, y_{N_r}\right]^T$ are the respective N_t-dimensional and N_r-dimensional transmitted and received complex vectors whose entries have real and imaginary parts that are integers, $\mathbf{H} \in \mathbb{C}^{N_r \times N_t}$ denotes the $N_r \times N_t$ channel matrix whose entries $h_{j,i}$ describe the coupling between the i^{th} transmit antenna and the j^{th} receive antenna, i.e., the Eigen modes of the MIMO channel. $\mathbf{n} \in \mathbb{C}^{N_r} = [n_1, n_2, \dots, n_r]^T$ is the independent and identically distributed (i.i.d) circularly symmetric, complex additive white Gaussian noise (AWGN) vector with zero-mean and covariance matrix $\sigma^2\mathbf{I}$ and $[\cdot]^T$ is the transpose operator. $\mathbb{C}$ denotes the set of complex numbers and $\mathbf{I}$ is the identity matrix. However, a real valued system will be considered in this thesis for simplicity. The elements of the vector $\mathbf{x}$ span an N_t-dimensional rectangular lattice $\mathcal{Z}^{N_t}$, where $\mathcal{Z}$ denote the set of integers. This system can be represented by the block diagram in Figure 5-1. The detection problem here is to find the vector $\hat{\mathbf{x}}$ belonging to the set of all possible transmitted vector symbols $\mathcal{Z}^{N_t}$ which minimizes the Euclidean norm with respect to the received vector $\mathbf{y}$, that

is, to find the lattice point **Hx** which is closest to **y**. Assuming **H** is known at the receiver, detection is carried out as:

$$\hat{\mathbf{x}} = arg\, min_{\mathbf{x}\in \mathcal{Z}^{N_t}} \|\mathbf{y} - \mathbf{H}\mathbf{x}\|^2 \tag{5-4}$$

where $\hat{\mathbf{x}}$ is the estimate for the transmitted vector **x**.

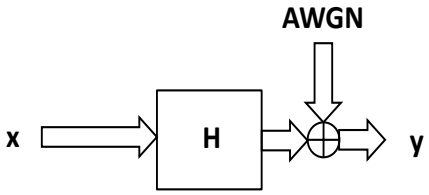

Figure 5-1 ML block diagram

The problem is further complicated as the received N_t-dimensional vector **Hx** , which spans a skewed lattice, has non-integer entries. This can be overcome by the process of quantization or slicing [18]. The system modelled by (5-4) represents the ML detection problem, which is computationally expensive for large constellations and large N_t and N_r thus rendering the ML detection impractical. This problem can be alleviated by restricting the search space to $\mathcal{L} \subset \mathcal{Z}^{N_t}$. However, the number of lattice points in $\mathcal{L}$ is still high. To demonstrate the above point, an example of a simple 4×4 space-time coded MIMO system which spreads $min(N_T,N_R)$T = 16 complex symbols from a 16-QAM constellation over T = 4 channel uses [61] is given where the code rate is $R_c = {}^{16}/_{4} \times \log_2 16 = 16$. The corresponding lattice generating matrix **H** has $m = 2 \times min(N_T, N_R)T = 32$ rows and n = $2N_R$T = 32 columns. Therefore, the resulting integer least-squares problem corresponds to dimension $m = 32$ and the entries of **x** each take on 4 integer values, say, $\{-3; -1;\ 1;\ 3\}$. The number of lattice points in $\mathcal{L}$ is $4^{32} \approx 1.84 \times 10^{19}$. It is therefore vitally important to confine the search to a sphere of radius R_0 which only includes a few lattice points inside the sphere.

Instead of conducting a brute-force (exhaustive) ML search, the SD solves the ML detection problem by restricting the search space $\mathbf{x} \in \mathcal{Z}^{N_t}$ to those lattice points that lie inside a hyper-sphere of radius R_0 centred at the received vector $\mathbf{y}$. The SD enumerates all lattice points inside a hyper-sphere centred at a given received vector using either the Finke-Pohst or the Schnorr-Euchner enumeration strategies [17], [109]. It keeps track of only a single node of the tree at any given time. The SD concept stems from the fact that the closest lattice point in $\mathcal{Z}$ is also the closest point in a hyper-sphere. If no point is found inside the hyper-sphere, then the algorithm increases the radius of the hyper-sphere and restart again. It is important recalling that a large sphere radius leads to increased detection complexity and a small radius leads to decoding failure. Figure 5-2 illustrates the principle of sphere detection where the empty circle is the received point.

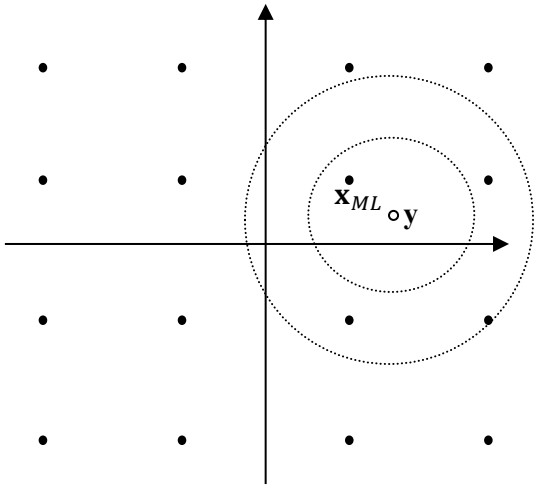

Figure 5-2 Geometric Representation of the Sphere Decoding Algorithm

The rest of this chapter provides a modification of the proposed SD (PSD) in Chapter 4, hence some of the equations used in Chapter 4 are repeated here for convenience. The SD detection problem can thus be expressed as:

$$\hat{\mathbf{x}} = \arg\min_{\mathbf{x} \in \mathcal{L} \subset \mathcal{Z}} \|\mathbf{y} - \mathbf{H}\mathbf{x}\|^2 \tag{5-5}$$

where $\mathcal{L}$ is the subset search space $\mathcal{Z}$.

Furthermore, the channel matrix $\mathbf{H}$ is a non-orthogonal random variable. The channel matrix can be orthogonalized by performing $\mathbf{QR}$ decomposition in order to obtain an upper triangular structure which enables the detection of the most reliably received signals first in a tree. Starting the detection process with the most reliably received signals increases the performance of schemes with fixed or upper bounded complexity [110] and reduces the complexity for schemes with variable complexity [92], [126]. Matrix decomposition also enables the sorting of the received vector in an upper triangular structure, with the most reliable signal in the N^{th} layer. This will be achieved by employing Sorted $\mathbf{QR}$ decomposition which combines layer ordering into matrix decomposition step at negligible overhead [93]. $\mathbf{QR}$ will be applied as follows [18]:

$$\mathbf{H} = \mathbf{Q}\begin{bmatrix}\mathbf{R_1}\\ \mathbf{0}\end{bmatrix} \tag{5-6}$$

where $\mathbf{R} = \begin{bmatrix}\mathbf{R_1}\\ \mathbf{0}\end{bmatrix}$ and $\mathbf{R_1}$ is an $N_t \times N_t$ upper triangular matrix, $\mathbf{0}$ is a $(N_r - N_t) \times N_t$ all-zero matrix and $\mathbf{Q}$ is an $N_r \times N_r$ orthogonal matrix. By multiplying the equation (5-1) with $\mathbf{Q^T}$, the Hermitian Transpose of $\mathbf{Q}$, the received signal can thus be written as:

$$\tilde{\mathbf{y}} = \mathbf{Q^T y} = \mathbf{Q^T Q R_1 x} + \mathbf{Q^T n} = \mathbf{R_1 x} + \tilde{\mathbf{n}} \tag{5-7}$$

where $\mathbf{Q^T Q} = \mathbf{I}$, the identity matrix and $\mathbf{Q^T n} = \tilde{\mathbf{n}}$ is the estimate of the noise. Equation (5-5) can be rewritten as:

$$\hat{\mathbf{x}} = \arg\min_{\mathbf{x}\in\mathcal{L}\subset\mathcal{Z}} \|\tilde{\mathbf{y}} - \mathbf{R_1 x}\|^2 \tag{5-8}$$

The SD radius R_{SD}^2 can thus be modelled by:

$$R_{SD}^2 \geq \|\tilde{\mathbf{y}} - \mathbf{R_1 x}\|^2 \tag{5-9}$$

The condition which guarantees the existence of at least a single lattice point inside the hyper-sphere of radius R_{SD} centered at the received signal $\mathbf{y}$ can be obtained by applying the constraint [18]:

$$R_{SD}^2 \geq \sum_{i=1}^{N_L}\left(\tilde{\mathbf{y}}_i - \sum_{j=i}^{N_L} r_{i,j}\mathbf{x}_i\right)^2 \tag{5-10}$$

where i represents the rows of $\tilde{\mathbf{y}}, \mathbf{R_1}$ and $\mathbf{x}$, and j represents columns of vectors $\mathbf{R_1}$, $N_L = N_t$ is the total number of layers in a tree structure. The details of the computation of the upper bound and the lower bounds of the signal space are provided in Section 4.3.4 in Chapter 4.

5.3 Linear detection schemes

The Zero-Forcing detector: A straightforward solution to the MIMO detection problem is to suppress the interference among the layers, i.e. the received data blocks. The Zero-Forcing (ZF) detector solves the unconstrained least-squares problem by multiplying the received signal by the Moore-Penrose pseudo-inverse $\mathbf{H}^{\dagger}$ of the lattice generating matrix to obtain $\hat{\mathbf{x}}$. Since the entries of $\hat{\mathbf{x}}$ are not necessarily integers, they can be rounded off to the closest integer, a process referred to as slicing [18] or quantization, to obtain:

$$\hat{\mathbf{x}}_{\mathrm{B}}=[\mathbf{H}^{\dagger}\mathbf{y}] \in \mathcal{Z} \tag{5-11}$$

where $\hat{\mathbf{x}}_{\mathrm{B}}$ is the Babai estimate and $\mathcal{Z}$ is the set of all constellation or lattice points. This strategy is also referred to as decorrelating [26] and is attractive where performance degradation due to noise enhancement can be accepted in order to achieve very low receiver complexity. The advantage of this detector is that it eliminates noise completely, i.e., it *'forces noise to zero'*, as its name suggests. Unlike the ML detector whose computational complexity per symbol rises exponentially with the number of multiple-access users, the decorrelating detector has a linear complexity per symbol. The receiver filter matrix $\mathbf{G}_{\boldsymbol{ZF}}$ can be expressed as [126]:

$$\mathbf{G_{ZF}} = (\mathbf{H}^{\boldsymbol{H}}\mathbf{H})^{-\mathbf{1}}\mathbf{H}^{\boldsymbol{H}} = \mathbf{H}^{\dagger} \tag{5-12}$$

where $\mathbf{H}^{\boldsymbol{H}}\mathbf{H} = \mathbf{G}$ is the Gram matrix and $\mathbf{H}^{\boldsymbol{H}}$ is the Hermitian transpose of the lattice generating matrix $\mathbf{H}$. Multiplying equation (5-12) with the received signal $\mathbf{y} = \mathbf{Hx} + \mathbf{n}$ yields:

$$\tilde{\mathbf{y}} = \mathbf{G_{ZF}}\mathbf{y} = \mathbf{G_{ZF}}\mathbf{Hx} + \mathbf{G_{ZF}}\mathbf{n} = \hat{\mathbf{x}} + \tilde{\mathbf{n}} \tag{5-13}$$

where $\tilde{\mathbf{n}}$ is the correlated noise at the ZF detector output. However, the ZF linear equalization shows poor performance particularly when the channel matrix $\mathbf{H}$ is ill-conditioned [126]. This problem can be solved by taking the receiver noise into account in the design of the filter matrix, i.e. the design of the MMSE detector.

The MMSE detector: The MMSE detector can be considered as the ZF detector which takes background noise into account and utilize the knowledge of received signal energies to improve detection. Unlike the ZF detector, the MMSE was designed to suppress noise enhancement and at the same time eliminate the residual interference. The linear mapping which incorporates noise minimizes the mean-squared error between the actual data and the soft output of the conventional detector by applying a partial or modified inverse of the correlation matrix. The MMSE optimization problem can be modelled as [127]:

$$\mathbf{G}_{MMSE} = \left(\mathbf{H}^{H}\mathbf{H} + {\sigma_n}^2\mathbf{I}_{N_t}\right)^{-1}\mathbf{H}^{H} \tag{5-14}$$

where ${\sigma_{\mathrm{n}}}^2\mathbf{I}_{N_t}$ is the $N_t \times N_t$ noise covariance matrix. The estimate for the transmitted signal can be obtained by applying the MMSE linear filter as follows:

$$\hat{\mathbf{x}} = \mathbf{G}_{MMSE}\mathbf{y} \tag{5-15}$$

The estimate $\hat{\mathbf{x}}$ can be remapped to a lattice point $\mathbf{H}\hat{\mathbf{x}}$ to yield:

$$\ddot{\mathbf{y}} = \mathbf{H}\hat{\mathbf{x}} = \mathbf{H}\mathbf{G}_{MMSE}\mathbf{y} \tag{5-16}$$

The MMSE initial radius can thus be modelled by:

$$R^2{}_{MMSE} = \|\mathbf{y} - \ddot{\mathbf{y}}\|^2 \tag{5-17}$$

5.4 The proposed sphere decoder

The method of choosing the initial radius based on the scaled variance of the noise proposed in [18] is given by:

$$r_c^2 = \alpha n \sigma^2 \tag{5-18}$$

where n is the degree of freedom of the random variable $\chi^2 = \left({}^{1}/_{\sigma^2}\right)\|\mathbf{y} - \mathbf{Hx}\|^2$. α is a variable parameter which is commonly based on experience and is chosen to ensure that at least a lattice point exists inside the sphere with a high probability. Throughout this thesis α will be referred to as the '*tuning factor'* (TF) in the proposed novel initial radius. This parameter can be determined from the computation of the probability of the existence of a lattice point inside a sphere as follows [8]:

$$\int_0^{\frac{\alpha n}{2}} \frac{\lambda^{\frac{n}{2}-1}}{\Gamma\left(\frac{n}{2}\right)} e^{-\lambda} d\lambda = 1 - \epsilon \tag{5-19}$$

$\Gamma(\cdot)$ is the gamma function. The parameter $1 - \epsilon$ is the probability of the existence of a lattice point in a sphere. It can be increased or decreased to vary α, which in turn fine tunes the radius to ensure the existence of quasi-optimal lattice points inside the sphere. It will be shown that the performance of the SD based on Schnorr-Euchner algorithm, i.e., the SE-SD [17], [109] will be improved significantly by using α to fine tune the proposed radius. From now on, the radius r_c will be referred to as the '*conventional radius*' and the proposed radius will be referred to as the '*novel radius*'. The corresponding SE-SD detectors will be referred to as the '*conventional SE-SD*' and the 'proposed *SE-SD*' respectively.

In the proposed method, the performance-complexity trade-off can be further enhanced, particularly in the low SNR regime, by using MMSE pre-processing [61] and taking into account the noise power spectral density of the received signal and the number of transmit antennas. An improved SD radius can thus be obtained by employing TF and the extended system model proposed in [128] where the respective $(N_t + N_r) \times N_t$ extended channel matrix $\bar{\bar{\mathbf{H}}}$ and $(N_t + N_r) \times N_t$ extended received vector $\bar{\bar{\mathbf{y}}}$ are denoted by:

$$\bar{\bar{\mathbf{H}}} = \mathbf{Q}\begin{bmatrix}\mathbf{H}\\ \sigma_n \mathbf{I}_{N_t}\end{bmatrix} \text{ and } \bar{\bar{\mathbf{y}}} = \begin{bmatrix}\mathbf{y}\\ \mathbf{0}_{N_t,1}\end{bmatrix} \quad \text{(5-20) [128]}$$

where $\mathbf{H}$ is the original $N_r \times N_t$ channel matrix and $\sigma_n = \alpha\sqrt{E_s/(N_t N_0)}$ is the new designed scaled variance of the noise based on the noise power spectral density N_0 and number of transmit antennas N_t. E_s is the energy per transmitted symbol, $\mathbf{I}_{N_t}$ is the $N_t \times N_t$ identity matrix and $\mathbf{y}$ is the original $N_r \times 1$ received vector. $\mathbf{0}_{N_t,1}$ is an all-zeros column vector of N_t elements.

Applying the ZF filter $\bar{\bar{\mathbf{G}}}_{ZF} = \left(\bar{\bar{\mathbf{H}}}^H \bar{\bar{\mathbf{H}}}\right)^{-1} \bar{\bar{\mathbf{H}}}^H$ to the above extended system model is equivalent to applying the MMSE filter $\mathbf{G}_{MMSE} = \left(\mathbf{H}^T\mathbf{H} + {\sigma_n}^2\, \mathbf{I}_{N_t}\right)^{-1}\mathbf{H}^T$ to the original system model as follows:

$$\bar{\bar{\mathbf{G}}}_{ZF}\bar{\bar{\mathbf{y}}} = \left(\bar{\bar{\mathbf{H}}}^H \bar{\bar{\mathbf{H}}}\right)^{-1} \bar{\bar{\mathbf{H}}}^H \bar{\bar{\mathbf{y}}} = \mathbf{G}_{MMSE}\mathbf{y} = \left(\mathbf{H}^H\mathbf{H} + \quad {\sigma_n}^2\, \mathbf{I}_{N_t}\right)^{-1}\mathbf{H}^H\mathbf{y} \quad \text{(5-21) [109]}$$

The extended system model can then be incorporated into **QR** detection algorithm for the purpose of tree search detection. This can be done by incorporating the MMSE extended channel matrix $\bar{\bar{\mathbf{H}}}$ into the Sorted **QR** Decomposition (SQRD).

$$\bar{\bar{\mathbf{H}}} = \bar{\bar{\mathbf{Q}}}\,\bar{\bar{\mathbf{R}}} = \begin{bmatrix}\bar{\bar{\mathbf{Q}}}_1 & \bar{\bar{\mathbf{Q}}}_3\\ \bar{\bar{\mathbf{Q}}}_2 & \bar{\bar{\mathbf{Q}}}_4\end{bmatrix}\begin{bmatrix}\bar{\bar{\mathbf{R}}}_1\\ \mathbf{0}\end{bmatrix} \quad \text{(5-22) [129]}$$

where $\bar{\bar{\mathbf{Q}}} \in \mathbb{R}^{\{(N_t+N_r)\times(N_t+N_r)\}}$, $\bar{\bar{\mathbf{R}}} = \begin{bmatrix} \bar{\bar{\mathbf{R}}}_1 \\ \mathbf{0} \end{bmatrix}$, $\bar{\bar{\mathbf{R}}}_1 \in \mathbb{R}^{(N_t\times N_t)}$, $\bar{\bar{\mathbf{Q}}}_1 \in \mathbb{R}^{(N_r\times N_t)}$, $\bar{\bar{\mathbf{Q}}}_2 \in \mathbb{R}^{(N_r\times N_t)}$, $\bar{\bar{\mathbf{Q}}}_3 \in \mathbb{R}^{(N_r\times N_t)}$, and $\bar{\bar{\mathbf{Q}}}_4 \in \mathbb{R}^{(N_r\times N_t)}$; $\mathbf{0}$ is a $N_r \times N_t$ matrix of all zeros. The Extended MMSE (EMMSE) radius $\bar{\bar{R}}_{MMSE}$ can then be computed based on the extended system model as follows:

$$\bar{\bar{d}}^2(\mathbf{x}) = \left\|\bar{\bar{\mathbf{y}}} - \bar{\bar{\mathbf{H}}}\mathbf{x}\right\|^2 = \left\|\bar{\bar{\mathbf{Q}}}_1^H\mathbf{y} - \bar{\bar{\mathbf{R}}}_1\mathbf{x}\right\|^2 + \left\|\bar{\bar{\mathbf{Q}}}_2^H\mathbf{y}\right\|^2 \tag{5-23}$$

$$\bar{\bar{d}}'^2(\mathbf{x}) = \bar{\bar{d}}^2(\mathbf{x}) - \left\|\bar{\bar{\mathbf{Q}}}_2^H\mathbf{y}\right\|^2 = \left\|\bar{\bar{\mathbf{Q}}}_1^H\mathbf{y} - \bar{\bar{\mathbf{R}}}_1\mathbf{x}\right\|^2 \tag{5-24}$$

The drawback of using MMSE pre-processing is the introduction of a bias $\eta = {\sigma_n}^2\|\hat{\mathbf{x}}\|^2$on the calculated distances:

$$\bar{\bar{d}}^{2\prime}(\mathbf{x}) = \left\|\bar{\bar{\mathbf{Q}}}_1^H\mathbf{y} - \bar{\bar{\mathbf{R}}}_1\mathbf{x}\right\|^2 = \|\mathbf{y} - \mathbf{H}\mathbf{x}\|^2 + \eta \tag{5-25}$$

Where ${\sigma_n}^2$ is the noise statistics at the receiver, $\hat{\mathbf{x}}$ is the estimate of the transmitted vector $\mathbf{x}$, $\|\mathbf{y} - \mathbf{H}\mathbf{x}\|^2 = {R^2}_{MMSE}$ is the original MMSE radius, see (5-17). The poor performance is attributed to strong noise enhancement, which often results from ill-conditioned channel matrix $\mathbf{H}$ upon the application of the ZF filter. The overall effect of strong noise enhancement is increased complexity which results in errors which cannot be dealt effectively with any error coding schemes. However, performance deterioration due to the EMMSE bias can be partially eliminated by obtaining knowledge of the structure of the bias and then using it to remove the bias before calculating the detector soft output [121]. The initial radius is further improved by scaling the bias with $|\mathbf{M}|$ for an $\mathbf{M}$-QAM modulator [118]:

$$\rho = \sqrt{\eta/_{|\mathbf{M}|}} \tag{5-26}$$

Therefore the novel EMMSE radius $\bar{\bar{R}}_{MMSE}$ is given by (5-27):

$$\bar{\bar{R}}_{MMSE}(\mathbf{x}) = d(\hat{\mathbf{x}}) + \rho \tag{5-27}$$

For the case of multi-level modulation, the bias will depend on $\hat{\mathbf{x}}$.

5.5 Performance Results and Discussion

In this section, the average number of nodes or lattice points visited and the performance of the SE-SD for different radii are compared with the results obtained using the proposed initial radius. The simulation setup is similar to that used in Chapter 4. A counter was introduced to count the number of nodes visited during the search operations. Figure 5-3 shows the performance results of the conventional radius and the proposed novel radius applied to the SE-SD, with and without scaling the bias for a 4x4 MIMO system with a 16-QAM constellation. With the search operations upper-bounded to 800 nodes, the complexity of the proposed SE-SD gets lower than the conventional SE-SD.

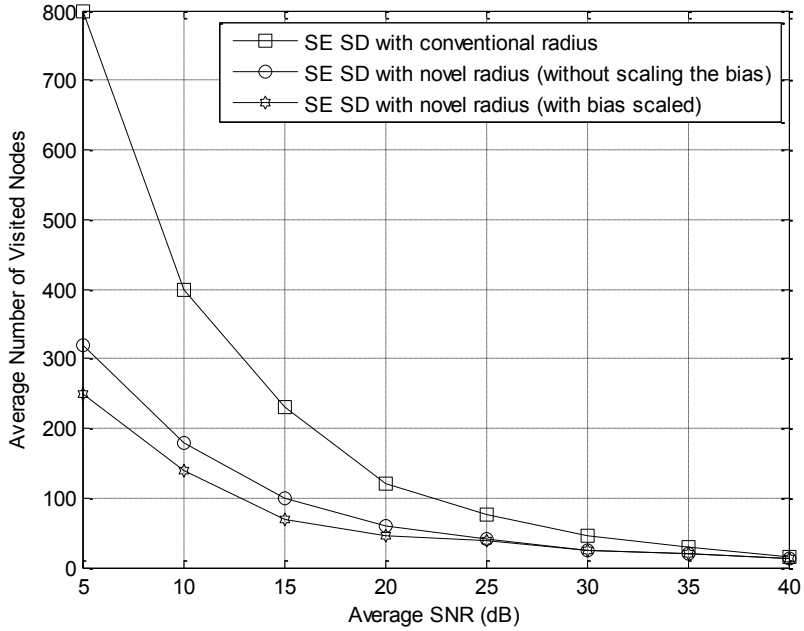

Figure 5-3 Complexity results for SE-SD 16-QAM-4x4 MIMO system

It can be clearly seen that the proposed approach has significant performance improvement compared to the conventional radius. Out of the 1.84×10^{19} lattices points generated in a

4x4 MIMO system with a 16-QAM constellation, only about 320 nodes are visited before a solution is obtained at an SNR of about 5dB. The effect of scaling of the EMMSE bias can also be seen as the number of nodes visited decreased to about 250 nodes compared to about 320 nodes before scaling.

In Figure 5-4, the complexity of the proposed novel radius is compared with the conventional radius and the original MMSE radius in terms of the number of visited nodes for a 4x6 MIMO system configuration. The search operations were upper-bounded to 35000 nodes. The proposed novel radius with bias scaled shows significant reduction in computational complexity of the proposed SE-SD compared to the conventional radius and the SE-SD radius without bias. The proposed initial radius reduces the computational complexity of the sphere by roughly a factor of 3.5 at a signal-to-noise ratio (SNR) of 5dB with bounded number of computations for 4x6 MIMO setup.

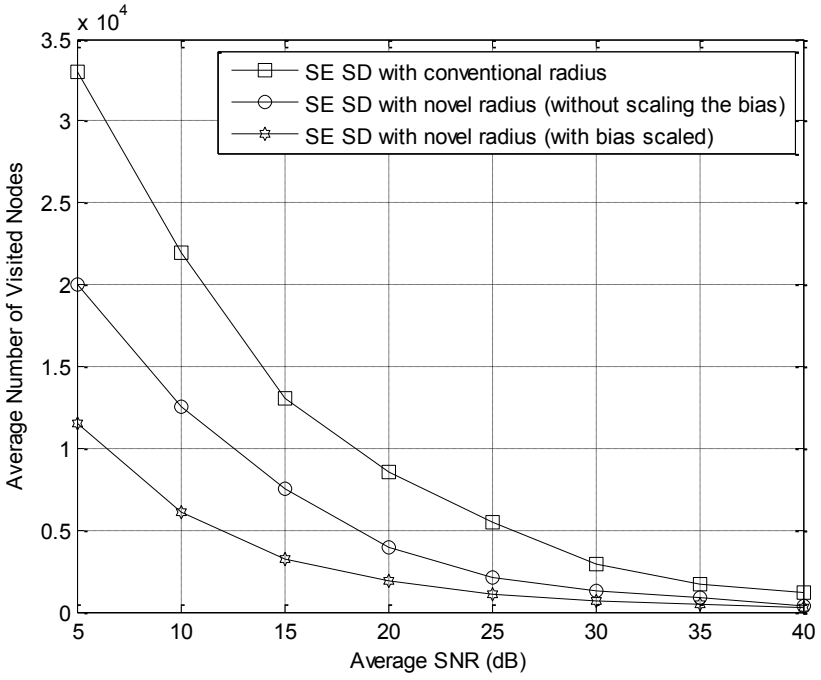

Figure 5-4 Complexity results for SE-SD 16-QAM-4x6 MIMO system

Observe the effect of the number of antennas on the complexity of the proposed SE-SD. The results in Figure 5-3 and Figure 5-4 demonstrate that the complexity of the proposed SE-SD

is dependent on the number of transmit and receive antennas. By equipping the transmitter with more antennas, the number of nodes visited increased from roughly 250 nodes for the 4x4 MIMO setup with 16-QAM transmission to about 12000 nodes for the 4x6 MIMO setup with 16-QAM transmission at an SNR of 5dB. If allowed to perform an unbounded number of computations with the proposed initial radius, the SD can achieve performance comparable to ML detection.

It is important mentioning that for each node visited the number of arithmetic operations is equal to N^L, where $N = \max(N_t, N_r)$ and L is the number of layers within the tree search structure. The assumption held during the computation of the arithmetic operations was that all multiplications, divisions, additions and subtractions have the same effect on the final count. However, it should be noted that the aforementioned arithmetic operations have different impacts on the complexity of the proposed SE-SD from a practical point of view, with the multiplications being the most expensive in terms of hardware resources.

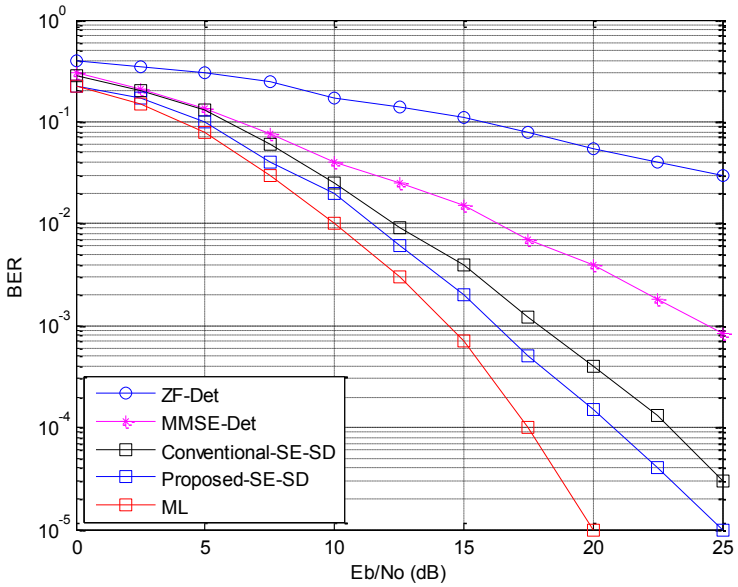

Figure 5-5 Performance of the proposed SE-SD for uncoded 64-QAM-4x4 MIMO setup

The BER performance of the ZF, MMSE, conventional SE-SD, ML and the proposed SE-SD for uncoded 4x4 MIMO setup with 64-QAM transmission are presented in Figure 5-5. In

conducting the simulations, a flat fading channel was assumed. The BER performance of the proposed SE-SD is evaluated by comparing it with the ML and conventional SE-SD, MMSE and the ZF detector. It can be clearly seen that the proposed SE-SD approaches the ML performance to within 1.5 dB in the low SNR regime. However, the BER performance of the proposed SE-SD gets worse compared to the ML performance in the high SNR regimes. The proposed SE-SD achieves performance improvement of about 5 dB at a BER of 10^{-2} over the performance of the MMSE detection scheme in the low SNR regimes.

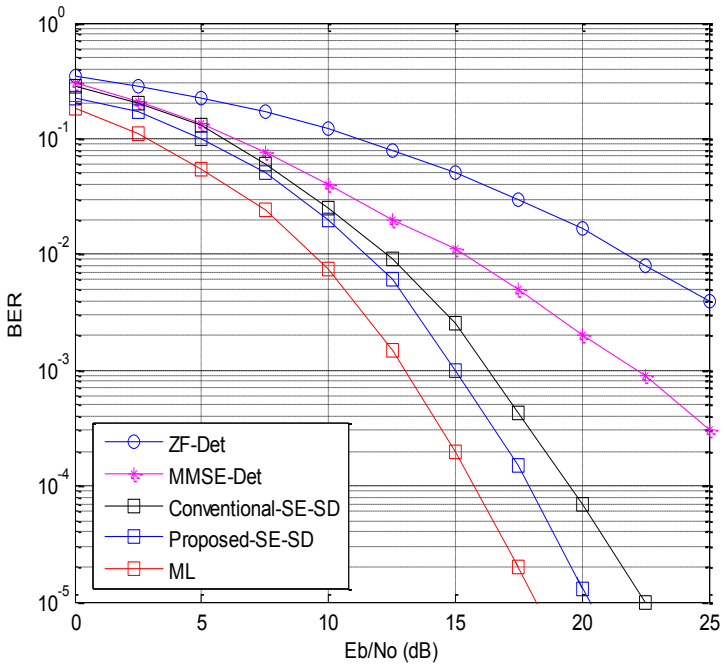

Figure 5-6 Performance results for the proposed SE-SD for uncoded 4x6 MIMO setup

Finally, equipping the transmitter with six antennas results in a performance improvement of about 4dB at the BER of 10^{-5}. The simulation results in Figure 5-6 show that the performance of the proposed SE-SD closely approaches the ML in the low SNR region. Again, the proposed SE-SD yields a performance gain of about 2.5dB over the conventional SE-SD while the performance of the MMSE and the ZF detectors get worse in high SNR range.

5.6 Conclusions

Currently existing sphere decoder based algorithms are capable of achieving maximum ML performance. However, optimal solution is achieved at the detriment of the NP-hard complexity of the sphere decoder. The choice of the initial radius for the SD has a significant impact on the complexity and the performance of the SD. The selection of the initial radius is NP-hard itself particularly in MIMO setups where large signal constellations or many transmit and receive antennas are employed. Currently, there is no well-established technique for computing the initial search radius. However, several techniques for computing the initial radius have been proposed in the literature.

A novel EMMSE initial sphere radius based on the received signal; noise statistics; the number of transmit antennas; the energy of the transmitted symbols and on the channel matrix was proposed in this Chapter. It was shown through simulation results that the proposed initial radius reduces the computational complexity of the sphere by roughly a factor of 3.5 at a SNR of 5dB with bounded number of computations for 4x6 MIMO setup. However, if the algorithm is allowed to perform an unbounded number of computations with the proposed initial radius, SD can achieve performance comparable to ML detection. The proposed sphere radius does not only result in reduced computational complexity of the sphere decoder, but also achieves performance gain over the conventional detection methods particularly at low SNRs.

6. The LRAD-SD-based Detection Schemes

6.1 Introduction

It has been demonstrated in [7] that Multiple-Input Multiple-Output (MIMO) technology is the most promising technology as it can improve link reliability without sacrificing bandwidth efficiency and transmit power. However, the major drawback of this technology is the increased complexity of the detector due to non-orthogonality of MIMO channels. Linear detectors are popularly known for their significantly reduced complexity however, the reduced complexity is achieved at strong performance penalty [130]-[135]. Non-linear detectors, including sequential detectors, yield better performance compared to linear detection schemes at the expense of one or more or a combination of the following problems: error propagation, performance degradation, increased computational complexity or increased processing delay [135]. To overcome these problems, a trade-off between performance and one or more of these issues has to be made. Currently, the solution to MIMO detection problem lies on tree search based detection algorithms.

Although the Maximum Likelihood (ML) detector yields an optimal solution to the MIMO detection problem, it cannot be implemented in practice as its computational complexity increases exponentially with the number of transmit and receive antennas and with the constellation size. Sphere Decoder (SD) based algorithms have been shown to be more efficient in estimating an ML solution [21], [136]. However, superior performance of the SD is achieved at the detriment of its variable NP-hard complexity [136] when the initial radius is too large. On the other hand, a small initial radius leads to decoding failure. The Depth-First-Search (DFS) SD-based algorithm was investigated in Chapter 4. The problem associated with the proposed DFS SE-SD is linked with $\left\lceil \frac{-R_{SD}{}'_{N_L-1}+\tilde{y}_{N_L-1|N_L}}{r_{N_L-1,N_L-1}} \right\rceil \leq x_{N_{L-1}} \leq$

$\left\lfloor \frac{R_{SD}{}'_{N_L-1}+\tilde{y}_{N_L-1|N_L}}{r_{N_L-1,N_L-1}} \right\rfloor$. If $r_{N_L-1,N_L-1} \ll 1$, the initial radius increases drastically. Thus, the number of the hypotheses $x_{N_{l-1}}$ rises exponentially with the increase in search radius leading to NP-hard complexity of the SD. In [137], the *K*-Best, also known as the Breadth-First Search (BFS), has been proposed to provide a sub-optimal solution to the MIMO detection problem. Here, *K* denotes the number of stored hypotheses $x_{N_{L-1}}$, also referred to as nodes or lattice points, at each layer during the tree search detection process. Although this technique yields a near-optimal solution to MIMO detection problem, the key issue is the reduction of the size *K* in order to achieve reasonably lower complexity.

The main objective of this chapter is to design an SD detection scheme that introduces a trade-off between performance, error propagation and complexity. First, the LRAD-MMSE-SIC detection scheme is proposed. The proposed LRAD-MMSE-SIC scheme will then be extended to the SD to reduce the search domain of the DFS based SD proposed in Chapter 4. The resulting reduced structure will be referred to as the LRAD-MMSE-SIC-SE-SD. It will be shown that its computational complexity is independent of the constellation size while it is polynomial with respect to the number of antennas and the signal-to-noise ratio.

6.2 System Model

The detection scheme for a symmetric MIMO system with N_t transmit and N_r receive antennas ($N_r = N_t$) is designed in this chapter. At the transmitter, data is de-multiplexed into N_t data sub-streams also referred to as layers. These sub-streams are encoded by the LDPC encoder and then interleaved bitwise by the inter-leaver before being mapped by the modulator **M** onto a $(N_t \times 1)$-complex valued transmit signal vector **x** of **M**-QAM symbols which are transmitted by the N_t transmit antennas simultaneously in parallel over the flat

fading channel, where M is the constellations size. In this chapter, 4-QAM and 64-QAM modulation schemes will be used.

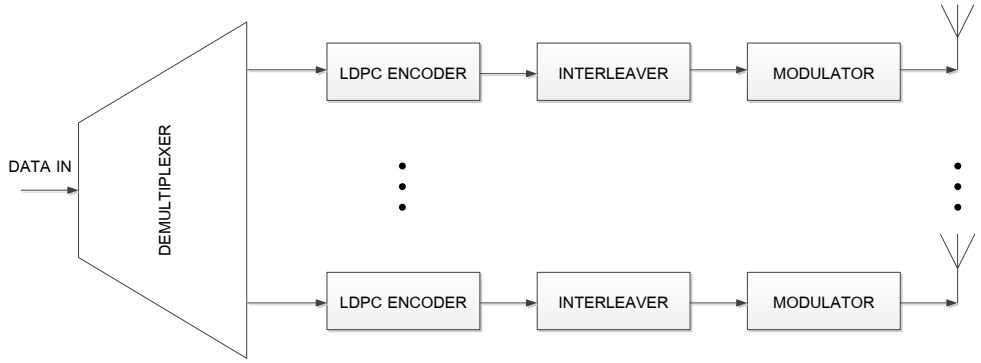

Figure 6-1 MIMO system transmission model

At the receiver, the received $N_r \times 1$ complex valued signal vector is modelled by:

$$\mathbf{y} = \mathbf{H}\mathbf{x} + \mathbf{n} \tag{6-1}$$

where $\mathbf{n}$ denotes the AWGN noise of variance σ_n^2 observed at the receiver. The average transmit power of each antenna will be normalized to 1, i.e. $E\{\mathbf{x}\mathbf{x}^H\} = \mathbf{I}_{N_t}$ and $E\{\mathbf{n}\mathbf{n}^H\} = \sigma_n^2\mathbf{I}_{N_r}$. $\mathbf{H}$ is the $N_r \times N_t$channel matrix whose elements are uncorrelated complex Gaussian fading gains with unit variance. In this design, a flat fading environment is assumed where the channel matrix $\mathbf{H}$ is constant over a time frame T and changes independently from frame to frame. It is also assumed that the channel matrix $\mathbf{H}$ is perfectly known at the receiver. The $N_r \times N_t$ complex valued system model in (6-1) can be decomposed into its $m \times n$ real-valued equivalent model which can be written as:

$$\begin{bmatrix}\Re\{\mathbf{y}\}\\ \Im\{\mathbf{y}\}\end{bmatrix} = \begin{bmatrix}\Re\{\mathbf{H}\} & -\Im\{\mathbf{H}\}\\ \Im\{\mathbf{H}\} & \Re\{\mathbf{H}\}\end{bmatrix}\begin{bmatrix}\Re\{\mathbf{x}\}\\ \Im\{\mathbf{x}\}\end{bmatrix} + \begin{bmatrix}\Re\{\mathbf{n}\}\\ \Im\{\mathbf{n}\}\end{bmatrix} \tag{6-2}$$

where $m = 2N_t$ and $n = 2N_r$ are the dimensions of the real valued channel matrix, $\begin{bmatrix}\Re\{\mathbf{y}\}\\ \Im\{\mathbf{y}\}\end{bmatrix}$ and $\begin{bmatrix}\Re\{\mathbf{n}\}\\ \Im\{\mathbf{n}\}\end{bmatrix}$ are $2N_r \times 1$vectors, $\begin{bmatrix}\Re\{\mathbf{H}\} & -\Im\{\mathbf{H}\}\\ \Im\{\mathbf{H}\} & \Re\{\mathbf{H}\}\end{bmatrix}$is a $2N_r \times 2N_t$ channel matrix and

$\begin{bmatrix}\Re\{\mathbf{x}\}\\ \Im\{\mathbf{x}\}\end{bmatrix}$ is a $2N_t \times 1$vector. The corresponding dimensions of the received, noise and transmit vectors are given by $\mathbf{y} \in \mathbb{R}^n$, $\mathbf{n} \in \mathbb{R}^n$ and $\mathbf{x} \in \chi^m$ respectively. χ denotes the finite set of real-valued transmit signals. The finite set χ generated using an **M**-QAM modulation scheme is given by:

$$\chi = \left\{\pm\frac{1}{2}x, \pm\frac{3}{2}x, \cdots \pm\frac{\sqrt{\mathbf{M}}-1}{2}x\right\} \tag{6-3}$$

where $\sqrt{\mathbf{M}}$ denotes the modulation index of the corresponding real-valued QAM modulator while the power normalisation factor $x(=\sqrt{\frac{6}{\mathbf{M}-1}})$ is used for normalizing the power of the complex valued transmit signals. In this design, it is chosen in such a manner that the transmit power is normalised to 1. Each noiseless received signal is viewed as a point of in a finite lattice spanned by **H** in the proposed design.

6.3 MIMO detection schemes

To recover the received signal, MIMO detection schemes are used to search for the received point located in the lattice generated by **H**. The optimum ML detector performs an exhaustive search over the uncut set of transmit signals $\mathbf{x} \in \chi^m$, and decides in favor of the transmit signal $\hat{\mathbf{x}}_{ML}$that minimizes the Euclidian distance to the receive vector **y** and can be expressed as:

$$\hat{\mathbf{x}}_{ML} = \arg\ \min_{\mathbf{x}\in\chi}\ \|\boldsymbol{y} - \mathbf{H}\mathbf{x}\|^2 \tag{6-4}$$

However, the brute force ML detection is not feasible for larger number of transmit antennas or higher order modulation schemes as the computational effort is of order $\mathbf{M}^{N_t}$. A feasible alternative is the SD discussed in Chapter 4 and Chapter 5, which restricts the search space to

a sphere of radius R_0. Nevertheless, the computational complexity is still high in comparison to simple, but suboptimal successive interference cancellation (SIC).

In this chapter, a less complex SD detection scheme based on the hybrid LRAD-MMSE-SIC is proposed. It is well known that the MMSE yields an ML solution in perfectly orthogonal channels. Unfortunately, practical MIMO channels are non-orthogonal. In order to improve the performance of MMSE in practical non-orthogonal MIMO channels, the LRAD is proposed to transform the channel matrix $\mathbf{H}$ into a near-orthogonal channel matrix $\bar{\mathbf{H}}$.

However, $\bar{\mathbf{H}}$ is still not perfectly orthogonal. It has been shown in [135]-[136] that the SIC detector is capable of achieving further improved performance compared to MMSE detector in non-orthogonal or near-orthogonal MIMO channels. It achieves performance improvements by successively cancelling out the interference due to adjacent signal layers starting with the influence of the largest signal first, until the signal with the smallest power is detected. To yield improved performance, the ordered SIC detection is thus proposed in this design. First, an overview of the LRAD detection scheme is provided in the next section before a detailed description of the proposed SD.

6.3.1 Lattice Reduction Aided Detection schemes

In this design, the columns $\boldsymbol{h}_l$ of the real-valued channel matrix $\mathbf{H}$ where$1 \leq l \leq N_t$ are regarded as the *basis* of a lattice spanned by the channel matrix $\mathbf{H}$. It is also assumed that the possible transmit vectors are given by $\mathbb{Z}^{N_t}$, the N_t-dimensional infinite integer space. First, the estimate of the transmitted symbols are mapped to the appropriate QAM decision regions by performing scaling and shifting operation of the received signal in accordance to the LRAD principles as follows: $\tilde{\mathbf{x}} = \frac{\mathbf{x}}{d} + \mathbf{1}_N/2$, where d is the minimum distance between QAM constellation points and $\mathbf{1}_N$ denotes an all-ones $(N_t \times 1)$-dimensional vector. Next, the MIMO channel matrix $\mathbf{H}$ is transformed into an effective near-orthogonal channel matrix $\bar{\mathbf{H}}$

which yields an effective equivalent received signal model. This is achieved by using Lenstra-Lenstra-Lovasz (LLL) algorithm which decomposes $\mathbf{H}$ into $\mathbf{H} = \bar{\mathbf{H}}\mathbf{T}^{-1}$ where $\mathbf{T}$ is an $N_t \times N_t$ *unimodular* matrix [102], i.e., $\mathbf{T}$ contains only integer entries and the determinant is det ($\mathbf{T}$) = 1 and $\mathbf{T}^{-1}$ is the inverse of the matrix $\mathbf{T}$. Mathematically, it is accepted that the inverse of a unimodular matrix always exist and contains only integer values, i.e., $\mathbf{T}^{-1} \in \mathbb{Z}^m$ ($m = 2N_t$). Thus, the effective transformed channel matrix $\bar{\mathbf{H}}$ which generates the *same* lattice as $\mathbf{H}$ is given by:

$$\bar{\mathbf{H}} = \mathbf{HT} \tag{6-5}$$

Finally, to further reduce the complexity of the proposed system, the channel matrix can be decomposed using $\mathbf{QR}$ decomposition, as $\mathbf{H} = \mathbf{QR}$ where the $N_r \times N_t$ matrix $\mathbf{Q} = [\boldsymbol{q}_1, \boldsymbol{q}_2, \cdots, \boldsymbol{q}_{N_t}]$ consists of orthogonal columns of unit length ($\mathbf{Q}^T\mathbf{R} = \mathbf{I}_{N_t}$). $\mathbf{R}$ is the upper triangular matrix which consists of elements $r_{i,j}$ where $1 \leq i, j \leq N_t$. Thus, each column vector $\mathbf{h}_k$ of the channel matrix $\mathbf{H}$ is given by $\mathbf{h}_k = \sum_{l=1}^{k} r_{l,k}\boldsymbol{q}_l$ where k ($1 \leq k \leq N_t$) is a counter. Here, the vector $\boldsymbol{q}_k$ denotes the direction of $\mathbf{h}_k$ perpendicular to the space spanned by $\boldsymbol{q}_1, \boldsymbol{q}_2, \cdots, \boldsymbol{q}_k$ and $r_{k,k}$ describes the corresponding length of $\mathbf{h}_k$. Furthermore, $r_{l,k} = \boldsymbol{q}_l^T\mathbf{h}_k$ is the length of the projection of $\mathbf{h}_k$ onto $\boldsymbol{q}_l$. The premise behind the LRAD technique is to transform a given basis $\mathbf{H}$ into a much better conditioned new basis $\bar{\mathbf{H}}$ with vectors of shortest length or, equivalently, into a basis consisting of near-orthogonal basis vectors. Likewise, the transformed channel matrix $\bar{\mathbf{H}}$ can be decomposed to $\bar{\mathbf{H}} = \bar{\mathbf{Q}}\bar{\mathbf{R}}$ in order to perform ordered SIC detection. The design description for the proposed MIMO detection scheme is provided in the next section.

6.3.2 LRAD-MMSE-SIC-SE-SD System Description

A detailed description of the proposed LRAD-MMSE-SIC-SE-SD MIMO detector is provided in this section. Figure 6-2 shows the block diagram of the proposed detection scheme. This consists of five main blocks namely LLL Algorithm, LRAD Preprocessing, MMSE-SIC, the SE-SD and the decision circuit. Each of the blocks addresses one or more the issues mentioned in Section 6.1. The LRAD linear detection performs nonlinear quantization on $\mathbf{z}$ instead of $\mathbf{x}$. The vector $\mathbf{z}$ resides in the transformed equivalent system model of the received signal.

First, the LLL and LRAD Preprocessing blocks address the problems associated with the ill-conditioned and non-orthogonality of the channel matrix $\mathbf{H}$. The LLL algorithm in the LRAD pre-processor generates $\mathbf{T}$ and $\mathbf{T}^{-1}$ which are used to transform the channel matrix $\mathbf{H}$ and the transmit vector $\mathbf{x}$ into the $\mathbf{z}$ domain as:

$$\bar{\mathbf{H}} = \mathbf{HT}, \quad \mathbf{z} = \mathbf{T}^{-1}\mathbf{x} \tag{6-6}$$

The transformed receive signal vector can then be rewritten as:

$$\mathbf{y} = \mathbf{Hx} + \mathbf{n} = \mathbf{HTT}^{-1}\mathbf{x} + \mathbf{n} = \bar{\mathbf{H}}\boldsymbol{z} + \mathbf{n} \tag{6-7}$$

Note that $\mathbf{Hx}$ and $\bar{\mathbf{H}}\boldsymbol{z}$ describe the same point in a lattice. The only difference is that the LLL-reduced channel matrix $\bar{\mathbf{H}}$ is much better conditioned and near-orthogonal than the original channel matrix $\mathbf{H}$. The condition of $\bar{\mathbf{H}}$ determines the noise amplification, hence the solution based on $\bar{\mathbf{H}}$ outperforms that based on $\mathbf{H}$. This solution does not only lead to performance gain of the overall system, but also reduces the computational complexity of the overall proposed LRAD-MMSE-SIC-SE-SD detector.

Since $\mathbf{x}$ belongs to the set $\mathbb{Z}^m$, $\mathbf{z}$ also belong to $\mathbb{Z}^m$, where $m = N_t$. Therefore, $\mathbf{x}$ and $\boldsymbol{z}$ stem from the same set. The only difference here is that for $\mathbf{M}$-QAM the lattice is finite and the

domain of $\mathbf{z}$ differs from $\boldsymbol{\chi}^m$. In other words, $\mathbf{z}$ now resides in a much reduced lattice. Further reduction in complexity is achieved by sorted $\bar{\mathbf{Q}}\,\bar{\mathbf{R}}$ decomposition of $\bar{\mathbf{H}}$. This leads to the generation of the estimate $\tilde{\boldsymbol{y}}$ of the received signal $\boldsymbol{y}$ with an ordered upper triangular matrix $\bar{\mathbf{R}}$. The modified signal $\tilde{\boldsymbol{y}}$ is then further processed by the SE-SD which utilises R_o computed by the MMSE-SIC processor. In the SIC block, signal detection starts with the most reliable signal, i.e., the signal with the largest amplitude. The details of the SIC algorithm is provided in Chapter 3 of this thesis.

Second, with the transformed received signal, the MMSE-SIC Preprocessing block generates a reliable initial radius R_{SE-SD} to be utilised in the SE-SD. The MMSE filter $\mathbf{G}_{MMSE} = (\bar{\mathbf{H}}^{-T}\bar{\mathbf{H}} + \sigma_n^2\mathbf{T}\mathbf{T}^{-1})^{-1}\bar{\mathbf{H}}^T$ is applied to improve the accuracy of the estimate $\bar{\mathbf{z}}_{LR-MMSE}$, of $\boldsymbol{z}$. Applying the MMSE-filter $\mathbf{G}_{MMSE}$ to the lattice-reduced system yields $\bar{\mathbf{z}}_{LR-MMSE}$ as follows:

$$\bar{\mathbf{z}}_{LR-MMSE} = \mathbf{G}_{MMSE}\mathbf{y} = \{(\bar{\mathbf{H}}^{-T}\bar{\mathbf{H}} + \sigma_n^2\mathbf{T}\mathbf{T}^{-1})^{-1}\bar{\mathbf{H}}^T\}\mathbf{y} \tag{6-8}$$

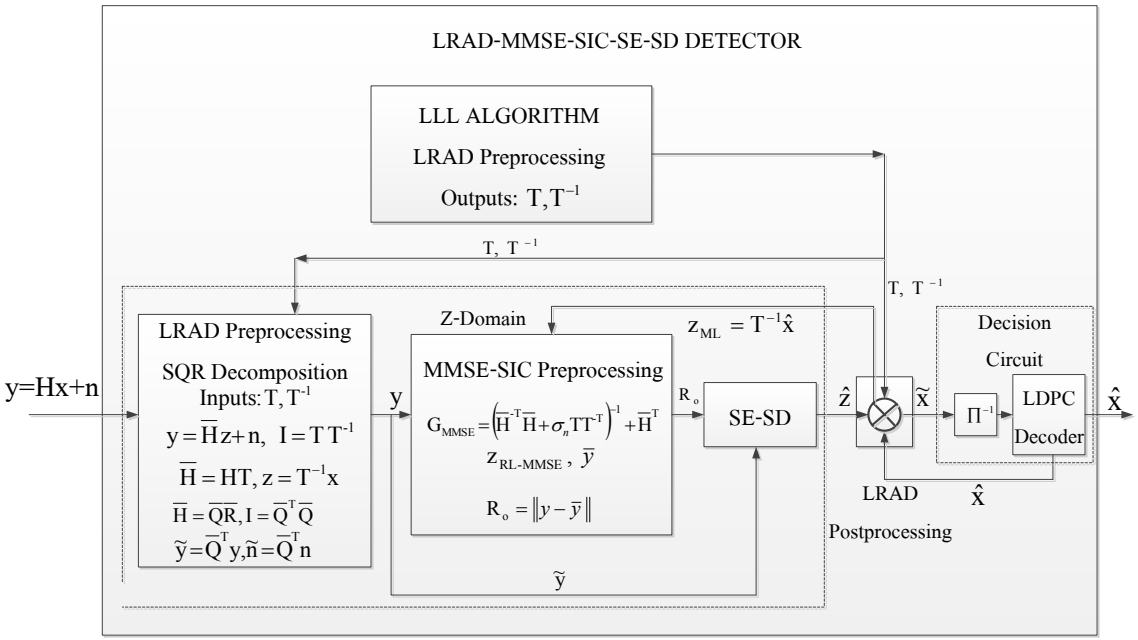

Figure 6-2 Proposed LRAD-MMSE-SIC-SE-SD block diagram

The output $\bar{\mathbf{z}}_{LR-MMSE-SIC}$ of the MMSE-SIC detector is equivalent to multiplying the original MMSE-SIC estimate $\bar{\mathbf{x}}_{MMSE-SIC}$ by$\mathbf{T}^{-1}$, the inverse of the unimodular matrix $\mathbf{T}$, that is:

$$\bar{\mathbf{z}}_{LR-MMSE-SIC} = \mathbf{T}^{-1}\bar{\mathbf{x}}_{MMSE-SIC} \tag{6-9}$$

The estimate $\bar{\mathbf{z}}_{LR-MMSE-SIC}$ can be remapped to a lattice point $\bar{\mathbf{H}}\bar{\mathbf{z}}_{LR-MMSE-SIC}$ to yield:

$$\bar{\mathbf{y}} = \bar{\mathbf{H}}\bar{\mathbf{z}}_{LR-MMSE-SIC} \tag{6-10}$$

The initial SE-SD radius can thus be modelled by:

$$R^2{}_{SE-SD} = R_0^2 = \|\mathbf{y} - \bar{\mathbf{y}}\|^2 \tag{6-11}$$

The initial radius R_o is fed into the input of the SE-SD. This is then processed using the SE-SD algorithm described in Chapter 4 to yield $\hat{\mathbf{z}}$. The SE-SD estimate can be recovered by multiplying $\hat{\mathbf{z}}$ by the unimodular matrix $\mathbf{T}$ as follows:

$$\tilde{\mathbf{x}} = \mathbf{T}\hat{\mathbf{z}} \tag{6-12}$$

This is fed into the decision circuit which finally generates the estimate $\hat{\mathbf{x}}$ of the received signal $\mathbf{x}$. To prevent error propagation in the MMSE-SIC preprocessing unit, the LDPC error corrected estimate $\hat{\mathbf{x}}$ is feedback via the LRAD post-processing unit where it is transformed into the z-domain as follows:

$$\mathbf{z}_{ML} = \mathbf{T}^{-1}\hat{\mathbf{x}} \tag{6-13}$$

The effect of this feedback does not only ensure that error propagation is effectively arrested, but it also ensures that the overall performance of the system improves significantly.

6.4 Performance Results and Discussion

The simulation results for the proposed LRAD-MMSE-SIC-SE-SD detection strategy are presented in this section. The simulation setup is similar to the setup described in Chapter 4.

The BER performance results are presented for different modulation orders and different number of transmit and receive antenna configurations. The performance results for the proposed LRAD-MMSE-SIC-SE-SD are evaluated by comparing them with the ML, LRAD-MMSE-SIC, and the MMSE-SIC detection schemes. The assumption made is that MIMO signals are transmitted through uncorrelated Rayleigh flat fading channels with the transmit power normalised to unit. Figure 6-3 shows the BER results for ½ rate LDPC coded and uncoded 4x4 MIMO setups for the proposed LRAD-MMSE-SIC-SE-SD. 4-QAM and 64-QAM modulation schemes were applied on each sub stream as representatives for the respective low and high spectral efficiency regimes.

It can be clearly seen that the proposed LRAD-MMSE-SIC-SE-SD achieves substantial performance improvements in comparison with the LRAD-MMSE-SIC and MMSE-SIC detection schemes. The results in Figure 6-3 (a) show that the proposed LRAD-MMSE-SIC-SE-SD scheme achieves performance improvement of about 2dB and 3dB at a BER of 10^{-3} for the cases of both coded and uncoded 4-QAM transmissions compared to the performance of the LRAD-MMSE-SIC and MMSE-SIC detection schemes respectively. The performance improvement arises from the combination of the reduced search space introduced by the LRAD schemes and the optimal ordering due to the MMSE-SIC.

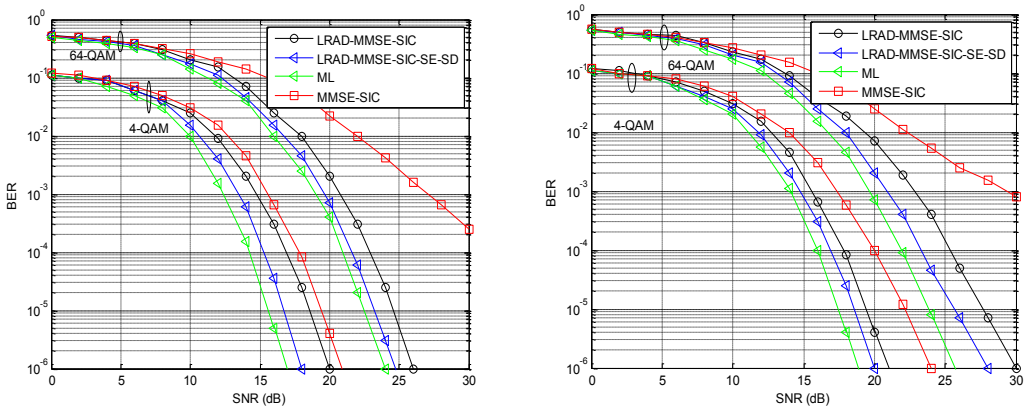

(a) Coded 4x4 MIMO System Setup (b) Uncoded 4x4 MIMO System Setup

Figure 6-3 Performance results for (a) coded and (b) uncoded 4x4 MIMO System Setup

However, there is a marginal overall performance loss of the proposed LRAD-MMSE-SIC-SD compared to the ML although the performance is 1dB within that of the ML throughout the SNR regimes. The performance loss comes with a benefit of significantly reduced computational complexity. A similar trend in BER performance is also observed for the cases of both coded and uncoded 64-QAM although there is a modulation efficiency improvement penalty of about 6dB decrease in performance at a BER of 10^{-3} compared to the case of the 4-QAM. The proposed scheme is about 2dB and 8dB better than the LRAD-MMSE-SIC and MMSE-SIC schemes respectively at a BER of 10^{-3} for the uncoded case shown in Figure 6-3 (b).

The benefit of equipping both the transmitter and the receiver is demonstrated in Figure 6-4. This is demonstrated by comparing the BER results for uncoded 4x4 MIMO setup and 4x6 MIMO setup where 4-QAM and 64-QAM modulation schemes are applied on each sub stream. Again, the proposed LRAD-MMSE-SIC-SD achieves substantial performance improvements in comparison to the LRAD-MMSE-SIC and MMSE-SIC detection schemes.

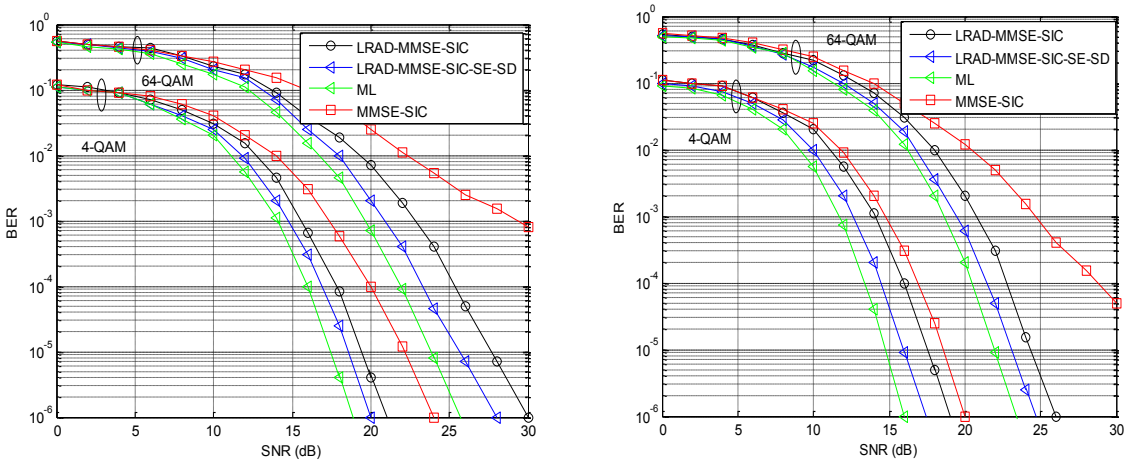

(a) Uncoded 4x4 MIMO System Setup (b) Uncoded 4x6 MIMO System Setup

Figure 6-4 Performance results for proposed LRAD-MMSE-SIC-SD

As can be clearly seen in Figure 6-4, the proposed LRAD-MMSE-SIC-SD benefits substantially from reduced error probability on the first layer by equipping the receiver with

more antennas (6 antennas in this case compared to 4 antennas in Figure 6-3). It can also be clearly seen that low order modulation schemes perform better than higher order modulation schemes at the cost of bandwidth inefficiency. These results demonstrate that equipping the transmitter and the receiver with more antennas in conjunction with higher order modulation schemes can be attractive where high data rates are the main target of the wireless communication system.

6.5 Computational Complexity Analysis

The goal of the MIMO detector is to solve the closest lattice point search (CLPS) problem as efficiently as possible with minimum computational complexity. However, the ML performs an exhaustive search which is impractical for real-time systems. Fortunately, the emergence of the SD has restored the lost hope for high data rate MIMO systems. This section investigates the complexity aspects of the proposed LRAD-MMSE-SIC-SE-SD for MIMO systems. The complexity analysis focuses on uncoded MIMO transmission, i.e., hard output detection.

So far, most of the available results on the complexity for sphere detection have focused on the average behaviour [11], [18], [113], [138] and complexity exponents at moderately high SNR [18]. It is stated in [139], that the SD has a considerably higher worst case, but lower average complexity than other tree search based detection algorithms.

In this thesis, the average complexity of the proposed LRAD-MMSE-SIC-SE-SD is investigated by estimating the number of arithmetic operations conducted to yield an estimate of the ML solution. This is then compared to the enumeration techniques in [12]. The simulation setup is equivalent to the one used in Section 2.8.3. For a brute force search (ML detection), the maximum number of arithmetic operations A_o required to compute an exhaustive ML solution is $A_o^{ML} = \sum_{l=1}^{N_L} \chi^l$. To make a fair comparison, the number of each

addition, multiplication, and extraction of a square-root will be counted as one operation as proposed in [12]. The upper limit for the original Fincke-Pohst (FP) is used as a figure of merit or yardstick against which the complexity of the proposed LRAD-MMSE-SIC-SE-SD is measured and is given by [12]:

$$\frac{1}{6}(2m^3+3m^2-5m)+\frac{1}{2}(m^2+12m-7)\times\left(\left(2\left\lfloor\sqrt{d^2t}\right\rfloor+1\right)\binom{\lfloor 4d^2t\rfloor+m-1}{\lfloor 4d^2t\rfloor}+1\right) \quad (6\text{-}14)$$

where $m=N_t$, d is the sphere radius and $t=\max\left(r_{1,1}^2,\cdots,r_{m,m}^2\right)$ while that in [124] require cubic $O\ (m^3)$ computations.

For a 4x4 MIMO with a 64-QAM constellation, the upper bound number of arithmetic operations used in simulations is $A_o=10000$. Figure 6-5 shows the average value of the arithmetic operations A_o for the proposed LRAD-MMSE-SIC-SE-SD plotted against SNR. According to the results obtained to date in the literature, the expected complexity of FP-SD is only polynomial in the problem size for a wide range of SNRs [18]. However, it was proven in [140] that there exists a lower bound exponent on the complexity of the FP-SD.

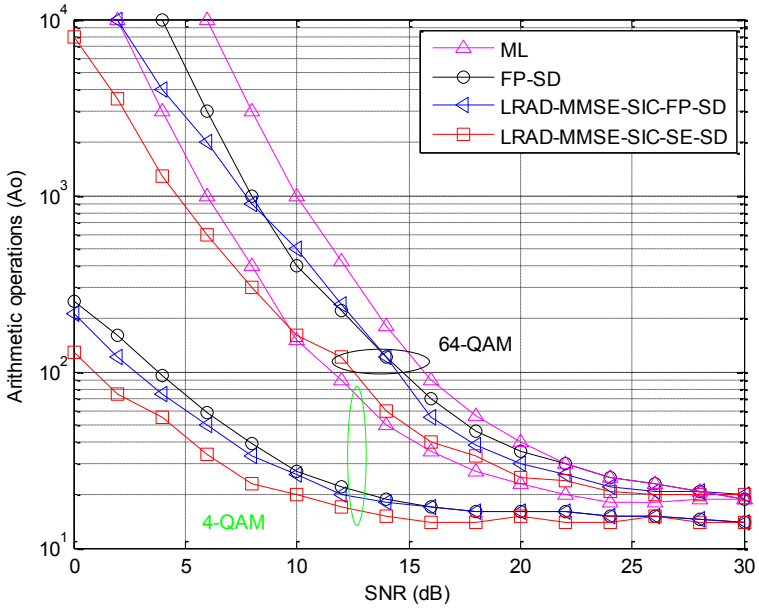

Figure 6-5 Average arithmetic operations without statistical pruning

While this implies that the complexity of the FP-SD will always grow exponentially with the problem size, the rate of exponential growth depends strongly on the SNR as is depicted in Figure 6-5. Here, the number of required arithmetic computations decreases substantially as the SNR is increased and the detection complexity eventually approaches that of linear suboptimal detectors, i.e., the detection complexity eventually approaches a constant value. Conversely, the number of arithmetic computations increases substantially as the SNR is decreased and the detection complexity eventually approaches that of a brute force search. The FP-SD complexity is also extremely sensitive to the choice of the search radius.

The goal of a wireless communication system is deliver high data rates at minimum transmit power and much reduced detector complexity. As can be seen in Figure 6-5, the proposed LRAD-MMSE-SIC-SE-SD can achieve the desired BER performance (see Figure 6-3 & Figure 6-4) at much reduced complexity within the whole range of the SNR regime (0-30dB) compared to the ML and original FP-SD for both cases of 4-QAM and 64-QAM transmissions.

The reduction in complexity of the proposed LRAD-MMSE-SIC-SE-SD is partly attributed to the MMSE-SIC preprocessing with layer ordering and partly due to the reduced search domain introduced by the LRAD scheme.

The complexity of the proposed LRAD-MMSE-SIC-SE-SD can be further reduced by applying statistical tree pruning, particularly in the low SNR regime. Figure 6-6 illustrates that the proposed LRAD-MMSE-SIC-SE-SD algorithm solves the CLPS problem far more efficiently than the original FP-SD with the application of statistical tree pruning, particularly in the low to medium SNR regime, and for the case of higher order modulation. The complexity of the proposed LRAD-MMSE-SIC-SE-SD can be reduced by several orders of magnitude for 64-QAM transmission at SNRs below 10dB. The average complexity of the

proposed LRAD-MMSE-SIC-SE-SD can be reduced by a factor of about 30 in the low SNR regime for the case of 64-QAM transmission as can be clearly seen in Figure 6-6. However, the reduction in complexity is not noticeable for the case of 4-QAM transmission.

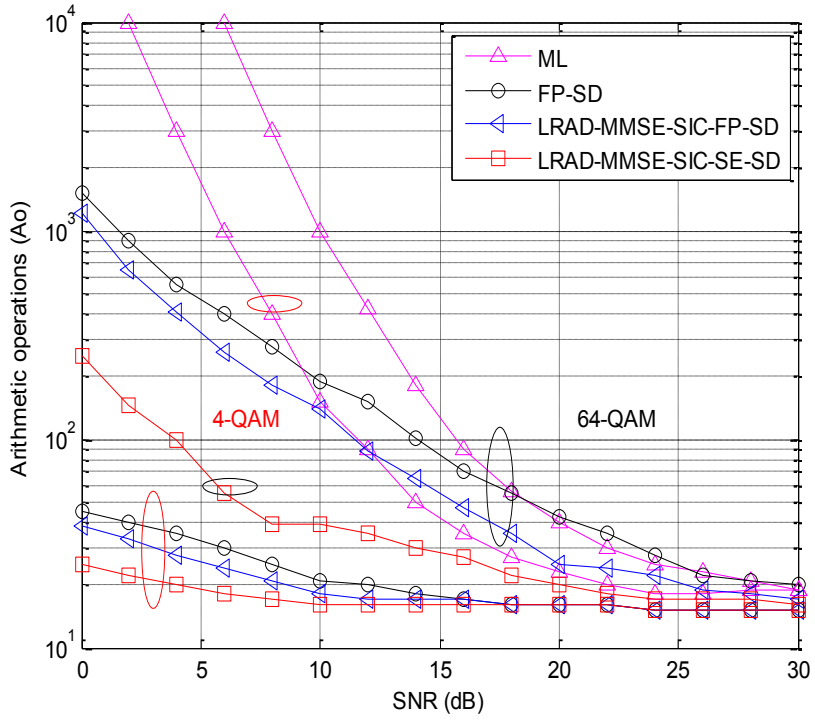

Figure 6-6 Average arithmetic operations with statistical pruning

The average complexity of the original FP-SD becomes largely independent of the operating SNR by employing LRAD-MMSE-SIC based preprocessing. A reduction of 80-90% compared to a FP-SD without tree pruning can be achieved. However, the complexity reduction is achieved at the expense of performance loss over the whole BER range arising from the suboptimality due to statistical tree pruning. Overall, the complexity for both the LRAD-MMSE-SIC-SE-SD and the LRAD-MMSE-SIC-FP-SD is much lower than the ML for both cases of 4-QAM and 64-QAM transmissions. Based on these results in Figure 6-5 and Figure 6-6 it can be concluded that the proposed SE-SD with LRAD-MMSE-SIC preprocessing is the most attractive option for solving the CLPS problem, i.e., the best option for solving the ML detection problem.

6.6 Summary

The simulation results shown in Figure 6-3 and Figure 6-4 are both consistent with theory. In both cases, coded transmissions show superior performance compared to uncoded transmissions. However, as the modulation order increases, the BER performance deteriorates. Simulations of the proposed LRAD-MMSE-SIC-SE-SD presented in this chapter show that the worst case computational complexity of the sphere detector largely is dependent on the number of transmit and receive antennas and the initial sphere of radius.

6.7 Conclusions

The LRAD-MMSE-SIC-SE-SD detection scheme which introduces a trade-off between performance, error propagation and complexity was designed in this chapter. The reduction in complexity mainly results from the transformation of the channel matrix into a near-orthogonal channel and SQRD. Computational complexity can also be minimized in the tree search process by using efficient enumeration strategies such as the Schnorr-Euchner and tree pruning techniques. The state-of-the-art LDPC were applied to stop errors from one stage propagating to the next stage of the detector. This has significant effect on performance improvement of the sphere detector.

7. Conclusion and Future Work

7.1 Conclusions

This thesis focused on the performance and complexity analysis of MIMO detection algorithms. A detailed study of the state-of-the-art sphere decoder for MIMO systems was conducted. The sphere detector for MIMO systems can be considered as an efficient ML detector whose search space is restricted to the hyper-sphere of radius R_o.

A detailed study of the ML and the heuristic suboptimal detection schemes was conducted in Chapter 3. It has also been shown that the MMSE detector performs very well in the detection of MIMO signals and will therefore, be considered in future work as a strong candidate for pre-coding schemes. Simulations of the NLD detection schemes in Chapter 3 show that NLD outperform LD, hence they are potential candidates for the pre-processing schemes for more powerful detection schemes such as the SD. It has also been shown that the channel capacity approaching LDPC coding can significantly improve the performance of MIMO detection schemes, thus laying the foundation for a bright future for high capacity MIMO systems.

The results for the proposed PSD in Chapter 4 show that the task of generating or recovering the transmitted MIMO signals at the receiver can be a significant challenge for the tree search based detection strategy. However, this challenge can be overcome by using a combination of the SD characterized by the Depth-First Search (DFS) with heuristic Multi-User Detection (MUD) methods, both linear and non-linear detectors. The BER curves of the PSD follow the error rate curve for the ML closely indicating that the PSD performance approaches the ML performance particularly in the low SNR regimes.

The choice of the initial radius is a crucial factor in the complexity of the sphere detector. A novel EMMSE radius based on the received signal, noise statistics, the number of transmit antennas, the energy of the transmitted symbols and on the channel matrix was developed in Chapter 5. The benefit associated with this approach is that it ensures that the number of lattice points inside the sphere is small, thus reducing the complexity of the SD detection scheme for MIMO systems.

The Schnorr-Euchner Sphere Decoder based on the DFS algorithm was investigated to depth in Chapter 5 where its ability to achieve near-optimal performance was demonstrated through simulation results. The complexity aspect of the sphere detector has been identified in this thesis as the central issue in MIMO detection, which can prohibit the realization of channel capacity in MIMO systems. It was shown through simulations in Chapter 6 that the computational complexity of the sphere detector is largely dependent on the number of transmit and receive antennas and the initial sphere of radius, which in turn determines the number of lattice points inside the sphere.

In Chapter 6, a new LRAD-MMSE-SIC-SE-SD detection scheme that introduces a trade-off between performance, error propagation and complexity was proposed. This detection scheme benefits largely from the transformation of the channel matrix into a near-orthogonal channel and SQRD. Computational complexity can also be minimized in the tree search process by using efficient enumeration strategies such as the Schnorr-Euchner and tree pruning techniques. The state-of-the-art LDPC were applied though at the expense of slight increase in complexity of the detector to stop errors from one stage propagating to the next stage of the detector. This has significant effect on performance improvement of the sphere detector.

7.2 Future Work

7.2.1 Tree search based Algorithms and sequential Detection

This thesis has concentrated on the sphere decoder for MIMO systems. It mainly focused on the DFS algorithm. A detailed analysis of the Metric First Search (MFS), Breadth First Search (BFS) and sequential detection remains an open research area, and thus remains a possible direction for this work. It would be also interesting to extend this analysis to other applications including Multi-User MIMO detection and cooperative communications.

7.2.2 MIMO Detection Problem Size

The MIMO detection problem size was limited to six real dimensions to yield real-time results at manageable computational complexity. For high data rate systems, an extension of the problem size beyond six will be a possible consideration in the future. For high data rate wireless communication systems, large constellation sizes and several transmit and receive antennas typically 16x16 MIMO configurations with 256-QAM will be investigated in the future.

7.2.3 Sphere Detection Computational Complexity Analysis

Research in the computational complexity analysis of the sphere decoder has largely focused on the number of arithmetic computations. To date, it has been shown that all studied tree search algorithms show very similar complexity. It has been thus difficult to determine which of the schemes is best suited for practical applications. A further extension of this work is the design of tree search based schemes which take practical implementation constraints such as parallelisation and latency issues into account. Further investigation of complexity reduction techniques such as MMSE preprocessing for real-time systems is a fascinating direction for this work.

7.2.4 Initial Radius Selection

The determination of an optimal initial search radius still remains the major challenge of the SD detection technique. The choice of the initial radius for the SD has a significant impact on the complexity and the performance of the SD [141]. To achieve the channel capacity, an optimal initial sphere radius which results in a sphere with a single point other than the received point is required. It would be very interesting designing such system that computes an optimal initial sphere radius in the future.

7.3.5 Hardware Implementation of the Proposed Detection schemes

Throughout this thesis, all detection schemes for MIMO systems investigated have been verified by computer simulations. The ultimate test for the validity of the proposed schemes is the real world application. A first step in this direction could be the evaluation of tree search algorithms using hardware-in-the-loop approach [132].

FPGA hardware based simulations have also received a lot of attention due to their improved performance advantages over software based simulations [143]. Hardware based simulations do not only provide real-time simulations but also enable the designers to effectively and accurately evaluate the hardware architectures of algorithms and systems. FPGA based simulations will therefore be an attractive optional future direction of this work.

References

[1] C. E. Shannon, "A mathematical theory of communication," *The Bell System Technical Journal*, vol. 27, pp. 379-423, 623-656, 1948.

[2] IEEE standard for local and metropolitan area networks Part 16: Air interface for broadband wireless access systems. *IEEE Std 802.16-2009*, pp. 29, 2009.

[3] M. Rachid, B. Daneshrad, "A low-complexity iterative mimo sphere decoding algorithm," *17th European Signal Processing Conference*, pp. 456-460, August 2009.

[4] A. Goldsmith, S. A. Jafar, N. Jindal, and S. Vishwanath, "Capacity limits of MIMO channels," *IEEE Journal on Selected Areas in Communications*, vol. 21, no. 5, pp. 684-702, June 2003.

[5] E. Zimmermann, G. Fettweis, D. L. Milliner, and J. R. Barry, "A Parallel Smart-Candidate-Adding Algorithm for Soft-Output MIMO Detection," *7th International ITG Conference on Source and Channel Coding*, Ulm, Germany, January 2008.

[6] C. Windpassinger and R. F. H. Fischer, "Low-complexity near maximum- likelihood detection and precoding for MIMO systems using lattice reduction," *In Proc. IEEE Information Theory Workshop*, Paris, France, pp. 345-348, March 2003.

[7] C. J. Foschini, "Layered space-time architecture for wireless communication in a fading environment when using multi-element antennas," *Technical Report 2, Bell Labs Technical Journal*, pp. 41-58, 1996.

[8] C.J. Foschini and M.J. Gans, "On limits of wireless communication in a fading environment when using multiple antennas," *Wireless Personal Communications*, vol. 6, no. 3, pp. 311-335, October 1998.

[9] D. Wubben, R. Rinas R. Bohnke, V. Kuhn and K. D. Kammeyer, "Efficient Algorithm for Detecting Layered Space-time Codes," *In Proc. ITG Conference on Source and Channel Coding*, Berlin, Germany, pp. 399-405, January 2002.

[10] A. Benjebbour, H. Murata, and S. Yoshida, "Comparison of Ordered Successive Receivers for Space-Time Transmission," *In Proc. IEEE Vehicular Technology Conference*, USA, Fall, vol.4, pp. 2053-2057, 2001.

[11] A.D. Murugan, H. El Gamal, M.O. Damen and G. Caire, "A unified framework for tree search decoding: rediscovering the sequential decoder," *IEEE Transaction on Information Theory*, vol. 52, pp. 933-953, March 2006.

[12] U. Finke, and M. Pohst, "Improved methods for calculating vectors of short length in a lattice, including a complexity analysis," *Mathematics of Computation*, vol. 44, no. 170, pp. 463-471, April 1985.

[13] V. T. Pham, Z. Lei and T.T. Tjhung, "Fano Detection Algorithm for MIMO Systems," *IEEE International Conference on Information Communication & Signal Processing*, pp. 1-5, Dec. 2007.

[14] Z. Ma, B. Honary, P. Fan, and E. G. Larsson, "Stopping Criterion for Complexity Reduction of Sphere Decoding," *IEEE Communications Letters*, vol. 13, no. 6, pp. 401-404, June 2009.

[15] H. Yao, and G.W. Wornell, "Lattice-reduction-aided detectors for MIMO communications systems," *In Proceedings of the IEEE Global Telecommunications Conference*, vol. 1, pp. 424-428, November 2002.

[16] E. Agrell, T. Eriksson, A. Vardy, and K. Zeger, "Closest point search in lattices," *IEEE Transaction on Information Theory*, vol. 48, no. 8, pp. 2201-2214, Aug. 2002.

[17] B. Shim, I. Kang, "Sphere Decoding With a Probabilitic Tree Pruning," *IEEE Transaction on Signal Processing*, vol. 56, no. 10, pp. 4867-4878, October 2008.

[18] H. Vikalo and B. Hassibi, "On the Sphere-Decoding Algorithm I. Expected Complexity," *IEEE Transactions on Signal Processing,* vol. 53, no. 8, pp. 2806-2818, August 2005.

[19] S. Qiao, "Integer least squares: Sphere decoding and the LLL algorithm," *Proceedings of C3S2E-08, ACM International Conference Proceedings Series*, pp. 23-28, May 2008.

[20] B. Shim, I. Kang, "On Radius Control of Tree-Pruned Sphere Decoding," *In Proceedings of the IEEE International conference on Communications*, pp. 2469-2472, 2009.

[21] H. Vikalo and B. Hassibi, "The Expected Complexity of Sphere Decoding, Part I: Theory, Part II: Applications," *IEEE Transactions on Signal Processing*, 2003.

[22] H. Liao, "A Zero Forcing and Sphere Decoding Joint Detector for Multiple Input Multiple Output LAS-CDMA System," *IEEE WRI International Conference on Communications and Mobile Computing*, pp. 246-249, 2009.

[23] E.G. Larsson, "MIMO Detection Methods: How they work," *IEEE signal Processing Magazine*, May 2009.

[24] K. Su, I. Berenguer, I. J. Wessell and X. Wang, "Efficient Maximum-Likelihood Decoding of Spherical lattice Codes," *IEEE Transactions On Communications*, vol.57, no. 8, pp. 2290-2300, Aug 2009.

[25] P. Li, and R. C. de Lamare, "Adaptive Decision-Feedback Detection with Constellation Constraints for MIMO Systems," *IEEE Transactions On Vehicular Technology*, vol. 61, no. 2, pp. 853-859, February 2012.

[26] S. Mhosvai, "Multi-user detection for DS-CDMA communications," *IEEE Personal Communications Magazine*, vol. 34, no. 10, pp. 124-137, October 1996.

[27] P.W Wolniansky, G. J. Foschini, G. D. Golden, and R. A. Valenzuela, "V-BLAST: an architecture for realizing very high date rates over the rich-scattering wireless channel," *In International Symposium on Signals, Systems and Electronics*, pp. 295-300, 1998.

[28] J. Tao, J. Wu, and Y. R. Zheng, "Low-Complexity Turbo Block Decision Feedback Equalization for MIMO Systems," *IEEE International Conference on Communications, Cape Town*, pp. 1-5, May 2010.

[29] H. Yagi, "Beam transmission of ultra-short waves," *Proceedings of the IRE*, vol. 16, pp. 715-741, June 1928.

[30] H.O. Peterson and H.H. Beverage, "Diversity telephone receiving system of R.C.A," *Communications, Inc., for radiotelegraphy*. *Proceedings of the IRE*, vol. 19, pp. 531-561, April 1931.

[31] J. Winters, "On the capacity of radio communication systems with diversity in a Rayleigh fading environment," *IEEE Journal on Selected Areas in Communications,* vol. 5, pp. 871-878, June 1987.

[32] D. N. Nguyen and M. Krunz, "Spectrum Management and Power Allocation in MIMO Cognitive Networks," *IEEE INFOCOM Proceedings,* pp. 2023-2031, March 2012.

[33] I. Emre Telatar, "Capacity of multi-antenna Gaussian Channels," *Technical Report, Bell Labs, Lucent Technologies*, June 1995.

[34] S. Lee, I. Pefkianakis, S. Choudhury, S. Xu, and S. Lu, "Exploiting Spatial, Frequency, and Multiuser Diversity in 3GPP LTE Cellular Networks," *IEEE Transactions on Mobile Computing,* vol. 11, no. 11, pp. 1652-1665, November 2012.

[35] C. Jeng-Yueng, Y. Mai, C. Yang, "Handover Enhancement in LTE-Advanced Relay Networks," *IEEE International Symposium on Computer, Consumer and Control,* pp. 224-227, 2012.

[36] S. Yuan, T. Luo, and M. Z. Win, "Neighboring Cell Search for LTE Systems," *IEEE Transactions on Wireless Communications*, vol. 11, no. 3, March 2012.

[37] S. B. Sedani, K. R. Borisagar, N. A. Kotak, G. R. Kulkarni, "Designing and Implementation of Quality Based Algorithms for Antenna Diversity Techniques Using Efficient Wireless Channels," *IEEE International Conference on Computational Intelligence and Computing Research*, 2010.

[38] W. Roh and A. Paulraj, "Outage performance of the distributed antenna systems in a composite fading channel," *In Proceedings of the 56th IEEE Vehicular Technology Conference*, vol. 3, pp. 1520-1524, 2002.

[39] S. Zhou, M. Zhao, X. Xu, J. Wang, and Y. Yao, "Distributed wireless communication system: a new architecture for future public wireless access," *IEEE Communications Magazine*, vol. 41, pp. 108-113, March 2003.

[40] S. Verdu, Multiuser Detection, Cambridge University Press, 1998.

[41] M. Cover, "Broadcast channels," *IEEE Transactions on Information Theory*, vol. 18, no. 1, pp. 2-14, January 1972.

[42] G. Caire and S. Shamai, "On the achievable throughput of a multiantenna Gaussian broadcast channel," *IEEE Transactions on Information Theory*, vol. 49, no. 7, pp. 1691-1706, July 2003.

[43] W. Yu and J. M. Cioffi, "Sum capacity of Gaussian vector broadcast channels," *IEEE Transactions on Information Theory*, November 2001.

[44] S. Vishwanath, N. Jindal, and A. Goldsmith, "Duality, achievable rates and sum-capacity of Gaussian MIMO broadcast channels," *IEEE Transactions on Information Theory*, vol. 49, no. 10, pp. 2658-2668, October 2003.

[45] P. Viswanath, and D. Tse, "Sum capacity of the multiple antenna Gaussian broadcast channel and uplink-downlink duality," *IEEE Transactions on Information Theory*, vol. 49, no. 8, pp. 1912-1921, August 2003.

[46] S. Haykin, "Adaptive Filter Theory," Prentice–Hall, Inc., Englewood Cliffs, NJ, USA, 4th edition, 2001.

[47] D. Gesbert, M. Shafi, D. Shiu, P.J. Smith, and A. Naguib, "From theory to practice: an overview of MIMO space-time coded wireless systems," *IEEE Journal on Selected Areas in Communications,* vol. 21, pp. 281-302, April 2003.

[48] A. Paulraj, R. Nabar, and D. Gore, "Introduction to Space-Time Wireless Communications," Cambridge University Press, 2003.

[49] M. Alamouti, "A simple transmit diversity technique for wireless communication," *IEEE Journal Select Areas Communications*, vol. 16, pp. 1451-1458, October, 1998.

[50] V. Tarokh, H. Jafarkhani, and A.R. Calderbank, "Space-time block codes from orthogonal designs," *IEEE Transaction on Information Theory*, vol. 45, no. 5, pp. 1456-1462, July 1999.

[51] H. Jafarkhani, "A quasi-orthogonal space-time block code," *IEEE Transaction on Communications,* vol. 49, pp. 1-4, January 2001.

[52] W. Su and X. Xia, "Signal constellations for quasi-orthogonal space-time block codes with full diversity," *IEEE Transaction on Information Theory*, vol. 50, pp. 2331-2347, October 2004.

[53] H. Bolcskei and A.J. Paulraj, "Space-frequency coded broadband OFDM systems," *In Proceedings of the IEEE Wireless Communications and Networking Conference,* Chicago, USA, September 2000.

[54] V. Tarokh, N. Seshradi, and A.R. Calderbank, "Space-time codes for high data rate wireless communications: Performance criteria and code construction," *IEEE Transaction on Information Theory*, vol. 44, no. 2, pp. 744-765, March 1998.

[55] L.C. Godara, "Application of antenna arrays to mobile communications. ii. Beamforming and direction-of-arrival considerations," *In Proceedings of the Proceeding of the IEEE*, vol. 85, pp. 1195-1245, August 1997.

[56] A.F, Molisch, "Wireless Communications," Second Edition, Publisher: Wiley-IEEE Press, pp. 445-498, Chichester, United Kingdom 2011.

[57] S.T. Chung, A. Lozano, and H.C. Huang, "Approaching eigenmode BLAST channel capacity using V-BLAST with rate and power feedback," *In Proceedings of the 54th IEEE Vehicular Technology Conference*, vol. 2, pp. 915-919, October 2001.

[58] H. Claussen, H.R. Karimi, and B. Mulgrew, "Low complexity detection of high-order modulation in multiple antenna systems," *IEE Proceedings*, vol. 152, pp. 789-796, December, 2005.

[59] G. Care, G. Taricco, and E. Biglieri, "Bit-Interleaved coded Modulation," *IEEE Transactions on Information Theory*, vol. 44, no. 3, May 1998.

[60] G.G Raleigh and J.M Cioffi, "Spatio-temperal coding for wireless communication," *IEEE Transactions on Communications,* vol. 46, pp. 357-366, March 1998.

[61] B. Hassibi and B. M. Hochwald, "High-rate codes that are linear in space and time," *IEEE Transactions on Information Theory*, vol. 48, no. 7, pp. 1804-1824, July 2002.

[62] U. Wachsmann, J. Thielecke, and H. Schotten, "Exploiting the data-rate potential of MIMO channels: multi-stratum space-time coding," *In Proceedings of the 53rd IEEE Vehicular Technology Conference,* vol. 1, pp. 199-203, May 2001.

[63] M. Stege, and G. Fettweis, "Multistratum-permutation codes for MIMO communication," *IEEE Journal on Selected Areas in Communications*, vol. 21, pp. 774-782, June 2003.

[64] R. Bohnke, V. Kuhn, and K. D. Kammeyer, "Efficient near-maximum likelihood detection of multi-stratum space-time codes," *In Proceedings of the IEEE Semiannual Vehicular Technology Conference,* Los Angeles, USA, September 2004.

[65] D. Tse, "Fundamental of Wireless Communication", Publisher: Cambridge University Press, 2004.

[66] J. G. Proakis, "Digital Communications," Fourth Edition, Publisher: McGraw-Hill, Singapore, 2001 pp. 247-254, 2001

[67] L. Zheng and D.N.C Tse, "Diversity and multiplexing: a fundamental trade-off in multiple-antenna channels," *IEEE Transaction on Information Theory*, vol. 49, pp. 1073-1096, May 2003.

[68] T.A. Huynh, D.C. Hoang, M. R. Islam and J. Kim, "Two-Level-Search Sphere Decoding Algorithm for MIMO Detection," *IEEE Transactions on Signal Processing*, pp. 448-452, 2008.

[69] R. Heath, Jr. and A. Paulraj, "Switching between multiplexing and diversity based on constellation distance," *In Proc. Allerton Conf. Communication, Control and Computing*, Oct. 2000.

[70] http://mathworld.wolfram.com/MutualInformation.html.

[71] T.J. Richardson and R.L Urbanke. "Modern Coding Theory," Cambridge University Press, November 2006.

[72] R. Gallager, "Low-density parity-check codes," *IRE Transactions on Information Theory*, vol. 8, pp. 21-28, January 1974.

[73] R. M. Tanner, "A recursive approach to low complexity codes," *IEEE Transactions on Information Theory*, vol. 27, pp. 533-547, September 1981.

[74] C. Berrou, S. Glavieux, and P. Thitimajashima, "Near Shannon limit error-correcting coding and decoding: Turbo-codes," *In Proceedings of the IEEE International conference on Communications*, pp. 1064-1070, Geneva, Switzerland, May 1993.

[75] D.J.C. MacKay and R. Neal, "Near Shannon limit performance of low-density parity check codes," *Electronic Letters*, vol. 33, no. 6, pp. 1645-1646, 1996. March 1997.

[76] J. Chien, H. Hsieh and S. Furui, "A new mutual information measure for independent component analysis," *IEEE International Conference on Acoustics, Speech and Signal Processing*, pp. 1817-1820, 2008.

[77] M. Kiessling, "Unifying Analysis of Ergodic MIMO Capacity in Correlated Rayleigh Fading Environments," *European Transactions on Telecommunications*, vol. 16, pp. 17-35, January 2005.

[78] G. J. Foschini and M. J. Gans, "On limits of wireless communication in a fading environment when using multiple antennas," *Wireless Personal Communications*, vol. 6, no. 3, pp. 311-335, October 1998.

[79] T. L. Marzetta and B. M. Hochwald, "Capacity of a mobile multiple-antenna communication link in Rayleigh flat fading," *IEEE Transactions on Information Theory*, vol. 45, no. 1, pp. 139-157, 1999.

[80] B. Hassibi and B. M. Hochwald, "How much training is needed in multiple-antenna wireless links?," *IEEE Transactions on Information Theory*, vol. 49, no. 4, pp. 951-963, 2003.

[81] B.M. Hochwald, T.L. Marzetta, and V. Tarokh, "Multiple-antenna channel hardening and its implications for rate feedback and scheduling," *IEEE Transactions on Information Theory*, vol. 50, pp. 1893-1909, September 2004.

[82] P. Grant, I Glover, "Digital Communications," Prentice Hall, Second Edition, pp. 239-247, 2004.

[83] H. L. Van Trees, "Detection, Estimation, and Modulation Theory," vol. I. John Wiley & Sons, Inc., New York, NY, USA, 1968.

[84] R. Fano, "A heuristic discussion of probabilistic decoding," *IEEE Transactions of Information Theory*, vol. 9, pp. 64-74, April 1963.

[85] M. Wiesel, Y.C Eldar, and S.S Shitz, "Semi definite relaxation for detection of 16-quam signalling in MIMO channels," *IEEE Signal Processing Letters*, vol. 12, pp. 653-656, September 2005.

[86] J. W. Choi, A. C. Singer, J. Lee, N. I. Cho, "Improved Linear Soft-Input Soft-Output Detection via Soft Feedback Successive Interference cancellation," *IEEE Transactions on Communications*, vol. 58, pp. 986-996, March 2010.

[87] C. Michalke E. Zimmermann and G. Fettweis, "Linear MIMO receivers vs. tree search detection: A performance comparison overview," *In 17th IEEE International Symposium on Personal, Indoor and Mobile Radio Communication*s, Helsinki, Finland, pp. 11-14, September 2006.

[88] E. Zimmermann and G. Fettweis, "Adaptive vs. hybrid iterative MIMO receivers based on MMSE linear and soft-SIC detection," *In 17th IEEE International Symposium on Personal, Indoor and Mobile Radio Communications*, Helsinki, Finland, pp. 11-14, September 2006.

[89] G. D. Golden, C. J. Foschini, R.A. Valenzuela and P.W. Wolniansky, "Detection algorithm and initial laboratory results using V-BLAST space-time communications architecture," *IEEE Electronics Letters*, vol. 35, no. 1, pp. 14-16, January 1999.

[90] M. Witzke, S. Baro, F. Schreckenbach, and J. Hagenuaer, "Iterative detection of MIMO signals with linear detectors," *In Proceedings of the 36th Asilomar Conference on Signals, Systems and Computers*, pp. 289-293, November 2002.

[91] Y. Wang, J. Wang, and Z. Xie, "Ordered successive interference cancellation mimo decision feedback equalization based on constant modulus property," *International Journal of Information and Systems Sciences*, vol. 4, no. 4, pp. 500-511, 2008.

[92] M.O. Damen, H. El Gamal, and G. Caire, "On maximum-likelihood detection and the search for the closest lattice point," *IEEE Transactions*, vol. 53, pp. 930-935, June 2005.

[93] D. Wubben, R. Bohnke, J. Rinas, V. Kuhn and K. D. Kammeyer, "Efficient algorithm for decoding layered space-time codes," *IEEE Electronics Letters*, vol. 36, no. 22, pp. 1348-1350, October 2001.

[94] E. Biglieri, A. Nordio, and G. Tarcco, "Doubly-Iterative Decoding of Space-Time Turbo Codes with a Large Number of Antennas," *IEEE International Conference on Communications Society*, vol.1, pp. 473-477, June 2004.

[95] W. Xu, Y. Wang, Z. Zhou, and J. Wang, "A flexible near-optimum detector for V-BLAST," *Proc. IEEE Circuits, Systems Symp. On Emerging Technologies*, Shanghai, China, pp. 681-684, May 2004.

[96] L. Yang C. Ming, S. Cheng and H. Wang, "Reduced Complexity Group Sphere Decoder Joint with Interference Cancellation for Multistream MIMO," *In Proceedings of the IEEE Information Theory*, vol. 2, pp. 895-898, September 2004.

[97] E. Zimmermann, S. Bittner, and G. Fettweis, "Complexity reduction in iterative MIMO receivers based on EXIT chart analysis," *In International Symposium on Turbo Codes & Related Topics*, Munich, Germany, April 2006.

[98] A. Boronka, D. Efinger, and J. Speidel, "Improving MIMO detection by l-valve analysis and adaptive threshold-based cancellation," *In Proceedings of the IEEE Global Telecommunications Conference*, vol. 4, pp. 2099-2013, December 2003.

[99] E. Viterbo and E. Bigleri, "A universal lattice decoder," *In 14eme Colloque GRETSI*, pp. 611-614, September 1993.

[100] C. Michalke and G. Fettweiss, "Simple broadband MIMO-OFDM transmission," *In International Symposium on Wireless Personal Multimedia Communications*, San Diego, USA, September 2006.

[101] D. Wubben and K. D. Kammeyer, "Parallel-SQRD for low complexity successive interference cancellation in per-antenna-coded MIMO-OFDM schemes," *In International Symposium on Turbo Codes & Related Topics*, Munich, Germany, April 2006.

[102] A. K. Lenstra, H. W. Lenstra, and L. Lovasz, "Factoring polynomials with rational coefficients," *Mathematische Annalen*, vol. 261, pp. 515-534, 1982.

[103] C.P Schonorr and M. Euchner, "Lattice basis reduction: Improved practical algorithms and solving subset sum problems," *Mathematical Programming*, vol. 66, pp. 181-199, August 1994.

[104] A.M. Chan, and 1. Lee, "A new reduced-complexity sphere decoder for multiple antenna systems," *In Proceedings of the IEEE International Conference on Communications*, vol. 1, pp. 460-464, May 2002.

[105] R. Kannan, "Improved algorithms for integer programming and related lattice problems," *In Proceedings of the 15th Symposium on the Theory of Computing,* pp. 99-108, ACM Press, 1983.

[106] D. L Milliner, E. Zimmermann, J. R. Fettweis, P. Gerhard, "A Framework for Fixed Complexity Breadth-First MIMO Detection," *IEEE 10th International Symposium on Spread Spectrum Techniques and Applications*, pp. 129-132, Aug 2008.

[107] M. Pohst, "On the computation of lattice vectors of minimal length, successive minima and reduced bases with applications," *ACM SIGSAM Bulletin*, vol. 15, pp. 37-44, February 1981.

[108] A.A. Nielsen, "Least Squares Adjustment: Linear and Nonlinear Weighted Regression Analysis", *National Space Institute/Informatics and Mathematical Modelling*, pp. 1-10, Oct 2008.

[109] F. Zhao, S. Qiao, "Radius Selection Algorithms for Sphere Decoding," 2009

[110] J. Lee and S.C. Park, "Novel Techniques of a Sphere Decoder for High Throughput," *Advanced Communication Technology, The 8th International Conference*, vol. 3, Feb 2006.

[111] E. Zimmermann and G. Fettweis, "Unbiased MMSE tree search MIMO detection," *In International Symposium on Wireless Personal Multimedia Communications*, San Diego, USA, pp.17.-20, September 2006.

[112] K.K. Wong and A. Paulraj, "On the decoding order of MIMO maximum-likelihood sphere decoder: linear and non-linear receiver," *In Proceedings of the 59th IEEE Vehicular Technology Conference*, vol. 2, pp. 698-702, May 2004.

[113] M. O. Damen, H. E. Gamal, and G. Caire, "On Maximum-Likelihood detection and the search for the closest lattice point," *IEEE Transactions on Information Theory* ,vol. 49, no. 10, pp. 2389-2402, Oct 2003.

[114] M. Samuel and F.M. Fitz, "Efficient iterative sphere detectors based on the Schnorr-Euchner enumeration," *IEEE Information Theory Workshop*, pp. 91-95, 2009.

[115] M. Samuel and F.M. Fitz, "Iterative sphere detectors based on the Schnorr-Euchner enumeration," *IEEE Transactions on Wireless communications*, vol. 9, no. 7, pp. 2137-2144.

[116] M. Stojnic, H. Vikalo, and B. Hassibi, "A branch and bound approach to speed up in sphere decoder," *A Proceedings of the IEEE International Conference on Acoustics, Speech, Signal Processing*, vol. 3, pp. 429-432, March 2005.

[117] M. Stojnic, H. Vikalo, and B. Hassibi, "Further results on speeding up the sphere decoder," *In Proceedings of the IEEE International Conference on Acoustics, Speech, and Signal Proceedings*, May 2006.

[118] G. Kapfunde, Y. Sun, N. Alinier, "An Improved Sphere Decoder for MIMO Systems," *3rd International Workshop on the Performance Enhancements in MIMO OFDM Systems (PEMOS)*, Barcelona, Spain, October, 2012.

[119] Q. Liu and L. Yang, "A novel method for initial radius selection of sphere decoding," *In Proceedings of the 60th IEEE Vehicular Technology Conference*, vol. 2, pp.1280-1283, September 2004.

[120] H. G. Kang, J. Park, T. An, J. Oh, and I. Song, "An ML Decoding Algorithm with Reduced Complexity for Multi-Input Multi-Output Systems," *International Symposium on Signals, Systems and Electronics*, pp. 339-342, August 2007.

[121] B.M. Hochwald and S. ten Brink, "Achieving near-capacity on a multiple-antenna channel", *IEEE Transactions on Communications*, vol. 51, pp. 389-399, March 2003.

[122] X. Xia, H. Hu, H. Wang, "Reduced initial searching Radius for Sphere Decoder," *The 18th Annual IEEE International Symposium on Personal, Indoor and Mobile Radio Communications*, pp. 1-4, September 2007.

[123] X.G. Dai, S. W Cheung and T.I. Yuk, "A new family of linear Dispersion Code for fast sphere decoding," *IEEE Transactions on Information Theory*, vol. 27, pp. 314-331, 2009.

[124] H. Vikalo and B. Hassibi, "On the sphere-decoding algorithm ii. Generalizations, second-order statistics, and applications to communications," *IEEE Transactions on Signal Processing*, vol. 53, pp. 2819-2834, August 2005.

[125] P. Marsch, E. Zimmermann, and G. Fettweis, "Improved methods for search radius estimation in sphere detection based MIMO receivers," *In 14th IST Mobile & Wireless Communications Summit*, Dresden, Germany, June 2005.

[126] G. Kapfunde, Y. Sun, "Performance Evaluation of Linear Detectors for LDPC-Coded MIMO Systems," *UCL Conference,* London, UK, 2010.

[127] E. Zimmermann, W. Rave, and G. Fettweis, "On the complexity of sphere decoding," *In 7th International Symposium Personal Multimedia Communications,* Abano Terme, Italy, pp. 12-15, September 2004.

[128] D. Seethaler, H. Artes and F. Hlawatsch, "Dynamic Nulling-and-Cancelling with Near-ML Performance for MIMO Communications," *In the Proceedings of the IEEE International Conference on Acoustics, Speech, and Signal Processing,* vol. 4, pp. 777-780, May 2004.

[129] B. Hassibi, "An efficient square root algorithm for BLAST," *In Proceedings of the IEEE International Conference on Acoustics, Speech, and Signal Processing*, vol. 2, pp. 737-740, Istanbul, Turkey, June 2000.

[130] D. Wubben, R. Bohnke, V. Kuehn, and K. D Kammeyer, "MMSE extension V-BLAST based on sorted QR decomposition," *In Proc. IEEE Semiannual Vehicular Technology Conference (Fall)*, vol.1, pp. 508-512, Orlando, USA, October 2003.

[131] J. Park, and J. Chun, "Efficient Lattice-Reduction-Aided Successive Interference Cancellation for Clustered Multiuser MIMO System," *IEEE Transactions on vehicular Technology*, vol. 61, no. 8, pp. 3646-3655, October 2012.

[132] J. Park, and J. Chun, "Improved Lattice Reduction-Aided MIMO Successive Interference Cancellation under Imperfect Channel Estimation," *IEEE Transactions on Signal Processing*, vol. 60, no. 6, pp. 3346-3351, June 2012.

[133] B. Gestner, X. Ma, and D.V. Anderson, "Incremental Lattice Reduction: Motivation, Theory, and Practical Implementation," *IEEE Transactions on Wireless Communications*, vol. 11, no. 1, pp. 188-198, January 2012.

[134] S. Aubert, Y. Nasser, and F. Nouvel, "Lattice Reduction-Aided Minimum Mean Square Error *K*-Best Detection for MIMO Systems," *International Conference on Computing, Networking and Communications, Wireless Communications Symposium*, pp. 1066-1070, 2012.

[135] D. Wubben and K.D Kammeyer, "Low complexity successive interference cancellation for MIMO–OFDM systems," *European Transactions on Telecommunications,* vol. 18, pp. 457-466, April 2007.

[136] L.A. Li, R.C. de Lamare, A.G. Burr, "Complex Sphere Decoding with a Modified Tree Pruning and Successive Interference Cancellation," *IEEE International Symposium on Wireless Communications Systems*, pp. 226-230, 2012.

[137] S. Han, T. Cui, and C. Tellambura, "Improved K-Best Sphere Detection for Uncoded and Coded MIMO Systems," *IEEE Transactions on Wireless Communications Letters*, vol. 1, no. 5, pp. 472-475, October 2012.

[138] C.F. Liao and Y.H. Huang, "Reduced-Complexity LLL Algorithm for Lattice-Reduction-Aided MIMO Detection," *IEEE Conference on Signals, Systems and Computers,* Conference Record of the Forty-Third Asilomar, pp. 1451-1455, 2009.

[139] Y. Dai, S. Sun, and Z. Lei, "A comparative study of QRD-M detection and sphere decoding for MIMO-OFDM systems," *In Proceedings of the IEEE 16th International Symposium on Personal, Indoor and Mobile Radio Communications*, vol. 1, pp. 186-190, September 2005.

[140] J. Jalden and B. Ottersten, "On the complexity of the sphere decoding in digital communications," *IEEE Transactions on Signal Processing*, vol. 53, pp. 1474-1484, April 2005.

[141] G. Kapfunde, F. Tade, Y. Sun, "A Sphere Decoder for MIMO Detection using Improved Initial Sphere Radius", *Applied Radio Systems Research and Smart Wireless Communications (ARSR/SWICOM),* Luton, UK, 2013.

[142] M. Stege, T. Hentschel, M. Lohning, M. Windisch, and G. Fettweis, "IEEE 802.11n MIMO-Prototyping with Dirty RF Using Hardware-in-the-loop Approach," *In 14th European Signal Processing Conference*, Florence, Italy, September 2006.

[143] Z. En, H. Xiaolin, C. Jianping, Z. Zhan and H. Kayama, "FPGA implementation and experimental performances of a novel timing synchronization method in MIMO-OFDM systems," in *14th IEEE Asia-Pacific Conference on Communications*, pp. 1-5*, 2008*.